LATERAL CONTROL OF A WEB USING ESTIMATED VELOCITY FEEDBACK

By

SHAIBAL SAILAZA MANDAL

Bachelor of Engineering

Sardar Patel College of Engineering

Mumbai, India

1998

Submitted to the Faculty of the
Graduate College of the
Oklahoma State University
in partial fulfillment of
the requirements for
the Degree of
MASTER OF SCIENCE
July, 2000

LATERAL CONTROL OF A WEB USING
ESTIMATED VELOCITY FEEDBACK

Thesis Approved:

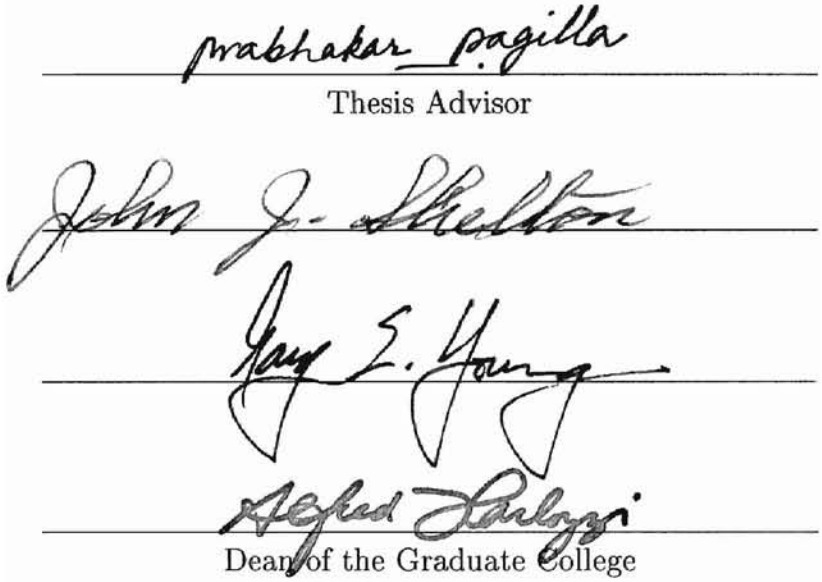

Thesis Advisor

Dean of the Graduate College

Acknowledgements

I would like to express my gratitude to Dr. Prabhakar Pagilla, my thesis advisor, for his guidance and advice throughout the development of this investigation. Without his help and supervision, I would not have completed this work. I am also grateful to my committee members, Dr. Gary Young and Dr. John J. Shelton, for their help and guidance. My sincere gratitude to Fife Corporation in Oklahoma City and Ken Hopcus for providing us with the equipments necessary for conducting the experiments.

I wish to thank Yongliang for setting up the real-time program. Finally, I wish to thank my colleagues Biao and Sun Yu for helping me with the experiments.

Table of Contents

List of Figures

Figure **Page**

Figure **Page**

Figure **Page**

Figure **Page**

Nomenclature

a	half contact width of rubber covered rolls
A	cross-sectional area of the web
A	durometer (chapter 2 only)
δ	radial deflection of rubber covered rolls
D	roll diameter
E	modulus of elasticity (Young's modulus)
F	force or load
F/W	effective nip load
G	modulus of elasticity in shear
I	moment of Inertia
K	constant for a given operating condition ($\sqrt{T/EI}$)
L	the length of a free span of a web
M	bending moment
M_0	bending moment at upstream roller
M_L	bending moment at downstream roller
n	a stress averaging factor
N	shear force normal to the elastic curve of the web
Q	shear force parallel to the original web centerline
R	roller radius
R_o	undeflected rubber covered roll radius
S	shape factor
t	rubber cover thickness
T	web tension
y	lateral position of web
v	velocity of the web

y_L	response at a Kamberoller guide
$y_0(s)$	the positional disturbance from upstream roller
w	side load per unit length
W	width of web
z	position of downstream roller relative to the ground
$\hat{X}_2$	estimated velocity of motor
U	control input
θ	angle between web and roller
θ_r	angle of rotation of roller
θ_0	angular disturbance at upstream roller
θ_L	angular input at downstream roller
β	angle of arc of lateral slippage
μ	coefficient of friction

Chapter 1

Introduction

A web refers to any material that is very long compared to its width and very wide compared to its thickness. Examples include paper rolls, thin aluminum foils, photo films, plastic films and metal strip. In a processing line, a web travels over a series of rollers that provide support, transport and control.

Web handling involves unwinding the material, feeding it to a processing plant and then winding it back on to a roll. Generally the web must follow a predetermined path which is in the longitudinal direction with a constant velocity. Deviation from this may result in inferior product quality. Too much lateral movement can cause slackness of the web. When this happens the slack web can go through a nip or be wound on to a roll causing wrinkles or creases to form. For this reason a tight control on the lateral displacement of the web is essential. Optical, pneumatic or ultrasonic sensors are used as edge detectors to sense the edge of the web.

The basic elements of an automatic system to control the lateral position of a web are (1) a sensor to detect web position, (2) a controller to receive input signals from the sensor and produce a higher power level output, (3) a guiding mechanism including some kind of actuator to receive the output of the controller and translate it into physical positioning of the web, and (4) the web itself, through which the sensor

detects lateral signals. Therefore a guiding installation is a system that consists of several components selected to function together to obtain the desired control. Proper selection and integration of the components is essential to obtaining optimum results.

The guiding system should be located as close as possible and immediately preceding the point in the process where accurate control is required. It should be designed and installed so that it is capable of correcting the maximum lateral deviation expected. It is important to remember that once the web leaves the guiding system, it is free to wander again, depending upon the many factors that may influence it, such as web properties and machine and process disturbances. All commonly used guide rollers today depend on a fundamental law of web behavior, that a web moves laterally on a roll it is approaching until its upstream span becomes perpendicular to that roll. The steering-type guide roller utilizes this principle by inclining itself to its entry span. As the web moves through the machine, it moves to align itself perpendicularly to the inclined guide roll and is laterally displaced in the entry span an amount depending upon the length of the span and the guide roll angle. A steering guide is useful where a relatively long, free web span is available. Lateral displacement of a web is also possible using differentially loaded nip guides.

1.1 Literature Review

This section will first review the statics and dynamics of a moving web and then briefly discuss nip rollers in the lateral control of web.

Modeling lateral dynamics is an important first step in an attempt to improve web process control and end-roll product quality. The model must provide an accurate description of the system and facilitate the implementation of online parameter and state estimation. Mathematical modeling of lateral web dynamics was introduced by Campbell (1958). Campbell's model was based on the assumption that the web

behaves like a string and makes sharp breaks at every roller. This basic assumption led to a first order model which was not very accurate. Shelton [1] , in his thesis (1968) developed an improved model based on the assumption that the web between two rollers behaves like a beam. The Shelton model can describe accurately the response of the web at a roller due to an input from a pure displacement guide but is limited to single span systems.

Shelton has been broad in his work on the lateral control of a web due to lack of previous literature on this subject. The fundamental static beam theory has been covered in considerable depth. He found the web lateral behavior to depend upon the dimensionless parameter KL. If KL is small (less than unity) and the shear modulus low, the static behavior was found to be quite dependent upon the shear deflection parameter $\frac{nT}{AG}$. Shelton has analysed the web for conditions considering only shear deflection (simplified model of first order) and for both bending deflection and shear deflection (accurate model of second order). The transfer functions of several practical web handling components and configurations were derived for each case. The accurate method of dynamic analysis confirmed the trends found in the simplified analysis to give a fair approximation at values of ωT_1 of less than two. If KL is less than unity and $\frac{nT}{AG}$ is less than 0.001, as is generally the case, the second order theory was found to be more accurate.

Although web conveyance systems have been widely used in the industry since the days of industrial revolution, the technical literature on the subject of lateral dynamics is very limited. The most significant work on lateral dynamics was done by Dr. J.J.Shelton. Shelton and Reid [2, 3] presented a comparison of the first order and the second order web dynamics to illustrate the inadequacies of the former for certain frequencies and operating conditions. Young and Reid [5] have given a clear insight into the fundamentals of lateral control of a web. Young, Shelton and Kardamilas [6]

use state estimation to predict lateral web position on a downstream sensor with use of the feedforward sensor to achieve improved control. The experiments provide with a solution when placement of an edge sensor near the web guide is prevented by physical constraints in the processing lines. Young and Kardamilas [7] and Kardamilas [8] have introduced a stochastic model, which represents non-ideal webs and disturbances at the entering span roll, based on experimental data. Little significant work has been done on the lateral control of web using differentially loaded nip rollers. Guiding by means of a higher loading on one side of a nip than on the other side causes a variation in velocity across the width of a web which is indicative of a variation in strain and therefore stress across the width. When integrated this stress will result in a moment which will be shown to produce the lateral deformation of the web. Guiding the web using differentially loaded nip guides would be particularly advantageous in applications where the entering and exiting spans are collinear. Young, Shelton and Fang [9] discuss the effects of low friction between the web and the roller between two web spans. The resulting slippage may cause the tension distribution in the downstream span to affect the tension distribution in the upstream span, resulting in a large lateral displacement. The primary purpose for the static analysis on the interactive web systems is to establish the governing function for each span. In [10], Young, Shelton and Fang develop the dynamics of interacting web spans based on the fundamental theory for web lateral motion developed by Shelton in his thesis.

Lindley [11] and Foreman [12] have been successful in controlling the lateral displacement using differentially loaded rubber covered rollers. Lindley presented a load-deformation relationship. Foreman used rubber covered rollers and found that the velocity of the web is proportional to the load on these rubber covered rollers. He stated that the increased velocity of the strip is due to the increased length of contact between the compressed rubber and the strip passing through. Shelton [13]

in his report to Fife Corporation on guiding with differential forces on rubber-covered nip rollers analysed the free and supported catenary conditions of the web for lateral movement. He found inadequacies in Foreman's analysis as it did not readily fit into a manageable theory. A few of the problems as specified by Shelton are (1) Extensive testing was done with hardness of rubber covers of 46, 50 and 58 Shore A durometer, well below the range of wringer rollers to have satifactory life expectancy. (2) The extensive testing was done with one rubber-covered and one steel roller. The thickness of the steel strip was not reported, but unless it was thick enough to remain planar within the nip, the nip behavior would be somewhat different from that with two identical rubber-covered rollers. (3) The web was dry, and the importance of friction was not determined. Ahmad [14] in his thesis experimentally verified the lateral deformations of a web due to non-uniform nip loading with rubber covered rollers. Shelton [15] has discussed the problems associated with cambered webs and how to eliminate or minimize the effects of camber. In his paper, Hopcus [4] discusses the practical application of terminal guides (unwind and rewind), the control system loop, sensor configurations, sensor locations and response of the system and equipment for the lateral control of a web.

1.2 Thesis Contribution

This research focuses on the control of lateral movement of the web and is an extension of the work done by Shelton for his PhD. thesis. The major achievements of this research are: (1) Investigation of existing models; (2) Investigation of the importance of the inner-loop velocity feedback; (3) Design and development of the experimental web platform; (4) Design and development of an open architecture real-time software system for easy implementation of lateral control strategies; (5) Implementation of a PID controller using the computer, bypassing the analog controller from Fife and

using it as an edge sensor signal amplifier.

Presently the industry uses different guiding mechanisms for lateral control of a web. A brief description of each of these guiding mechanisms and control system is explained in Chapter 2. The guiding mechanism used for the experiments in this research is a Fife Kamberoller guide, which is a remotely pivoted guide. The control system for this guiding mechanism uses the velocity feedback from the motor. At steady state, the position of the motor is directly proportional to the position of the web. The motor velocity can therefore be estimated using the velocity of the web, which can be estimated by using a minimum order observer design. The objective of this research is to eliminate the inner-loop velocity feedback in the motor using an observer based controller, thus reducing the cost of the motor. It is experimentally verified that the digital control using the computer gives a better response than the A9 analog controller used by Fife.

1.3 Thesis Outline

The organization of this report is as follows. Chapter 2 gives a brief overview of the work done by Shelton, Lindley and Foreman. Some of Shelton's work has been reproduced in this chapter since it forms the fundamental basis for web lateral behavior. Different types of automatic control systems and guiding mechanisms have been described in Chapter 3. The observer design to estimate the velocity of the web for eliminating the inner-loop velocity feedback in the motor has been done in Chapter 4. Chapter 5 describes the open-architecture experimental platform that is developed for lateral control experiments. Chapter 6 shows the experimental results obtained after conducting lateral control experiments. Chapter 7 lists some remarks of this work and suggestions for future research.

Chapter 2

Background

Dr. Shelton's [1] work has been extensively reviewed and a summary of this is presented in this chapter. It clearly explains the statics and dynamics of a moving web. He assumed the following conditions for the lateral behavior (static and dynamic) of a web. (1) Standard beam theory assumptions: (i) The web is initially straight and uniform; (ii) All deflections are small. (2) The area of contact between the web and the roller is small compared to the length of the web span. (3) Friction between the web and the roller is sufficient to prevent slippage and moment transfer, so that a moment in one span is isolated from its adjacent span. (4) Stress distribution in the normal section of a web is linear.

2.1 Static behavior of a web

Using the elementary beam theory Shelton analyzed the static behavior of a web to derive a fourth order differential that is used for web analysis. Fig. 2.1 shows a schematic diagram of a section of the web with tension forces on it. The web span is assumed to be long so that deflections due to shear stress can be neglected.

The moment and the normal forces acting on the web is given by the following

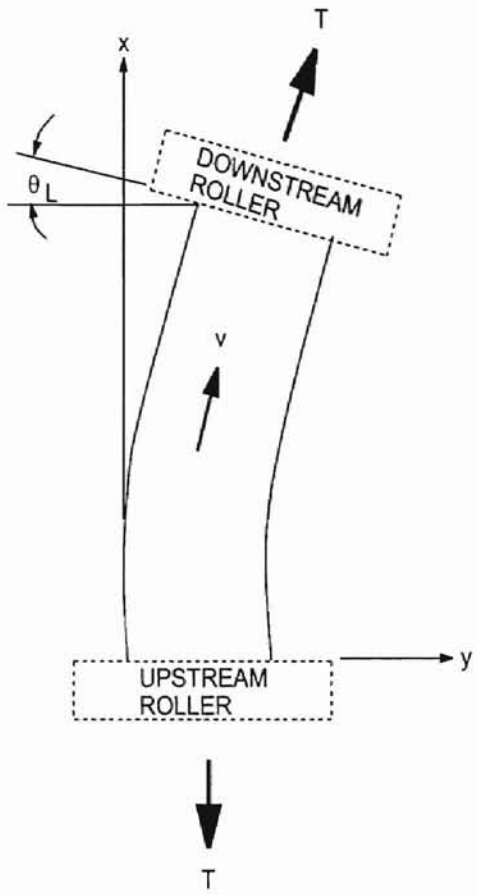

Figure 2.1: Schematic diagram of web on rollers

equations:

$$M = -\frac{Ed}{dx}\left(\frac{Idy}{dx}\right) \tag{2.1}$$

$$N = -\frac{Ed}{dx}\left(\frac{Id^2y}{dx^2}\right) \tag{2.2}$$

$$w = \frac{Ed^2}{dx^2}\left(\frac{Id^2y}{dx^2}\right) \tag{2.3}$$

Fig. 2.2 shows the free body diagrams of a free web span, a horizontal section and a normal section. These are used to derive the fourth order differential equation

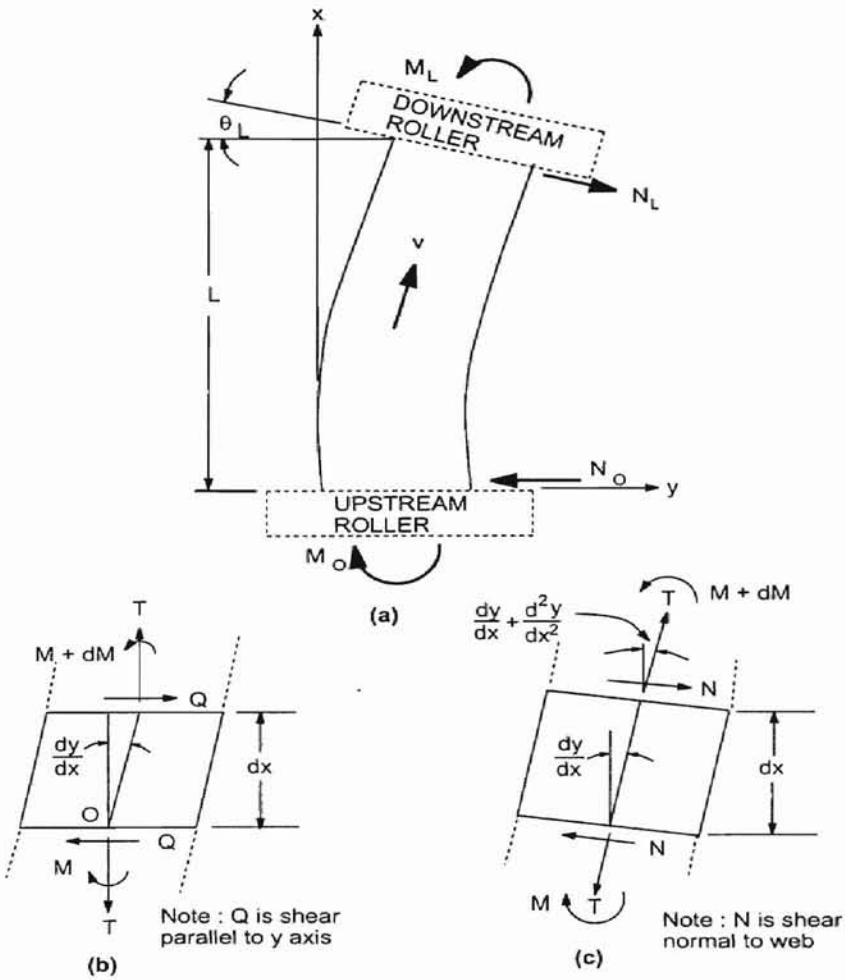

Figure 2.2: Freebodies and symbols for steady-state analysis

used for web analysis. Since all deflections are assumed to be small the tension T in both (b) and (c) of Fig. 2.2 are equal. A summation of all moments about point O gives us the following relation:

$$Q = \frac{dM}{dx} + T\frac{dy}{dx} \tag{2.4}$$

Taking the derivative of equation (2.1) and substitution into equation (2.4) gives the following equation

$$Q = -\frac{EId^3y}{dx^3} + \frac{Tdy}{dx} \tag{2.5}$$

Q is a constant since there is no side load assumed in the free span, and EI is a constant because it is assumed that the entire span is taut.

Differentiating equation (2.5) and dividing it by EI yields the fourth order differential equation of the elastic curvature of a web.

$$\frac{d^4y}{dx^4} - K^2\frac{d^2y}{dx^2} = 0 \tag{2.6}$$

The solution for the linear differential equation (2.6) is

$$y = C_1 \sinh Kx + C_2 \cosh Kx + C_3x + C_4 \tag{2.7}$$

Four boundary conditions are applied to evaluate the constants in equation (2.7):

- The lateral displacement at the upstream roller is assume to be zero which means $x = 0$ and $y = 0$.
- Friction is assumed to be sufficiently large to prevent circumferential slippage which means at $x = 0$, $\frac{dy}{dx} = 0$.
- The web approaches a roller perpendicularly to the roller axis. Shelton has experimentally verified this condition which lead to the following equation

$$C_1 \cosh KL + C_2 \sinh KL + C_3 = \theta_L$$

- The moment on the guide roller is assumed to be zero at steady state, that is $M_L = 0$.

Considering the above boundary conditions the constants are found to be:

$$C_1 = -\frac{\theta_L}{K}\frac{\cosh KL}{\cosh KL - 1} \tag{2.8}$$

$$C_2 = \frac{\theta_L}{K}\frac{\sinh KL}{\cosh KL - 1} \tag{2.9}$$

$$C_3 = \theta_L\frac{\cosh KL}{\cosh KL - 1} \tag{2.10}$$

$$C_1 = -\frac{\theta_L}{K}\frac{\sinh KL}{\cosh KL - 1} \tag{2.11}$$

2.2 Dynamic behavior of a web

2.2.1 Ideal moving web

In this case the physical properties of the web are ignored. The web is assumed to have no shear strength and hence can be assumed to be a straight line between two rollers. A web approaching a roller will align itself perpendicular to the roller as shown in Fig. 2.3

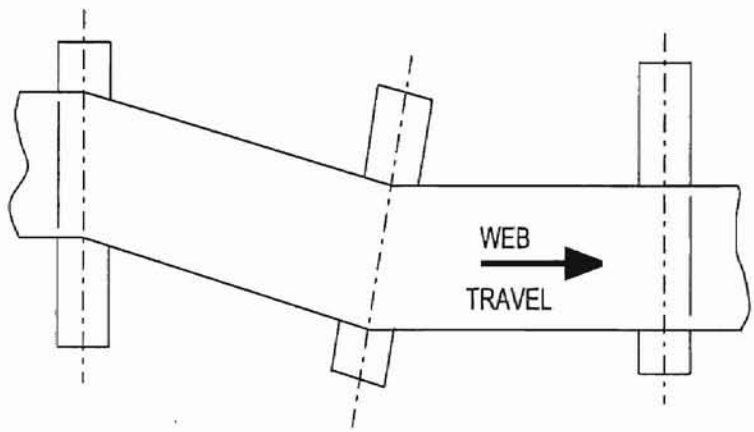

Figure 2.3: Web passing over a series of non-parallel rollers

On account of lateral movement of the roller the velocity of the web edge relative to the ground is the summation of the velocity of the web relative to roller and the velocity of the roller relative to the ground.

If the roller is moving laterally, the total velocity of the web edge relative to the ground is equal to the sum of the velocity of steering of the web and the velocity of lateral transport of the web. The following equation expresses the web velocity at the downstrean roller.

$$\frac{dy_L}{dt} = -v\theta + \frac{dz}{dt} \tag{2.12}$$

The negative sign in equation (2.12) accounts for the fact that a positive angle results in a negative velocity.

Shelton [1] has given an explained derivation of the transfer function and the frequency response for each of the following cases:

- Response at a fixed roller to input at the previous roller.
- Steering guide response.
- Response at a point between two parallel rollers.

A time response for each of the above cases has been done in this thesis with $\tau = 0.625$.

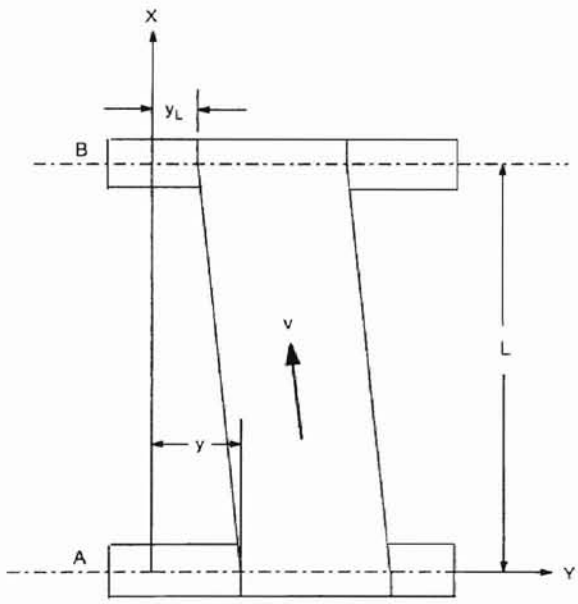

Figure 2.4: Symbols for the derivation of response at a fixed roller

Figures 2.4, 2.5 and 2.6 show all symbols used in the derivation of the transfer function for each of the above cases respectively. Their transfer functions are given as follows:

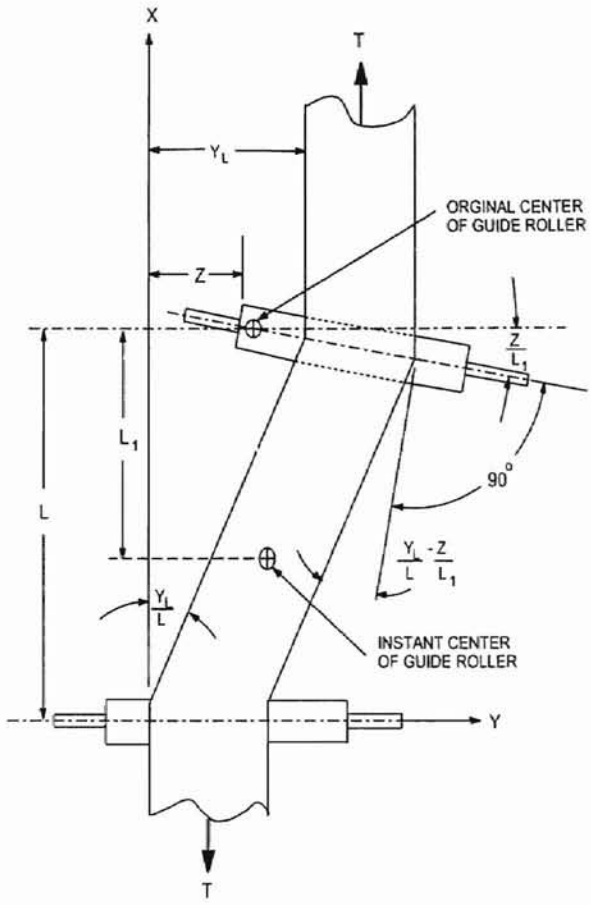

Figure 2.5: Symbols for the derivation of response at a steering guide

1. Response at a fixed roller to input at the previous roller.

$$\frac{Y_L(s)}{Y_0(s)} = \frac{1}{T_1 s + 1} \tag{2.13}$$

2. Steering Guide Response.

$$\frac{Y_L(s)}{Z(s)} = \frac{T_1 s + \dfrac{L}{L_1}}{T_1 s + 1} \tag{2.14}$$

3. Response at a point between two parallel rollers.

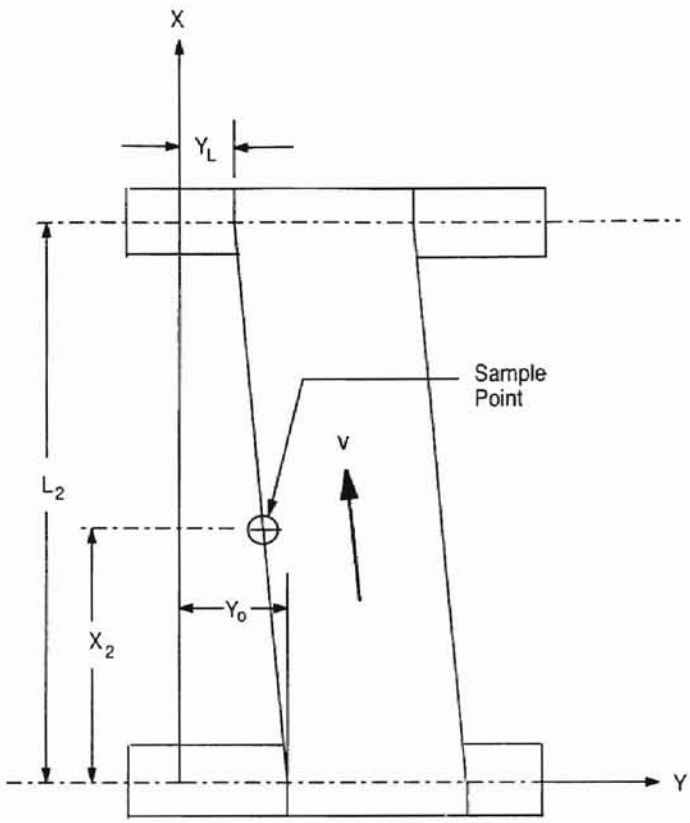

Figure 2.6: Symbols for the derivation of response at a point between two rollers

$$\frac{Y_2(s)}{Y_0(s)} = \frac{T_2(1 - \frac{x_2}{L_2})s}{T_2 s + 1} \tag{2.15}$$

Figures 2.7, 2.8 and 2.9 show the time response at a fixed roller due to input at the previous roller, steering guide response and response at a point between two parallel rollers respectively. Fig. 2.8 shows that the time to reach steady state depends on the distance of the instant center of the guide roller from the guide roller. As the distance decreases the amplitude of response increases. Fig. 2.9 indicates that as the distance of the sampling point from the upstream roller increases the time required to reach steady state increases.

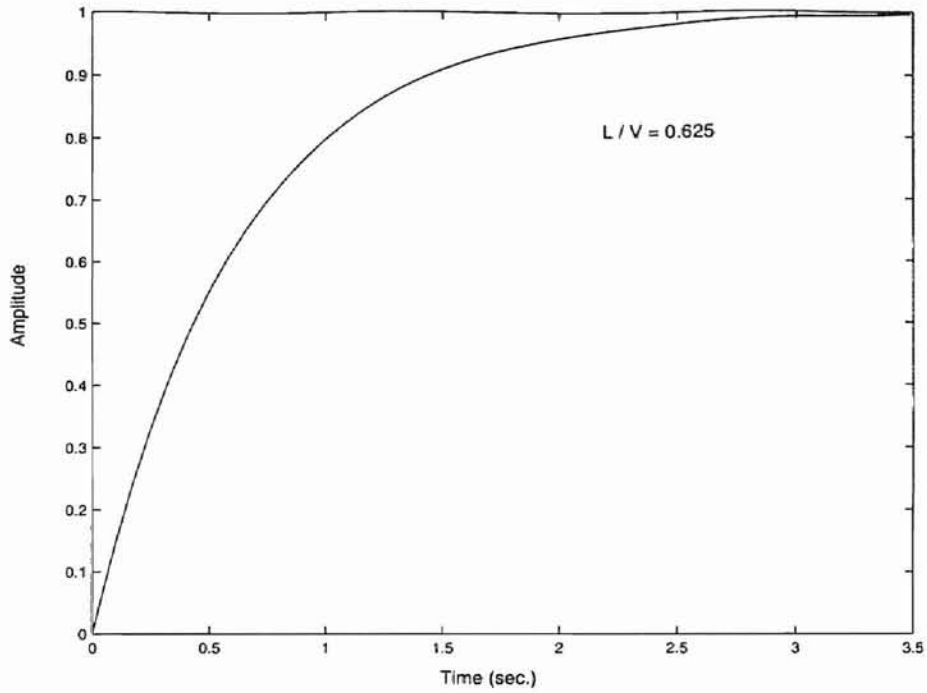

Figure 2.7: First order time response at a fixed roller due to input at the previous roller

2.2.2 Real moving web

Equation (2.6), applied to a web is independent of its steady state condition, if the web mass is neglected. But only the boundary conditions change. Shelton has rewritten the equation in the partial derivative form since time and location are both variables in the dynamic condition. Therefore equation (2.6) becomes:

$$\frac{\partial^4 y}{\partial x^4} - K^2 \frac{\partial^2 y}{\partial x^2} = 0 \tag{2.16}$$

He developed partial differential equations showing a relation between the downstream end of a web to its dynamics of steering. Dynamic analysis of the downstream end of the web is done with the statics as the fundamental basis. The static conditions are broken into two parts for dynamic analysis which are then superimposed to develop a differential equation of dynamic steering.

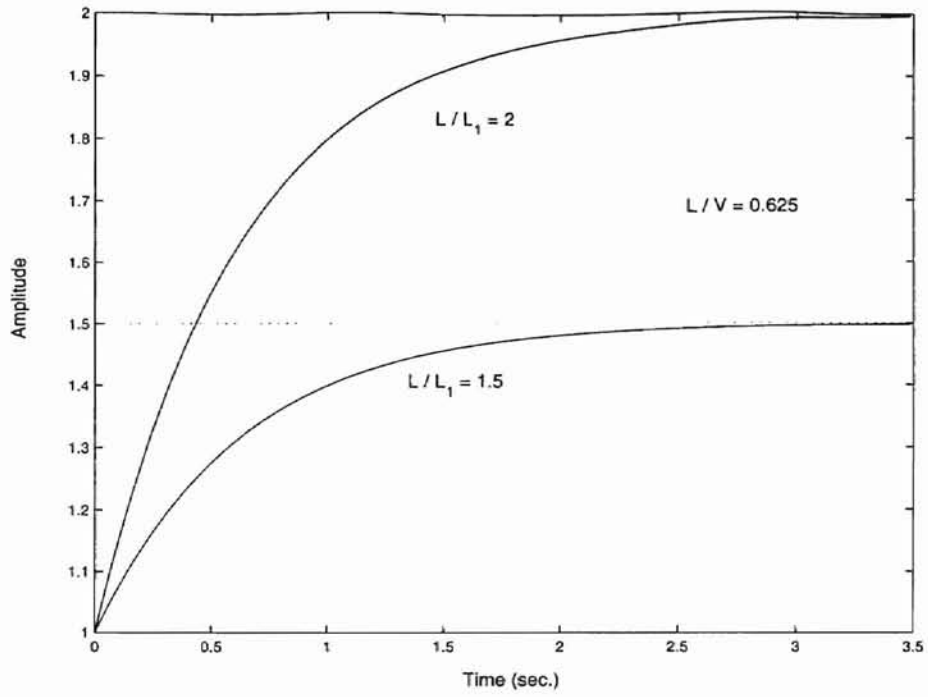

Figure 2.8: First order time response of a steering guide

Equations of dynamic steering

Fig. 2.10 shows a shiftable roller with curved web passing over it. All roller and web angles are assumed to be positive. The lateral velocity of the web is the summation of the velocity of the web relative to the roller and the velocity of the roller relative to the ground. As seen in Fig. 2.10 point A lies on the line of entering contact, hence the subscript is used to identify it as a point on the downstream roller. The above reasoning can be expressed in the form:

$$\frac{dy_L}{dt} = v\left(\theta_r - \left.\frac{\partial y}{\partial t}\right|_L\right) + \frac{dz}{dt} \tag{2.17}$$

where

$\left.\frac{\partial y}{\partial x}\right|_L$ = the slope of the web evaluated at L.

As point B on the web passes the line of entering contact, the lateral velocity of the web relative to the roller is equal to the product of slope of the web relative to the roller at point B and the longitudinal velocity v of the web. As points A and B

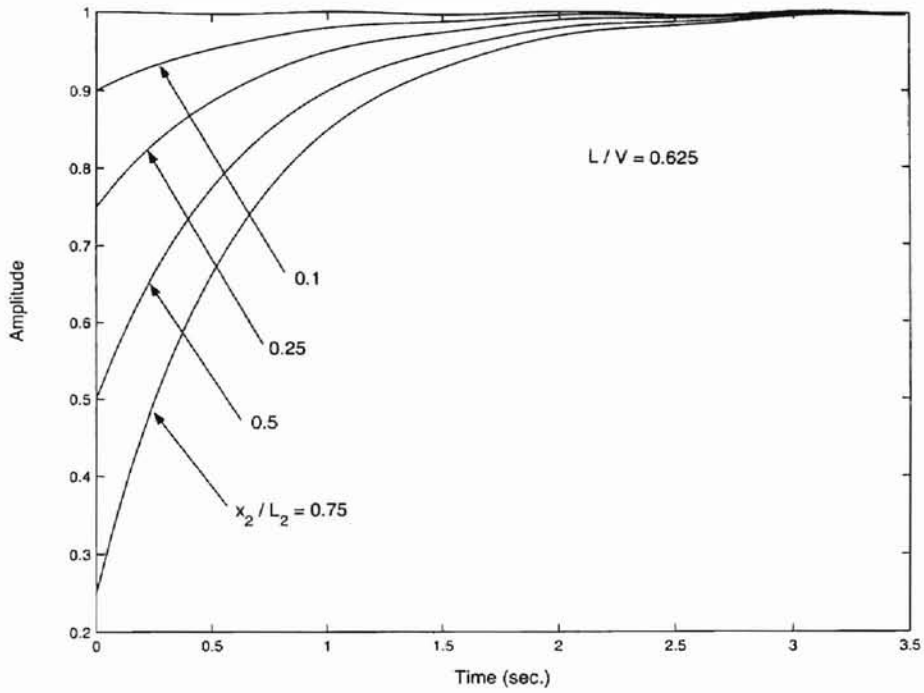

Figure 2.9: First order response at a point between two parallel rollers

enter the line of contact, the lateral velocity of the web relative to the roller in that period is given by:

$$\left.\frac{dy_L}{dt}\right|_A - \left.\frac{dy_L}{dt}\right|_B = v\left(\left.\frac{\partial y}{\partial x}\right|_A - \left.\frac{\partial y}{\partial x}\right|_B\right) \tag{2.18}$$

Dividing the left hand side of equation (2.18) by Δt and the right hand side by $\frac{\Delta x}{v}$, Shelton developed the equation of lateral acceleration to be:

$$\frac{d^2 y_L}{dt^2} = v^2 \left.\frac{\partial^2 y}{\partial x^2}\right|_L + \frac{d^2 z}{dt^2} \tag{2.19}$$

which is the summation of the acceleration due to steering and acceleration due to lateral transport.

Analysis of web mechanics for bending

Fig. 2.11 shows the symbols used for the derivation of relations for pure translation of the end of web. Ignoring deflection due to shear forces and considering the following boundary conditions:

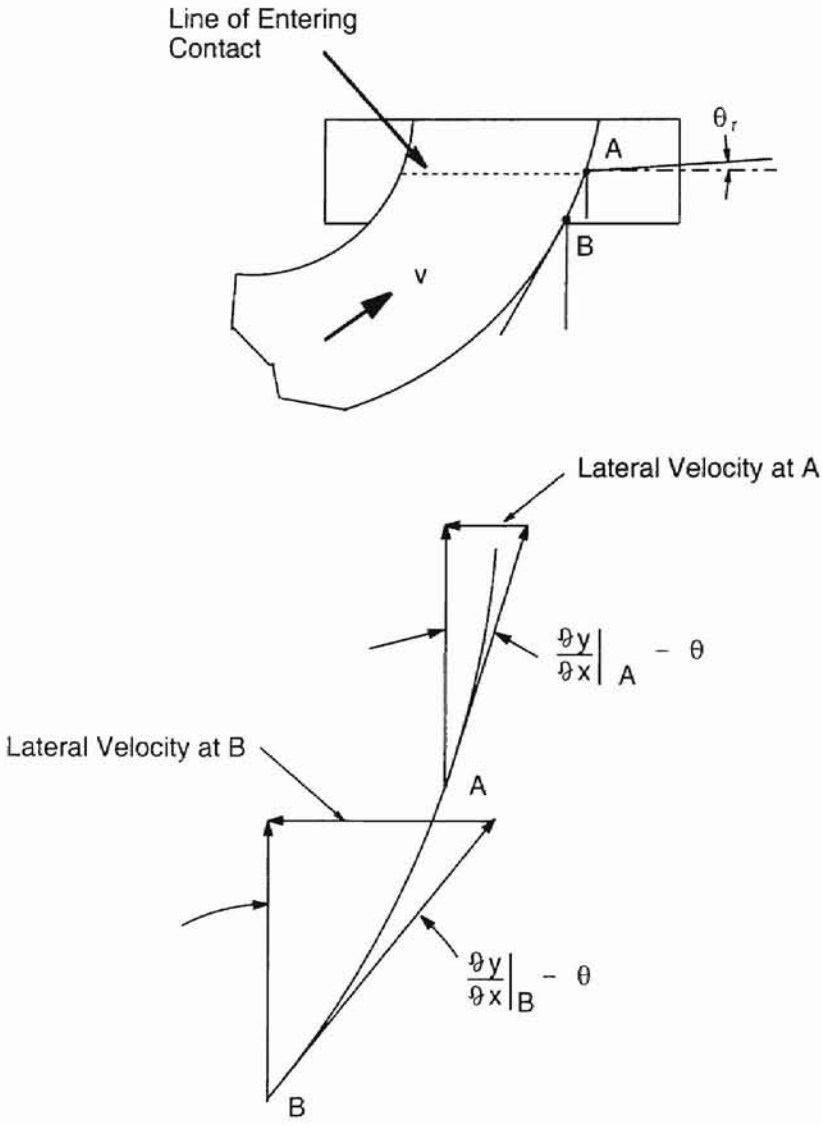

Figure 2.10: Steering action of a web with induced curvature

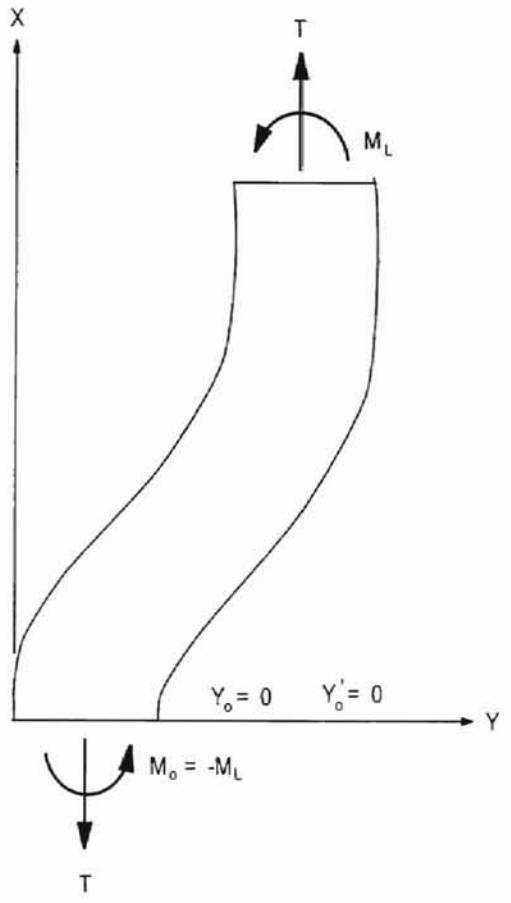

Figure 2.11: Boundary conditions for translation of end of web

1. y_0 is zero

2. $\dot{y}_0$ is zero

3. $M_0 = -M_L$

the coefficients of equation (2.7) are evaluated to be:

$$C_1 = -\frac{y_L(1+\cosh KL)}{KL(1+\cosh KL) - 2\sinh KL} \tag{2.20}$$

$$C_2 = \frac{y_L \sinh KL}{KL(1+\cosh KL) - 2\sinh KL} \tag{2.21}$$

$$C_3 = \frac{y_L K(1+\cosh KL)}{KL(1+\cosh KL) - 2\sinh KL} \tag{2.22}$$

$$C_4 = -\frac{y_L \sinh KL}{KL(1+\cosh KL) - 2\sinh KL} \tag{2.23}$$

The primary parameter of evaluation of equation (2.19) is $\ddot{y}_L$ and M_L. Because $\ddot{y}_L$ is equal to $K^2(C_1 \sinh KL + C_2 \cosh KL)$ and EIK^2 is equal to T, simplification leads to the results:

$$\ddot{y}_L = -K^2 y_L \left(\frac{\sinh KL}{KL(\cosh KL + 1) - 2\sinh KL} \right) \tag{2.24}$$

$$M_L = T y_L \left(\frac{\sinh KL}{KL(\cosh KL + 1) - 2\sinh KL} \right) \tag{2.25}$$

Considering

$$f_1(KL) = \frac{KL^2 \sinh KL}{KL(\cosh KL + 1) - 2\sinh KL} \tag{2.26}$$

so that,

$$\ddot{y}_L = -\frac{y_L}{L^2} f_1(KL) \tag{2.27}$$

$$M_L = \frac{T y_L}{KL^2} f_1(KL) \tag{2.28}$$

A similar derivation is done for pure rotation. Fig. 2.12 shows the boundary conditions. The constants of equation (2.7) are found out to be:

$$C_1 = \frac{\theta_L}{K} \frac{\cosh KL - 1}{KL \sinh KL - 2(\cosh KL - 1)} \tag{2.29}$$

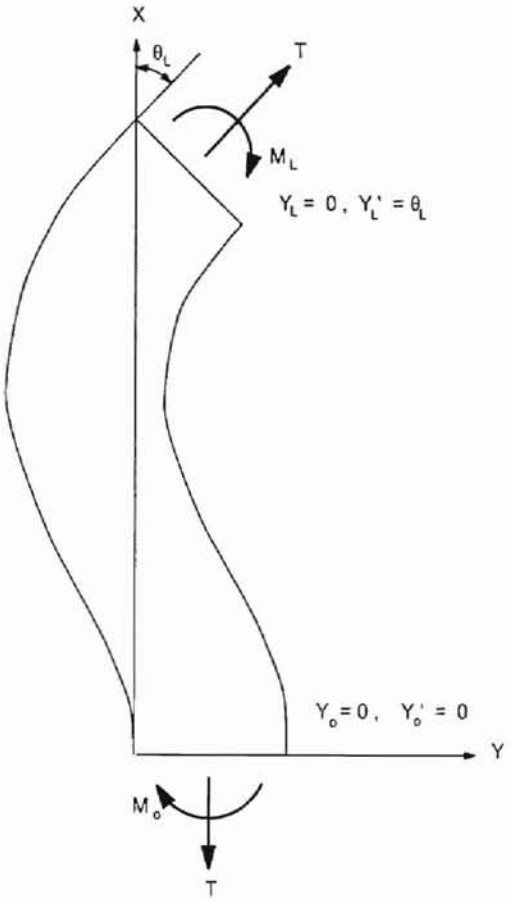

Figure 2.12: Boundary conditions for rotation of the end of web

$$C_2 = \frac{\theta_L}{K} \frac{KL - \sinh KL}{KL \sinh KL - 2(\cosh KL - 1)} \tag{2.30}$$

$$C_3 = -\theta_L \frac{\cosh KL - 1}{KL \sinh KL - 2(\cosh KL - 1)} \tag{2.31}$$

$$C_4 = -\frac{\theta_L}{K} \frac{KL - \sinh KL}{KL \sinh KL - 2(\cosh KL - 1)} \tag{2.32}$$

The equations of interest similar to those for end translation are:

$$\ddot{y}_L = -\frac{\theta_L}{L} f_2(KL) \tag{2.33}$$

$$M_L = \frac{TL\theta_L}{KL^2} f_2(KL) \tag{2.34}$$

where,

$$f_2(KL) = KL\left(\frac{KL\cosh KL - \sinh KL}{KL\sinh KL - 2(\cosh KL - 1)}\right) \tag{2.35}$$

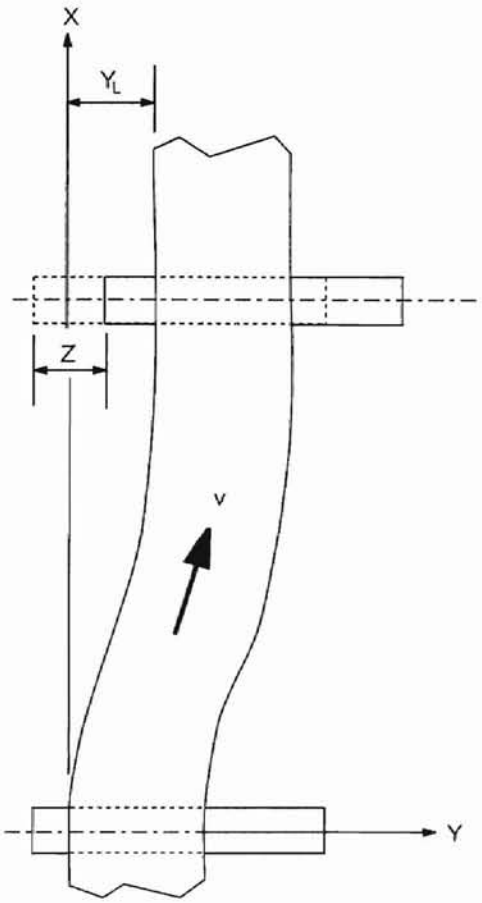

Figure 2.13: Translation

Shelton used the fundamental equations derived here and applied them to the following cases and evaluated their second order transfer functions to be:

1. Response at a fixed roller to input at the previous roller.

$$\frac{Y_L(s)}{Y_0(s)} = \frac{1}{\frac{T_1^2}{f_1(KL)}s^2 + \frac{f_2(KL)}{f_1(KL)}T_1 s^2 + 1} \tag{2.36}$$

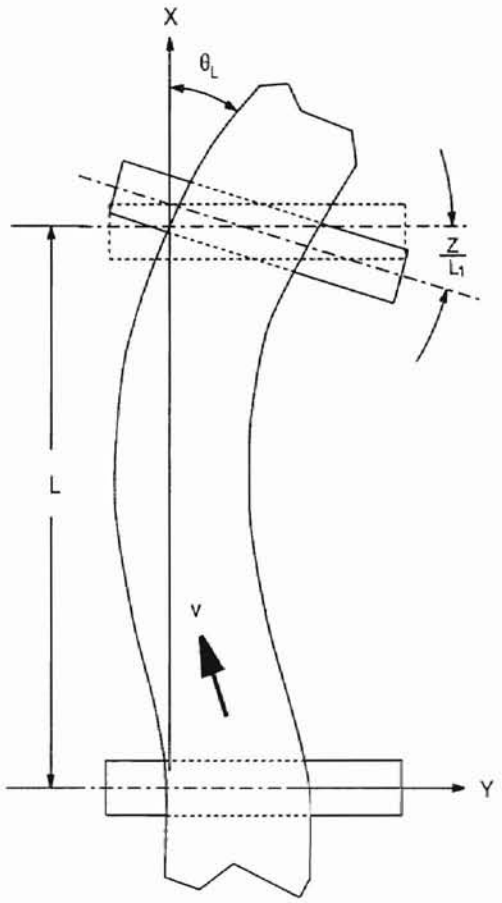

Figure 2.14: Rotation

2. Steering guide response.

   Fig. 2.5 shows the arrangement and nomenclature. Figures 2.13 and 2.14 show the scheme of superposition of translation and rotation of the end.

$$\frac{Y_L(s)}{Z(s)} = \frac{\frac{T_1^2}{f_1(KL)}s^2 + K_C T_1 s + \frac{LK_C}{L_1}}{\frac{T_1^2}{f_1(KL)}s^2 + K_C T_1 s + 1} \tag{2.37}$$

3. Response at a point between two parallel fixed rollers.

   Figures 2.16 and 2.15 show the two components of web shape used in this

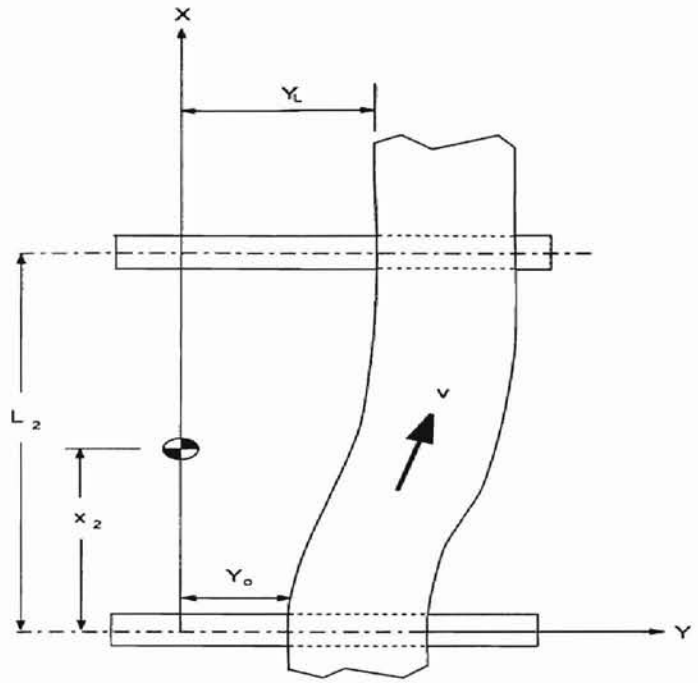

Figure 2.15: Translation : Deflection of a web between two parallel rollers

derivation. The transfer function of the system is given by:

$$\frac{Y_2(s)}{Y_0(s)} = \frac{\frac{T_2^2}{f_1(KL)}(1-f_5)s^2 + T_2(K_C(1-f_5)+f_4)s+1}{\frac{T_2^2}{f_1(KL)}s^2 + T_2K_Cs+1} \tag{2.38}$$

where

$$\begin{aligned} f_4(KL,\frac{x_2}{L}) &= \frac{-1}{KL\sinh KL - 2(\cosh KL-1)}(\cosh KL-1)\frac{\sinh KL(\frac{x_2}{L})}{KL} \\ &\quad -\frac{x_2}{L} - \frac{\sinh KL - KL}{KL}(\cosh KL(\frac{x_2}{L})-1) \end{aligned} \tag{2.39}$$

$$\begin{aligned} f_5(KL,\frac{x_2}{L}) &= [\frac{1}{KL(\cosh KL+1)-2\sinh KL}][(\cosh KL+1)(KL(\frac{x_2}{L}) \\ &\quad -\sinh KL(\frac{x_2}{L})) + \sinh KL(\cosh KL(\frac{x_2}{L})-1)] \end{aligned} \tag{2.40}$$

Fig. 2.17 shows the second order time response of a web at fixed roller to input at previous roller. It can be seen that as the value of KL increases the time required

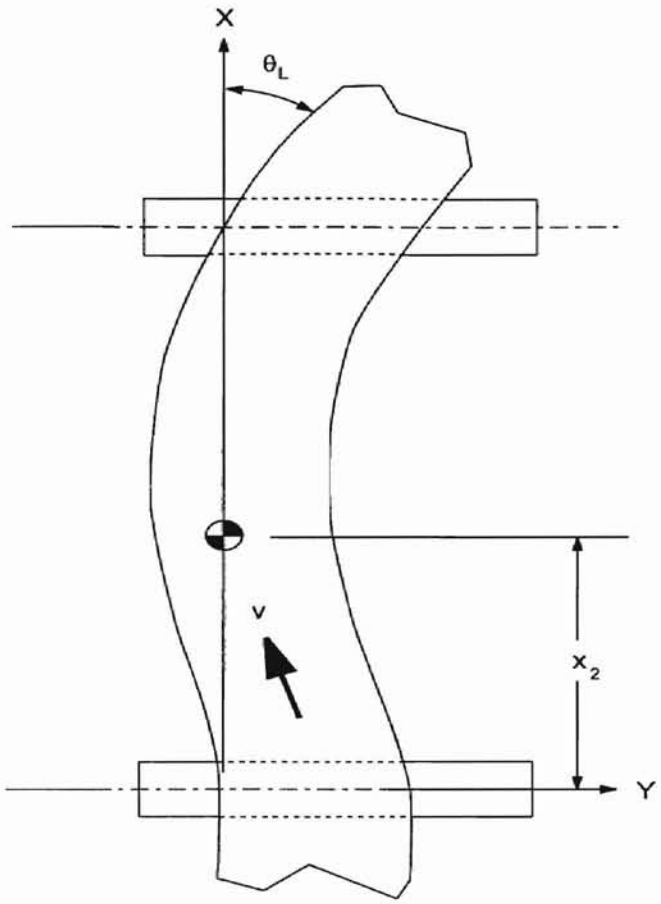

Figure 2.16: Rotation : Deflection of a web between two parallel rollers

to reach steady state value increases. As KL increases the response is similar to the first order response.

Fig. 2.18 shows the second order response of a steering guide. The amplitude of the step response depends on the distance of the instant center from the guide roller. As the distance decreases the response increases. The second order system reaches steady state value faster than the first order system.

Fig. 2.19 shows the second order time response at a point between two parallel rollers. It is seen that the system reaches steady state value faster when the sampling point is near the upstream roller. When compared to the first order system it is seen that the second order system reaches steady state faster at all conditions.

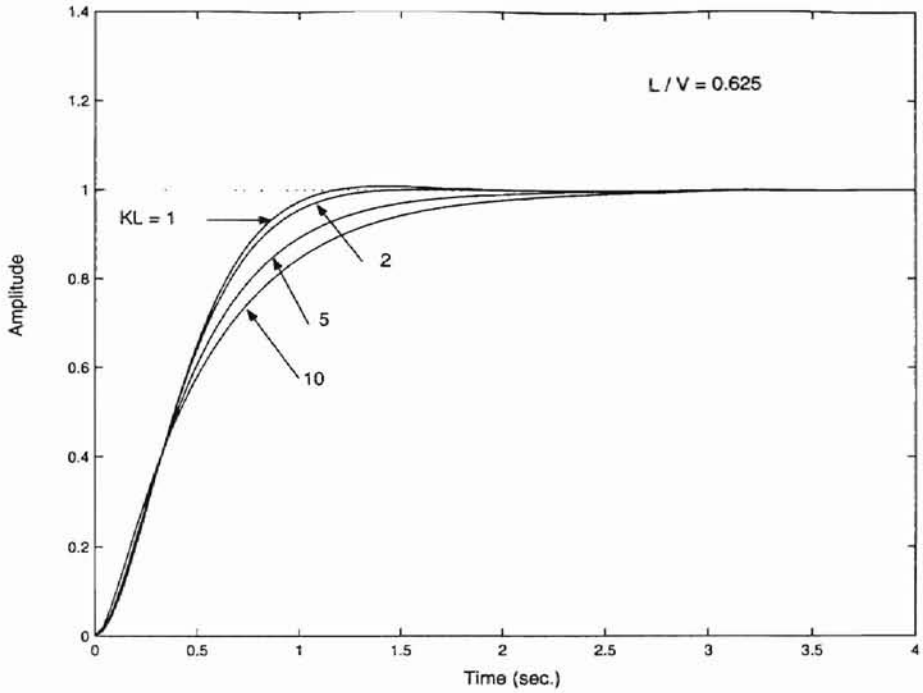

Figure 2.17: Second order time response of a web at fixed roller to input at previous roller

2.3 Lateral control of a web using nip rollers

Lateral control of a web can also be achieved by the use of nip rollers. These rollers are usually rubber covered. A nip is any two rollers in contact as shown in Fig. 2.20.

2.3.1 Concept used in the use of rubber covered rollers

Consider Fig. 2.21. Let A, B and C be three chambers filled with water and let water from chamber A be allowed to flow to chamber C through chamber B. The velocity of flow of water in chamber B increases since the cross-sectional area of flow decreases, that is if the mass flow rate of incompressible fluid is assumed to be constant then the velocity of the fluid must increase as it passes through the constriction, which in this case is chamber B. This same principle could be applied to the nip rollers to deflect the web laterally.

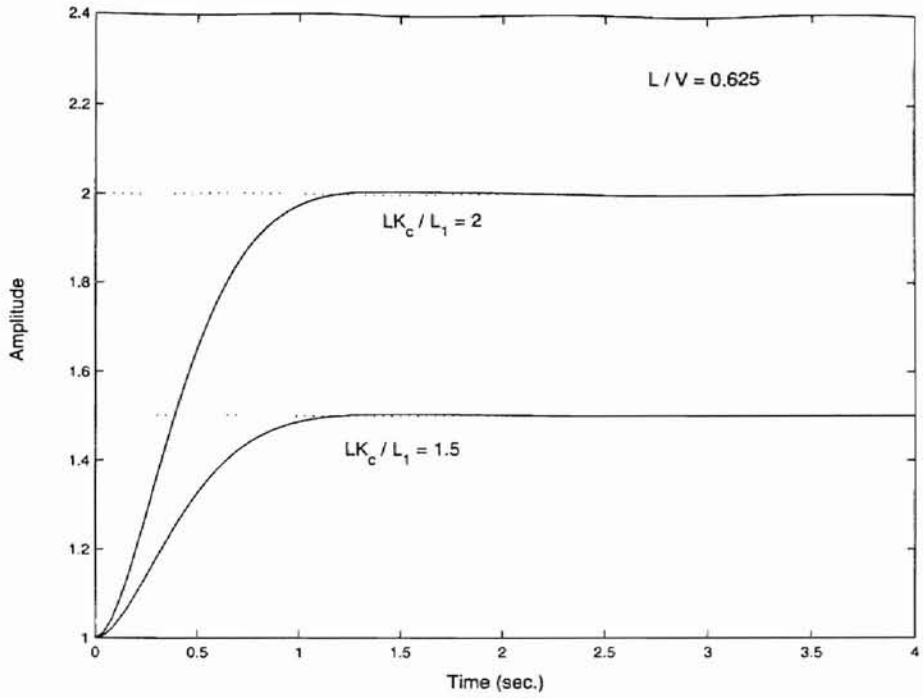

Figure 2.18: Second order time response for a steering guide

Due to the differential loading of the nip rollers there is a differential velocity across the width of the rollers and the web that passes through these rollers also has a differential velocity. This variation in the velocity of the web will also cause a variation in the strain and stress across the width of the web. When integrated, the stress will result in a moment which will be shown to produce the lateral deformation of the web.

2.3.2 Lindley's analysis

Lindley used the relations derived for load compression of rubber blocks at low strain to derive relationships between rubber covered rollers at large deformation. Considering Young's modulus to be independent of the strain in the material, the effective nip load is:

$$\frac{F}{W} = E\sqrt{(tD)}\left(\alpha_R + \frac{kD}{t}\beta_R\right) \tag{2.41}$$

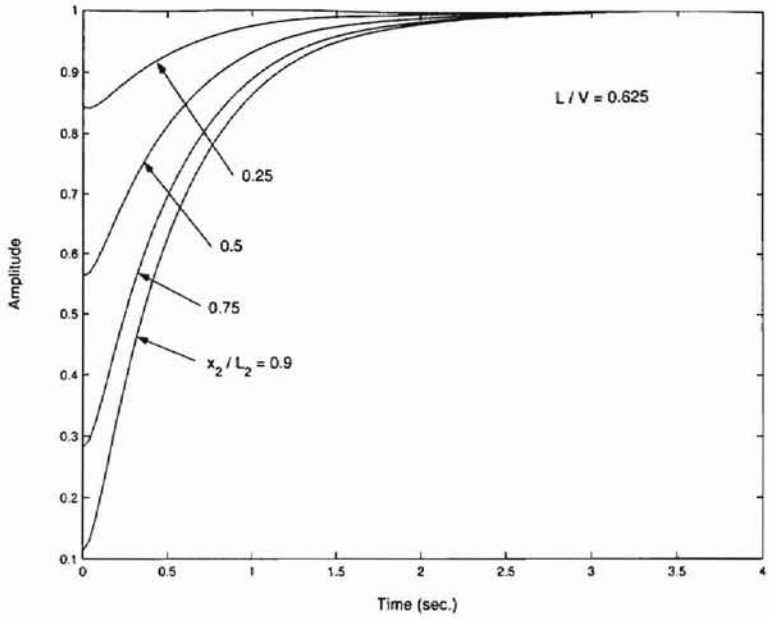

Figure 2.19: Second order time response at a point between two parallel rollers

where

$$\alpha_R = \frac{8}{3} ln \left(\frac{1+\sqrt{u}}{1-\sqrt{u}} \right) - \frac{16}{3}\sqrt{u}$$

$$\beta_R = ln \left(\frac{1+\sqrt{u}}{1-\sqrt{u}} \right) - \frac{10\sqrt{u}}{3(1-u)} + \frac{4\sqrt{u}}{3(1-u)^2}$$

$$u = \frac{\delta}{t}$$

$$E_c = \frac{4}{3} E(1 + kS^2) \tag{2.42}$$

$$S = \frac{\sqrt{D\delta}}{(1-\delta)}$$

The factor, k, is determined empirically from equation (2.42)

2.3.3 Foreman's analysis

In 1964, Foreman performed experiments to show the relationship between rubber compression and velocity of the strip passing through the pinch rolls. Foreman used

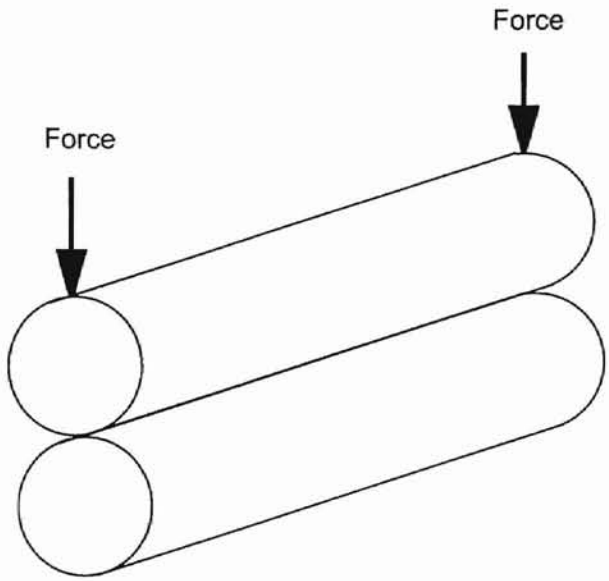

Figure 2.20: Illustration of a nip

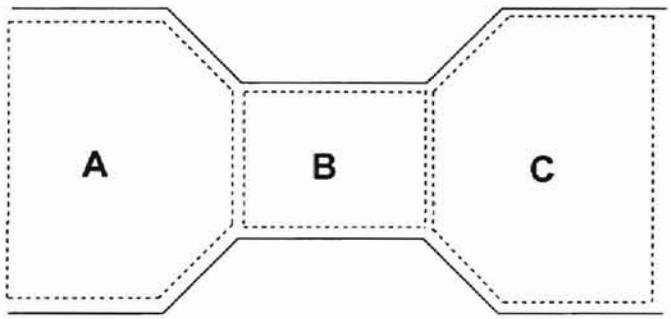

Figure 2.21: Concept for rubber covered rollers

two sets of rubber covered rollers, one of which was 11 inches in diameter with a $\frac{3}{4}$ inch rubber covering. The second roller was 30 inches in diameter with 1 inch rubber covering. The hardness of the rubber ranged from 60 to 70 durometer. The strip was passed between these two rollers and the upper roller was loaded. The lower roller was rotated using a hand lever by one revolution. After this, the length of movement of the strip was measured. The length of movement of the strip without any load was calculated using the diameter of the roller. A difference was found between these two values. It was found that with increase in load, the length of movement of the strip increased. Increases upto 2 percent were found. Foreman also showed relationships

between compression of rubber and the movement of the strip for different durometer and rubber thickness. Fig. 2.22 shows the setup for Foreman's experiments.

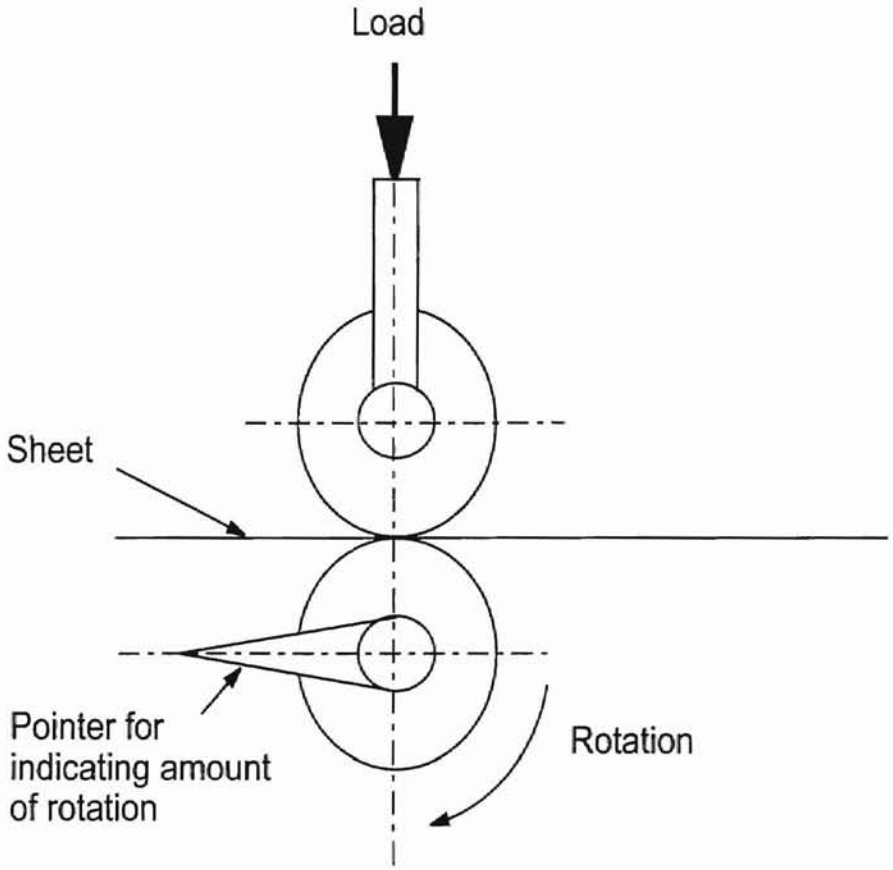

Figure 2.22: Foreman's experimental setup

2.3.4 Shelton's analysis

In one of his reports to Fife Corporation, Shelton gave an outline on web steering due to a differentially loaded nip across the width of the web. Shelton presented a relationship for calculating the effective nip load due to radial deformation of the rubber.

The following assumptions were made by him:

1. The covering material behavior is similar to that of natural rubber and when in the form of a roll covering it is relatively incompressible.

2. Rubber covered rolls are identical in size and durometer (durometer is the measure of hardness of rubber).

3. Small deflections of the rubber covered rolls occur when they are loaded.

4. The entering span prior to the nip guide is very long. So shear deformation can be neglected.

Shelton [13] points out that, for the proper application of the differentially loaded nip guide the entering web span needs to be long. Hence he analyzed the longitudinal stiffness of a free catenary (see Fig. 2.23) and a supported catenary (see Fig. 2.24. Fig. 2.25 shows an equivalent free catenary of the supported catenary.) which are necessary for the proper application of the differentially loaded nip guide.

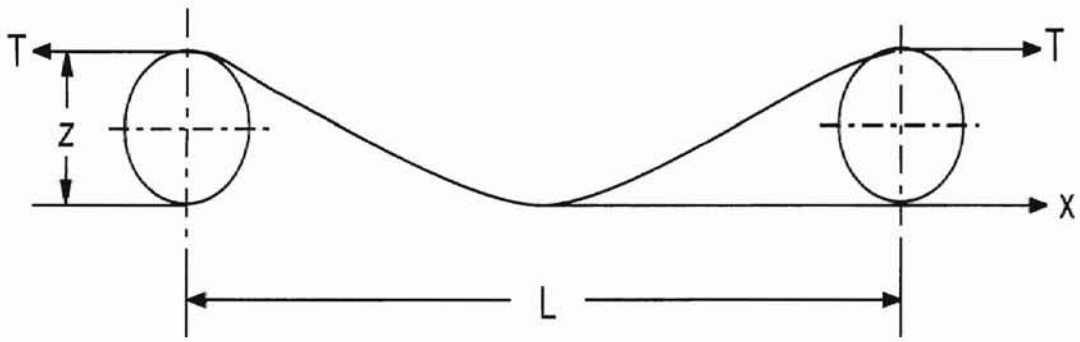

Figure 2.23: A free catenary

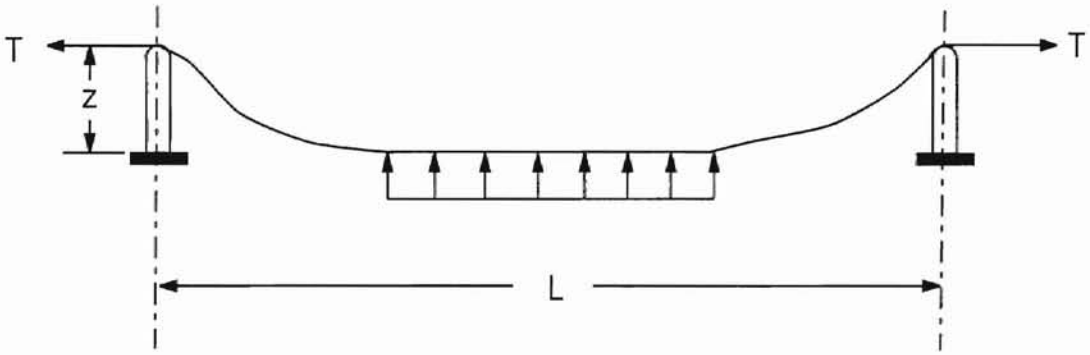

Figure 2.24: A supported catenary

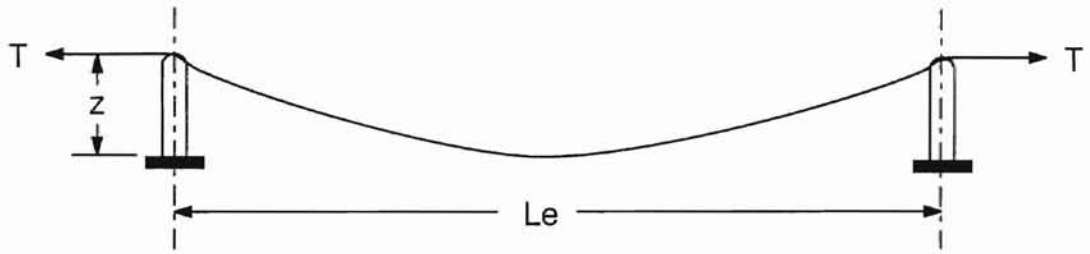

Figure 2.25: Equivalent free catenary of the supported catenary

Fig. 2.26 shows a portion of a roller and the symbols used by Shelton to find out the expression for effective nip load.

The effective nip load formulated by Shelton was :

$$\frac{F}{W} = t\left(41.3e^{0.048A}\left(\frac{2R_o}{t}\right)^{0.5}\left(\frac{\delta_f}{t}\right)^{1.5} + \frac{105.4e^{0.048A}}{(2.5-0.002A)}\left(\frac{2R_o}{t}\right)^{(1.5-0.002A)}\left(\frac{\delta_f}{t}\right)^{(2.5-0.002A)}\right) \tag{2.43}$$

Shelton's frequency response plots and the time response plots shown indicate that the second order system gives a more appropriate results. Lateral control of a web using nip rollers has been studied and further research in that area will come in the future.

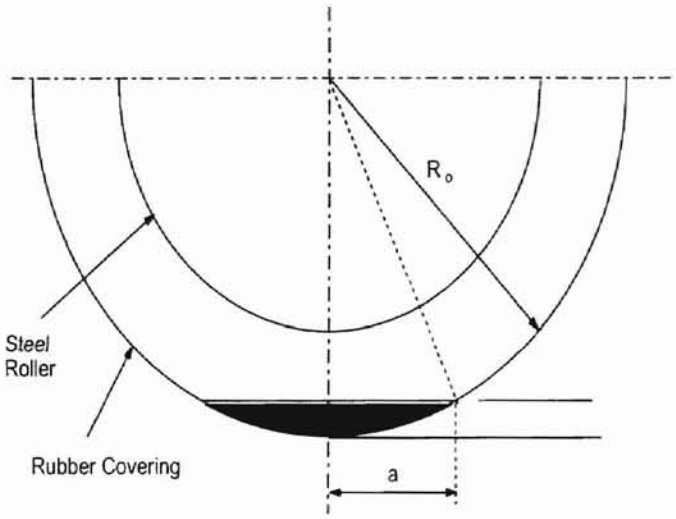

Figure 2.26: Schematic diagram of roller

Chapter 3

Automatic Guiding Mechanisms and Control Systems

This chapter describes the basic types of guiding mechanisms and automatic control systems used in the web handling industry for the lateral control of web. Hopcus [4] has briefly discussed different types of control systems used for the lateral control of a web.

3.1 Basic types of automatic control systems

There are four types of automatic guiding control systems: Pneumohydraulic, Electrohydraulic, Pneumomechanical and Electromechanical systems. All systems are closed-loop proportional control systems.

3.1.1 Hydraulic types

The two hydraulic types function in a similar manner. A sensor monitors the lateral position of the web. The sensor signal is transmitted either directly to the power unit servo valve (Pneumohydraulic systems) or to a signal processor which then sends a signal to the power unit servo valve (Electrohydraulic systems). Hydraulic output from the power unit through the servo valve, proportional to the lateral error of

the web, positions the guide structure, which moves the web to the correct lateral position. These systems are attractive for extremely heavy loads and harsh environments. Figures 3.1 and 3.2 show a block diagram of the pneumohydraulic and the electrohydraulic types of automatic guiding systems, respectively.

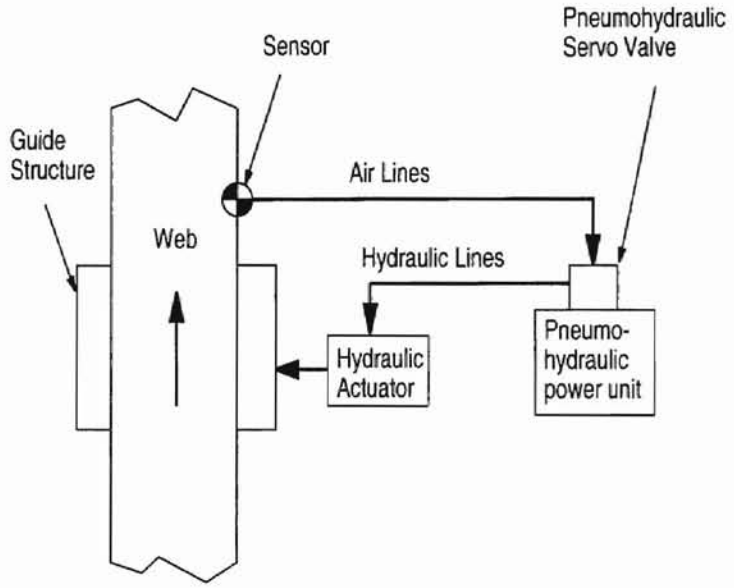

Figure 3.1: Pneumohydraulic guiding control system

3.1.2 Mechanical types

The two mechanical types of control systems also function in a similar manner. A sensor, either electronic for electromechanical systems or pneumatic for pneumomechanical systems, monitors the lateral position of the web. The sensor signal is either transmitted directly to the processor (electromechanical system) or is first converted from an air pressure signal to an electrical signal with a transducer (pneumomechanical system). The processor then sends a signal, proportional to the amount of error detected by the sensor, to the DC drive motor on the electromechanical actuator. The actuator positions the guide structure which moves the web to the correct lateral

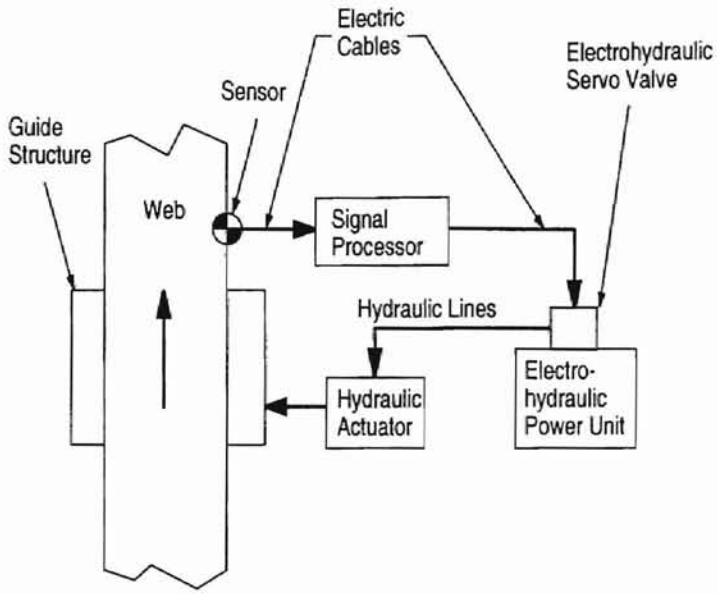

Figure 3.2: Electrohydraulic guiding control system

position in the sensor. These systems are especially attractive for applications demanding a high frequency response and where hydraulics are not desirable. Figures 3.3 and 3.4 show a block diagram of the pneumomechanical and electromechanical types of guiding control systems, respectively.

3.2 Guiding mechanisms

The basic guiding applications can be listed as: End pivoted guide, Center pivoted guide, Remotely pivoted guide and Offset pivot guide. A brief description of each guide is given in the following.

3.2.1 End pivoted guide

Fig. 3.5 shows a schematic diagram of an end pivoted guide. When the guide is stationary, it does not affect the web position. As the guide is steered about its pivoted end the web is displaced to the desired position since the web always travels perpendicular to the roller.

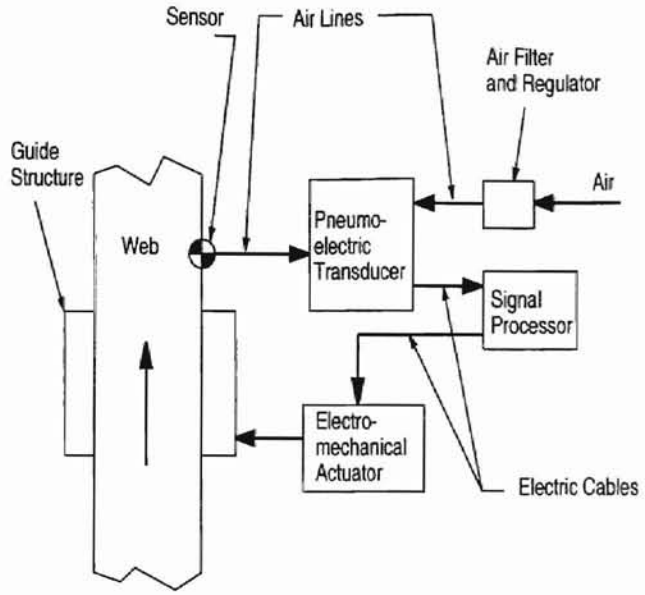

Figure 3.3: Pneumomechanical guiding control system

3.2.2 Center pivoted guide

Fig. 3.6 shows a schematic diagram of the center pivoted guide. This guide is very similar to the end pivoted guide except that the pivoted point is at the center of the roller.

The transfer function for the end pivoted and center pivoted guides for figures 3.5 and 3.6 respectively is given by equation (3.1)

$$Y_L(s) = \left(\frac{\frac{f_3(KL)}{\tau^2}}{s^2 + \frac{f_2(KL)}{\tau}s + \frac{f_1(KL)}{\tau^2}} \right) \theta_0(s) + \left(\frac{-\frac{f_3(KL)}{\tau}s + \frac{f_1(KL)}{\tau^2}}{s^2 + \frac{f_2(KL)}{\tau}s + \frac{f_1(KL)}{\tau^2}} \right) Y_0(s) + \left(\frac{\frac{f_2(KL)}{\tau^2 c}}{s^2 + \frac{f_2(KL)}{\tau}s + \frac{f_1(KL)}{\tau^2}} \right) U(s) \quad (3.1)$$

3.2.3 Remotely pivoted guide

Fig. 3.7 shows a schematic diagram of the remotely pivoted guide. These are steering type guides in that the roller is moved laterally and angularly to accomplish lateral

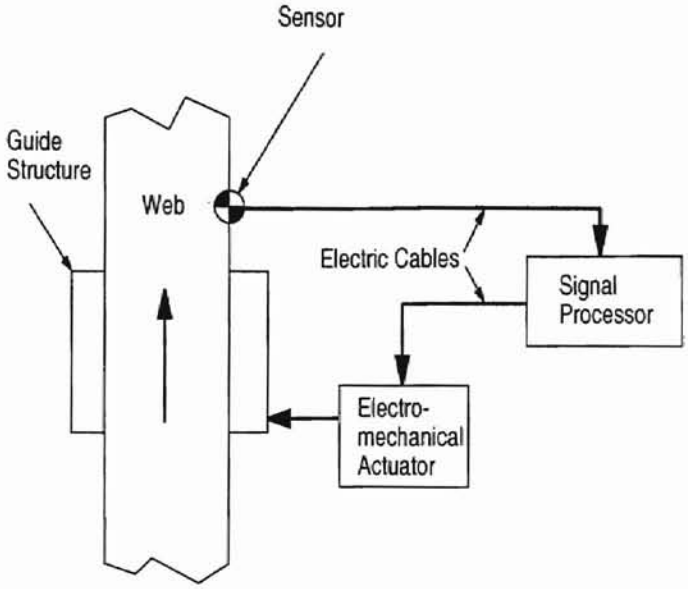

Figure 3.4: Electromechanical guiding control system

web correction. This action steers the web laterally in the entering span. The point about which the guide assembly rotates in reaching the angular position required for a given correction is called the 'center of rotation'.

For a remotely pivoted steering guide shown in Fig. 3.7, the transfer function is

$$Y_L(s) = \left(\frac{\frac{f_3(KL)}{\tau^2}}{s^2 + \frac{f_2(KL)}{\tau}s + \frac{f_1(KL)}{\tau^2}} \right) \theta_0(s) + \left(\frac{-\frac{f_3(KL)}{\tau}s + \frac{f_1(KL)}{\tau^2}}{s^2 + \frac{f_2(KL)}{\tau}s + \frac{f_1(KL)}{\tau^2}} \right) Y_0(s) + \left(\frac{s^2 + \frac{f_2(KL)}{\tau}s + \frac{f_2(KL)}{\tau^2 x_1}}{s^2 + \frac{f_2(KL)}{\tau}s + \frac{f_1(KL)}{\tau^2}} \right) Z(s) \tag{3.2}$$

$$Y_L(s) = G_1(s)Z(s) + G_2(s)\theta_0(s) + G_3(s)Y_0(s)$$

3.2.4 Offset pivot guide

Fig. 3.8 shows a schematic diagram of the offset pivoted guide. These are displacement-type guides which provide web position co[illegible]ion with minimum entry and exit span

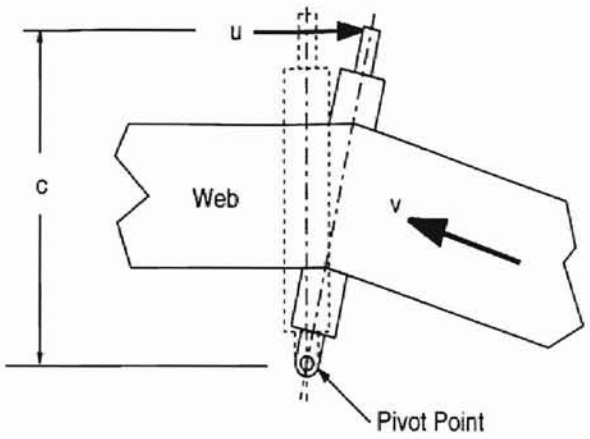

Figure 3.5: End pivoted guide

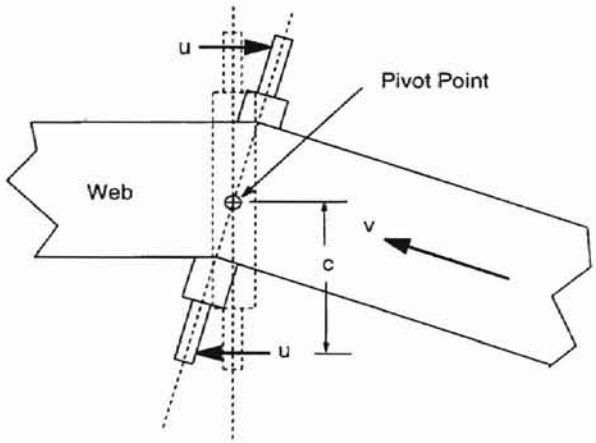

Figure 3.6: Center pivoted guide

requirements. When the guide is centered, it does not affect the web position. As the guide moves to a position other than the center, the web is displaced to the desired position as it moves across the guide span.

For a displacement guide shown in Fig. 3.8, the transfer function is

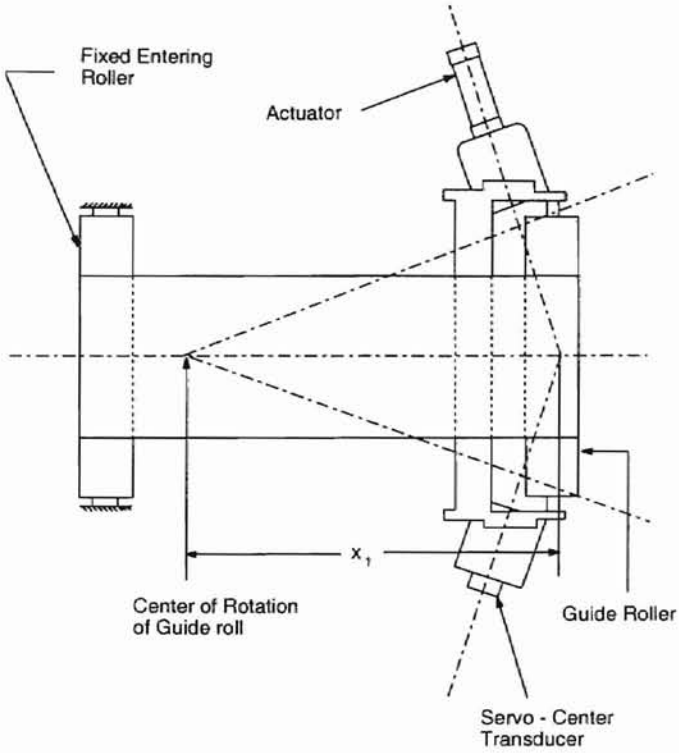

Figure 3.7: Remotely pivoted guide

$$
\begin{aligned}
Y_L(s) \;=\; & \left(\frac{\dfrac{f_1(KL_3)}{\tau_3^2}\dfrac{f_1(KL)}{\tau^2}}{[s^2 + \dfrac{f_2(KL_3)}{\tau_3}s + \dfrac{f_1(KL_3)}{\tau_3^2}][s^2 + \dfrac{f_2(KL)}{\tau}s + \dfrac{f_1(KL)}{\tau^2}]} \right) Y_0(s) \\
& + \left(\frac{\dfrac{f_1(KL)}{\tau^2}[s^2 + \dfrac{f_2(KL_3)}{\tau_3}s]\dfrac{L_1 - L}{L_1}}{[s^2 + \dfrac{f_2(KL_3)}{\tau_3}s + \dfrac{f_1(KL_3)}{\tau_3^2}][s^2 + \dfrac{f_2(KL)}{\tau}s + \dfrac{f_1(KL)}{\tau^2}]} \right. \\
& \left. + \frac{s^2 + \dfrac{f_2(KL)}{\tau}s + \dfrac{f_2(KL)}{\tau^2}\dfrac{L}{L_1}}{[s^2 + \dfrac{f_2(KL)}{\tau}s + \dfrac{f_1(KL)}{\tau^2}]} \right) Z(s), \qquad (3.3)
\end{aligned}
$$

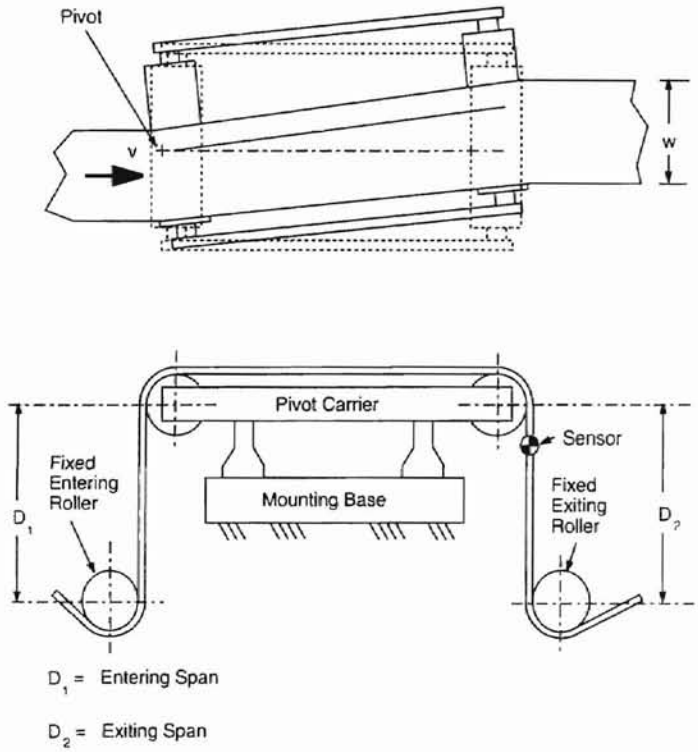

Figure 3.8: Offset pivoted guide

Chapter 4

Observer Design and Simulation Results

This chapter justifies the need for an observer based controller and explains the procedure followed for the design.

4.1 Present controller

The present controller on the experimental platform which is the A9 signal processor (courtesy : Fife Corporation, Oklahoma City) uses position feedback signal from the edge sensor and motor velocity feedback signal from the tachometer. A block diagram of the present controller is shown in Fig 4.1.

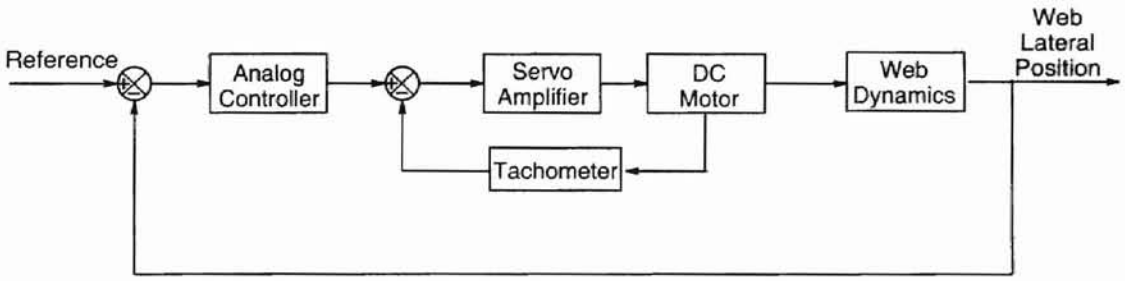

Figure 4.1: Block diagram of controller using tachometer

4.2 The importance of inner-loop velocity feedback

To investigate the importance of the velocity inner-loop, a digital lateral controller without the velocity inner-loop is implemented for the following three conditions, i.e. no disturbance, step disturbance and pulse disturbance. By tuning the control gains for computer control, similar performance as that of Fife A9 controller is obtained. Figures 4.2 and 4.3 show the experimental results of computer control. The following observation can be made from the experimental results.

1. When there is no disturbance then the results with and without inner-loop velocity feedback are similar. But when there is step and pulse disturbances, the performance of the control system deteriorates. Therefore, inner-loop velocity feedback is essential in maintaining stability of the guide system in the presence of any lateral disturbances.

2. As shown in Figures 4.2 and 4.3, when the step disturbance is not that large, it is still possible to push the web edge to the reference position. However, the overshoot becomes very large, and the oscillations last longer. During this oscillation period the motor may saturate.

3. If the disturbance magnitude is large, then the system can go unstable. From the third row plot in Figures 4.2 and 4.3 the oscillation does not subside.

Thus, inner-loop velocity feedback is critical to stable closed-loop system performance in presence of disturbances.

The cost of a motor increases because of the presence of the inner-loop velocity feedback. Therefore a need arises to circumvent the use of tachometer signals for inner-loop feedback with a motor velocity estimator.

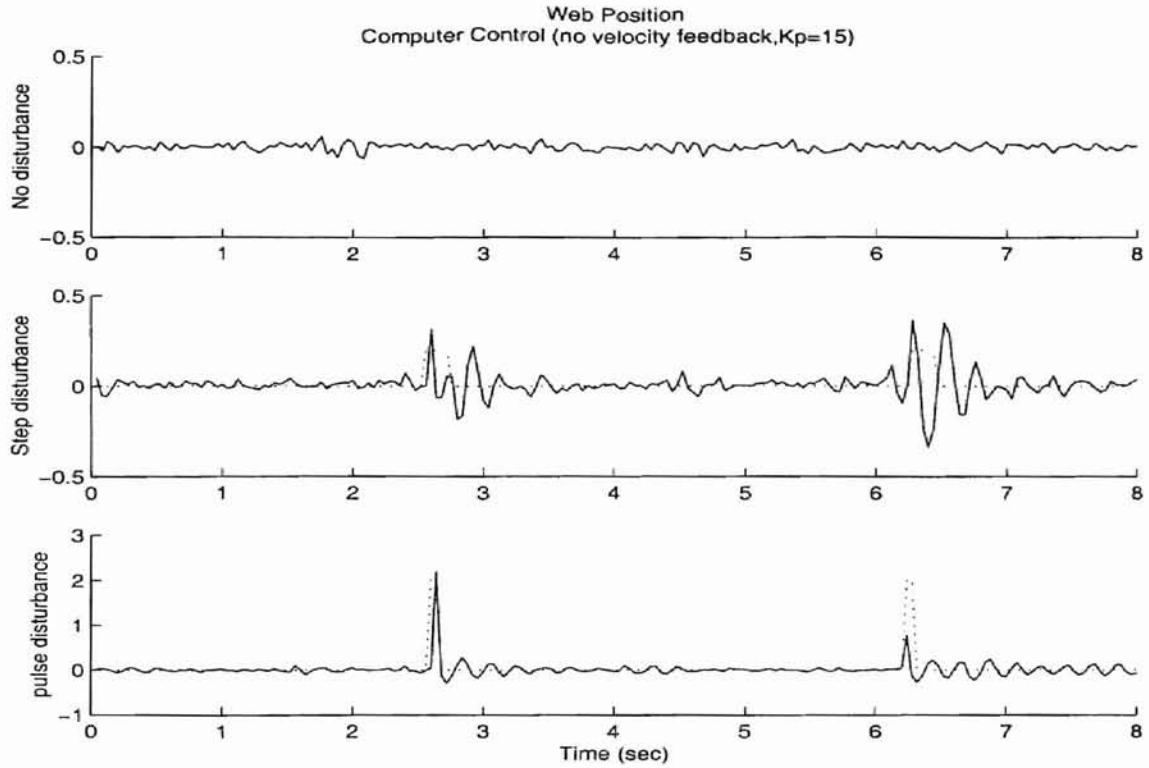

Figure 4.2: Web position: computer control without velocity feedback

4.3 Observer design

The analog controller (A9 signal processor) used by Fife for the lateral control of a web uses velocity feedback from the tachometer of the motor as stated earlier. Research was undertaken to replace the tachometer feedback signal since it would greatly reduce the cost of the motor and the lateral guide on the whole.

Considering the angular and lateral disturbance to be zero, equation (3.2) can be rewritten as

$$Y_L(s) = \left(\frac{s^2 + \frac{f_2(KL)}{\tau} s + \frac{f_2(KL)}{\tau^2 x_1}}{s^2 + \frac{f_2(KL)}{\tau} s + \frac{f_1(KL)}{\tau^2}} \right) Z(s) \tag{4.1}$$

Equation (4.1) shows that at steady state the lateral position of web and the guide which means the position of the motor are proportionally related. Since the system is observable the velocity of the web can be estimated using a minimum order observer

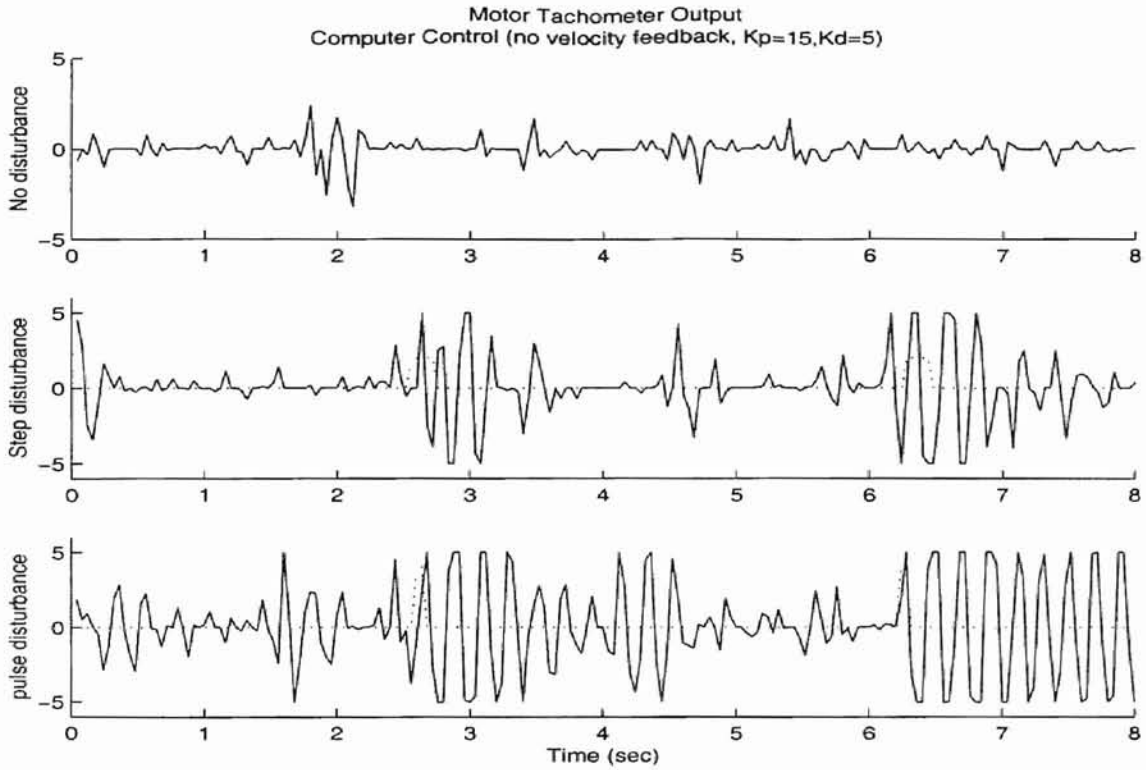

Figure 4.3: Motor velocity: computer control without velocity feedback

design. The velocity of the motor can then be estimated using the relation between the motor position and web position.

Fig. 4.4 shows the analog controller used by Fife. Fig. 4.5 shows the block diagram of the system used to replace the inner-loop velocity feedback. Note that the analog controller used by Fife has been replaced with a digital controller. The web dynamics is given by equation (4.1).

4.3.1 Developing the state space form

From Fig. 4.5 the open-loop actuator dynamics can be written as:

$$\frac{Z(s)}{U_m(s)} = \frac{k_m}{s^2 + a_m s} \tag{4.2}$$

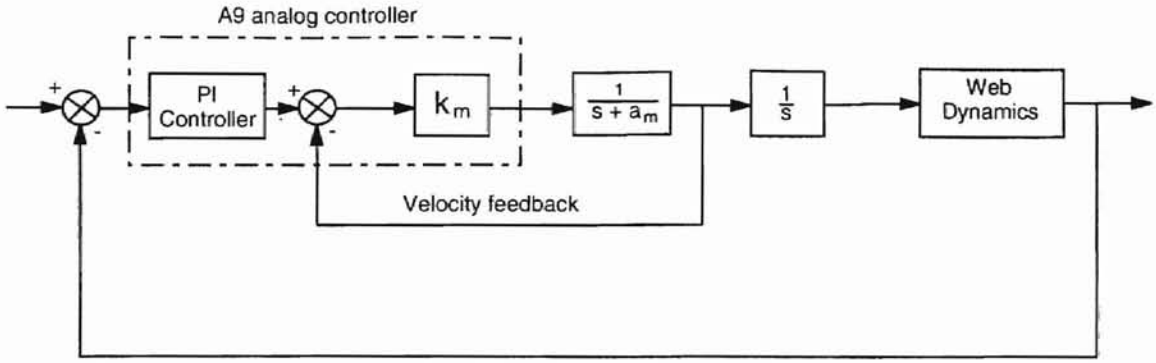

Figure 4.4: Block diagram of controller using tachometer

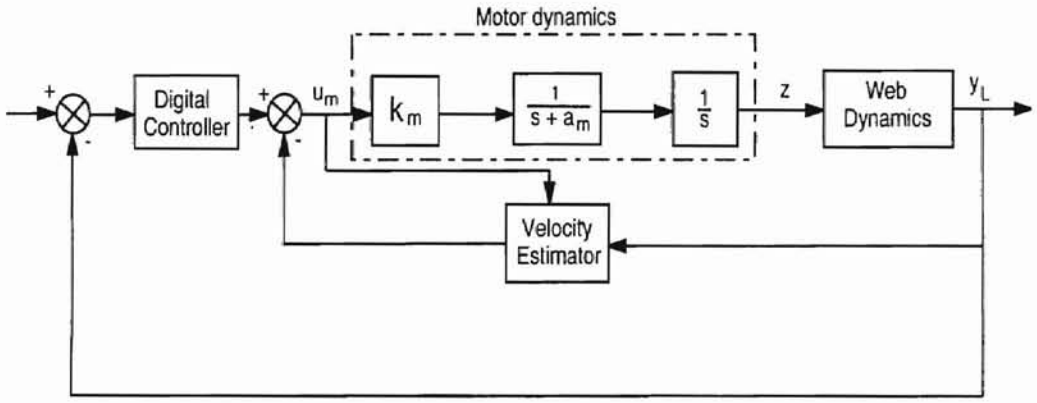

Figure 4.5: Block diagram of controller using velocity estimator

If an inverse laplace transform is applied to equation (4.2) then the following differential equation results.

$$\ddot{z} + a_m \dot{z} = k_m u_m \tag{4.3}$$

For simplicity equation (4.1) is written in the form:

$$\frac{Y_L(s)}{Z(s)} = \frac{s^2 + \alpha_2 s + \beta}{s^2 + \alpha_2 s + \alpha_1} \tag{4.4}$$

where

$\alpha_1 = \frac{f_(KL)}{\tau^2}$

$$\alpha_2 = \frac{f_2(KL)}{\tau}$$

$$\beta = \frac{f_2(KL)}{\tau^2 x_1}$$

Taking an inverse laplace transform of equation (4.4) yields the following differential equation.

$$\ddot{y}_L(t) + \alpha_2 \dot{y}_L(t) + \alpha_1 y_L(t) = \ddot{z}(t) + \alpha_2 \dot{z}(t) + \beta z(t) \tag{4.5}$$

Consider x_1 and x_2 to be the state variables of equation (4.3) and, x_3 and x_4 to be the state variables of equation (4.5). Let us assume $x_1 = z$ and $x_2 = \dot{z}$, which give the following relations:

$$\dot{x}_1(t) = x_2(t) \tag{4.6}$$

$$\dot{x}_2(t) = -a_m x_2(t) + k_m u_m(t) \tag{4.7}$$

Let us assume $x_3 = y_L$ and $x_4 = \dot{y}_L$, and equation (4.5) and broken into two state equations and written as:

$$\dot{x}_3(t) = x_4(t) \tag{4.8}$$

$$\dot{x}_4(t) = \ddot{z}(t) + \alpha_2 \dot{z}(t) + \beta x_1(t) - \alpha_1 x_3(t) - \alpha_2 x_4(t) \tag{4.9}$$

Since z, the position of the motor is expected to be a constant $\ddot{z}$ and $\dot{z}$ are zero. Therefore equation (4.9) can be rewritten to include the above condition.

$$\dot{x}_4(t) = \beta x_1(t) - \alpha_1 x_3(t) - \alpha_2 x_4(t) \tag{4.10}$$

Putting equations (4.6), (4.7), (4.8) and (4.10) in matrix form yields the following state space model of the system.

$$\begin{pmatrix} \dot{x}_1(t) \\ \dot{x}_2(t) \\ \dot{x}_3(t) \\ \dot{x}_4(t) \end{pmatrix} = \begin{pmatrix} 0 & 1 & 0 & 0 \\ 0 & -a_m & 0 & 0 \\ 0 & 0 & 0 & 1 \\ \beta & 0 & -\alpha_1 & -\alpha_2 \end{pmatrix} \begin{pmatrix} x_1(t) \\ x_2(t) \\ x_3(t) \\ x_4(t) \end{pmatrix} + \begin{pmatrix} 0 \\ k_m \\ 0 \\ 0 \end{pmatrix} u_m \tag{4.11}$$

Note that x_1, x_2, x_3 and x_4 are state variables which denote the position of the motor, velocity of motor, position of web and velocity of web respectively. Since x_3 is the only state variable that can be measured the output equation is given by:

$$y(t) = \begin{pmatrix} 0 & 0 & 1 & 0 \end{pmatrix} \begin{pmatrix} x_1(t) \\ x_2(t) \\ x_3(t) \\ x_4(t) \end{pmatrix} + \begin{pmatrix} 0 \end{pmatrix} + u(t) \tag{4.12}$$

4.4 State Observers

In a practical system, not all state variables can be measured. Hence, it is necessary to estimate the state variables that are not directly measurable. Such estimation is commonly called observation. Estimation of the unmeasurable state variables can be done using the output and control variables. State observers can be designed if and only if the observability condition is satisfied.

Full order state estimation means that we observe (estimate) all n state variables regardless of whether some state variables are available for direct measurement. Here we design a minimum order observer to estimate the velocity of the motor. From Fig. 4.5, the state observer will have y_L and u_m as inputs and x_2 as output. For the system under consideration the state and output equations are given by equations (4.11) and (4.12) respectively. Suppose the state vector x is a n-vector and the y vector is a m-vector. Hence we need to estimate only $(n - m)$ variables. The reduced-order observer becomes an $(n - m)$th-order observer.

The minimum-order observer can be designed by first partitioning the state vector into two parts, as shown

$$x = \begin{pmatrix} x_a(t) \\ x_b(t) \end{pmatrix} \tag{4.13}$$

where $x_a(t)$ is that portion of the state vector that can be directly measured and

$x_b(t)$ is the unmeasureable portion. The partitioned state and output equations of the system can then be written as follows

$$\begin{pmatrix} \dot{x}_a(t) \\ \dot{x}_b(t) \end{pmatrix} = \begin{pmatrix} A_{aa} & A_{ab} \\ A_{ba} & A_{bb} \end{pmatrix} \begin{pmatrix} x_a(t) \\ x_b(t) \end{pmatrix} + \begin{pmatrix} B_a \\ B_b \end{pmatrix} u(t) \tag{4.14}$$

$$y = \begin{pmatrix} I & 0 \end{pmatrix} \begin{pmatrix} x_a(t) \\ x_b(t) \end{pmatrix} \tag{4.15}$$

Rewriting the above equations, the measured portion of the state equation becomes

$$\dot{x}_a(t) = A_{aa}x_a(t) + A_{ab}x_b(t) + B_a u(t)$$

or,

$$\dot{x}_a(t) - A_{aa}x_a(t) - B_a u(t) = A_{ab}x_b(t) \tag{4.16}$$

Equation (4.16) has all measurable quantities on the left hand side and unmeasurable quantities on the right hand side. Equation (4.16) is also the output equation for minimum order observer design. The unmeasured portion of the state, which is also the state equation for minimum order observer design is as follows

$$\dot{x}_b(t) = A_{ba}x_a(t) + A_{bb}x_b(t) + B_b u(t) \tag{4.17}$$

Let us assume that the state $x_b(t)$, to be approximated by the state $\hat{x}_b(t)$ is of the dynamic model

$$\dot{\hat{x}}_b(t) = A_{ba}\hat{x}_b(t) + B_b u(t) + K_e(y(t) - C\hat{x}_b(t)) \tag{4.18}$$

where

$C\hat{x}_b$ is the approximated output.

K_e is a weighing matrix.

Substituting equation (4.16) as the output equation in equation (4.18) and $C = A_{ab}$, we get the following equation

$$\dot{\hat{x}}_b(t) = (A_{bb} - K_e A_{ab})\hat{x}_b(t) + K_e\dot{y}(t) + (A_{ba} - K_e A_{aa})y(t) + (B_b - K_e B_a)u(t) \tag{4.19}$$

Let us define the observer error dynamics

$$e(t) = x_b(t) - \hat{x}_b(t) \tag{4.20}$$

$$\dot{e}(t) = \dot{x}_b(t) - \dot{\hat{x}}_b(t) \tag{4.21}$$

Expanding equation (4.21) using equations (4.17), (4.19) and (4.20) we get the following equation

$$\dot{e}(t) = (A_{bb} - K_e A_{ab})e(t) \tag{4.22}$$

The characteristic equation for the minimum-order observer is obtained from equation (4.22)

$$|sI - A_{bb} + K_e A_{ab}| = 0 \tag{4.23}$$

From equation (4.23) we see that the dynamic behavior of the error signal is determined by the eigenvalues of $A_{bb} - K_e A_{ab}$. If $A_{bb} - K_e A_{ab}$ matrix is a stable matrix, the error vector will converge to zero for any initial error $e(0)$.That is, $\hat{x}(t)$ will converge to $x(t)$ regardless of the values of $x(0)$ and $\hat{x}(0)$

K_e can be evaluated from equation (4.23) and the unmeasured states can be estimated using the value K_e and equation (4.19).

A complete derivation of the minimum order observer has been given in appendix A. The velocity observer is given by the following equation:

$$\hat{X}_2(s) = \frac{\beta_3 s^3 + \beta_2 s^2 + \beta_1 s + \beta_0}{s^3 + \gamma_2 s^2 + \gamma_1 s + \gamma_0} Y(s) \quad \frac{\lambda_2 s^2 + \lambda_1 s + \lambda_0}{s^3 + \gamma_2 s^2 + \gamma_1 s + \gamma_0} U(s) \tag{4.24}$$

4.5 Lateral dynamics : Simulated results

4.5.1 Open-loop response

In this section, open-loop response of the web lateral dynamics is investigated. A Fife Kamberoller guide (a remotely pivoted steering guide) is used for this investigation. Fig. 4.6 shows a web span with a Kamberoller guide and an edge sensor immediately downstream of the guide roller.

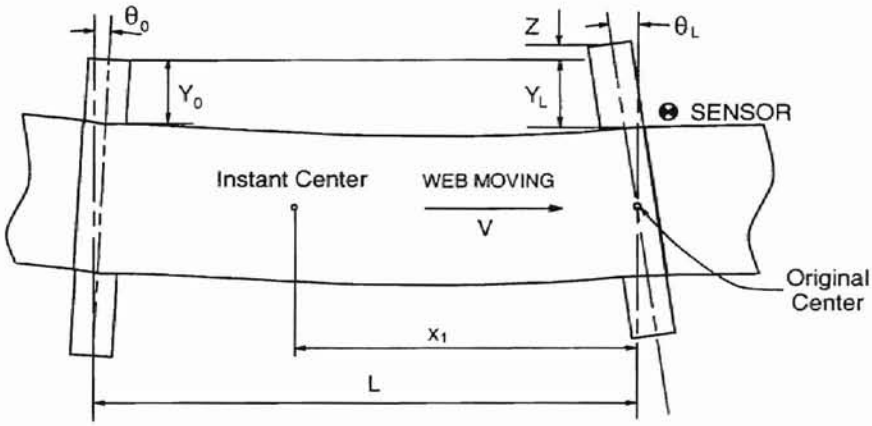

Figure 4.6: A web system

The lateral dynamics for the web span shown in Fig. 4.6 is given by equation (4.25), which is

$$\begin{aligned} Y_L(s) &= \left(\frac{\frac{f_3(KL)}{\tau^2}}{s^2 + \frac{f_2(KL)}{\tau}s + \frac{f_1(KL)}{\tau^2}} \right) \theta_0(s) + \left(\frac{-\frac{f_3(KL)}{\tau}s + \frac{f_1(KL)}{\tau^2}}{s^2 + \frac{f_2(KL)}{\tau}s + \frac{f_1(KL)}{\tau^2}} \right) Y_0(s) \\ &\quad + \left(\frac{s^2 + \frac{f_2(KL)}{\tau}s + \frac{f_2(KL)}{\tau^2 x_1}}{s^2 + \frac{f_2(KL)}{\tau}s + \frac{f_1(KL)}{\tau^2}} \right) Z(s) \end{aligned} \tag{4.25}$$

Equation (4.25) can be rewritten in the form:

$$Y_L(s) = G_1(s)Z(s) + G_2(s)\theta_0(s) + G_3(s)Y_0(s)$$

where $G_1(s), G_2(s), G_3(s)$ are as given in equation (4.25) and

$Y_L(s)$: response at a Kamberoller guide;
$Y_0(s)$: the positional disturbance from upstream roller;
$\theta_0(s)$: angular disturbance at upstream roller;
$Z(s)$: positional input at steering guide;
$\theta_L(s)$: angular input at steering guide.

The following simulation investigates the response at a Kamberoller guide, under the assumption that a disturbance $Y_0(s)$ is introduced at upstream roller. Other terms in equation (4.25), which are the angular disturbance, $\theta_0(s)$, at upstream roller and input at Kamberoller guide, $Z(s)$, are taken to be zero. Under this condition, the web dynamic behavior is described by

$$Y_L(s) = G_3(s)Y_0(s)$$

The parameter and experimental conditions used in this simulation are those of the Kamberoller guide in our experimental web platform, and are given in the following table.

K	$L(in)$	$v(in/sec)$	$x_1(in)$
0.0292	46	80	88

Simulation on a web system described by Fig. 4.6 is accomplished. The responses at a Kamberoller guide to impulse, step and sinusoidal disturbance are investigated. The simulation results are shown in Figures 4.7, 4.8 and 4.9 respectively. The simulation results show that the studied web system can follow the disturbance after a short time period. Please note that when the disturbance is introduced, the web edge first moves toward the direction contrary to that of the disturbance. This can be understood from the term $G_3(s)$ in equation (4.25), which has the initial value as $-\frac{f_3(KL)}{\tau}$. Moreover, from Fig. 4.9, the open-loop dynamics of the system appears to be characterized by a low-pass filter.The goal of lateral control of a web is

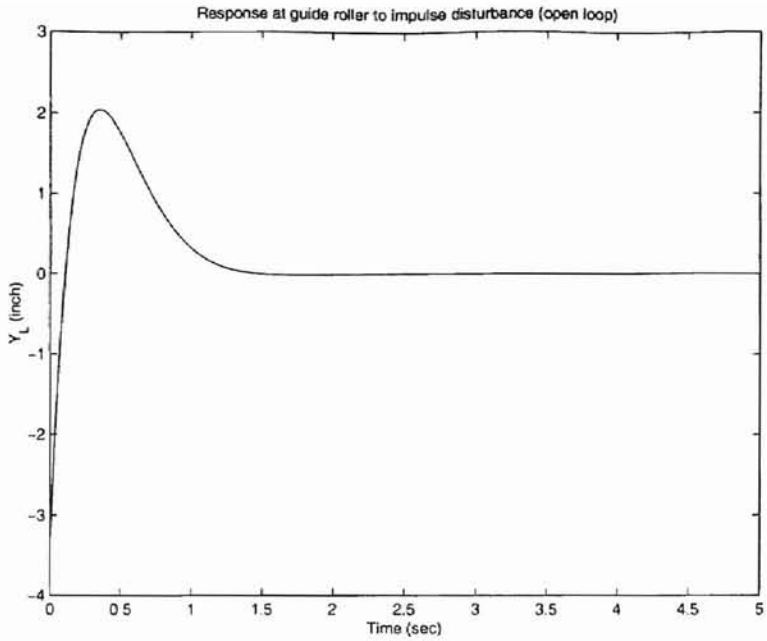

Figure 4.7: Response at Kamberoller guide to an impulse disturbance

to minimize the lateral position error by applying appropriate control strategies to the intermediate steering guide. The lateral control system to be discussed is given in Fig. 4.10, where

$Y_L(s)$: response at the remotely pivoted guide;
$Y_R(s)$: web reference position at the remotely pivoted guide;
$Y_0(s)$: positional disturbance from upstream roller;
$\theta_0(s)$: angular disturbance at upstream roller;
$G_C(s)$: transfer function of controller;
$G_M(s)$: transfer function of motor dynamics;
$U_M(s)$: control input to the motor;
$V_M(s)$: motor angular position;
C_m : constant relating motor angle to the lateral displacement of the guide.

4.5.2 PI Control

Proportional and integral control strategy is applied for web lateral control system. To test the performance of PI control at steering guide, computer simulation was

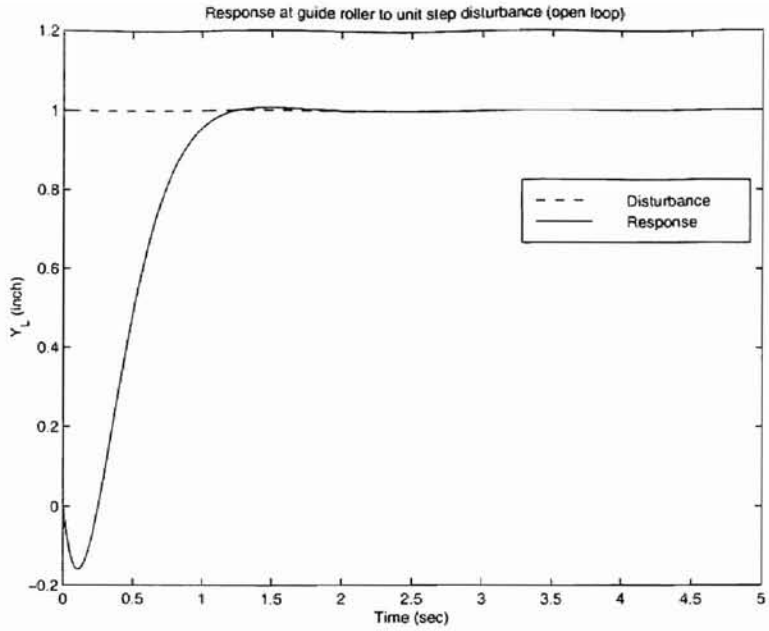

Figure 4.8: Response at Kamberoller guide to unit step disturbance

done with different proportional and integral gains. Because in the real web system, roller axes are parallel to each other, the angular disturbance at upstream roller θ_0 in the equation (4.25) is taken as zero. Simulink block diagram for simulations is given in Fig. 4.15. The parameters used in the simulations are computed in the Matlab script file given in Appendix, from the parameters given in the following table.

K	$L(in)$	$v(in/sec)$	$x_1(in)$
0.0292	46	80	88

4.5.3 Control with estimated motor velocity

According to modern control theory, for an observable system, the state variables can be estimated based on the system input and output information. Following this idea, a minimum-order estimator is designed which estimates the velocity of the DC motor. Fig. 4.14 shows the block diagram of a lateral control system with estimated motor velocity feedback, where the steering guide takes the form of remotely pivoted guide (Kamberoller guide) whose dynamics is described by equation (4.25). where

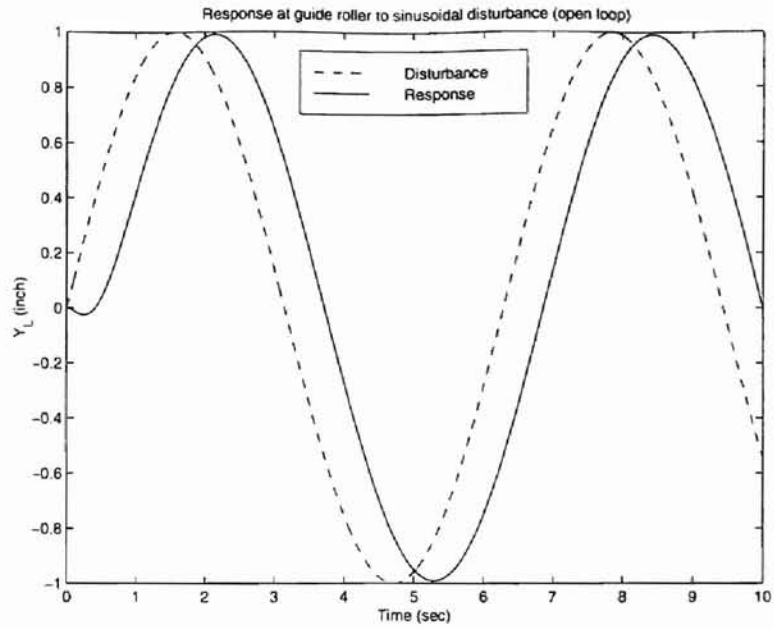

Figure 4.9: Response at Kamberoller guide to sinusoidal disturbance

$Y_g(s)$: response at the guide;

$Y_r(s)$: reference position at the guide;

$Y_0(s)$: position disturbance from upstream roller;

$\theta_0(s)$: angular disturbance at upstream roller;

$G_c(s)$: transfer function of controller;

$G_M(s)$: transfer function of motor;

$G_{vu}(s)$: transfer function from input u to estimated velocity;

$G_{vy}(s)$: transfer function from measured web position y to estimated velocity;

$V_M(s)$: actual motor velocity (from tachometer);

$\widehat{V}_M(s)$: estimated motor velocity;

C_m : constant relating motor angle to the guide displacement.

Simulink block diagram of the lateral control system given in Fig. 4.14 using tachometer feedback is shown in Fig. 4.15. Simulink block diagram of estimated motor velocity feedback is shown in Fig. 4.16. The variables used in the Simulink block diagram can be obtained from the Matlab script file in appendix B.

To test the effect of motor velocity observer, computer simulation is accomplished on a web lateral system with estimated motor velocity feedback. Three types of

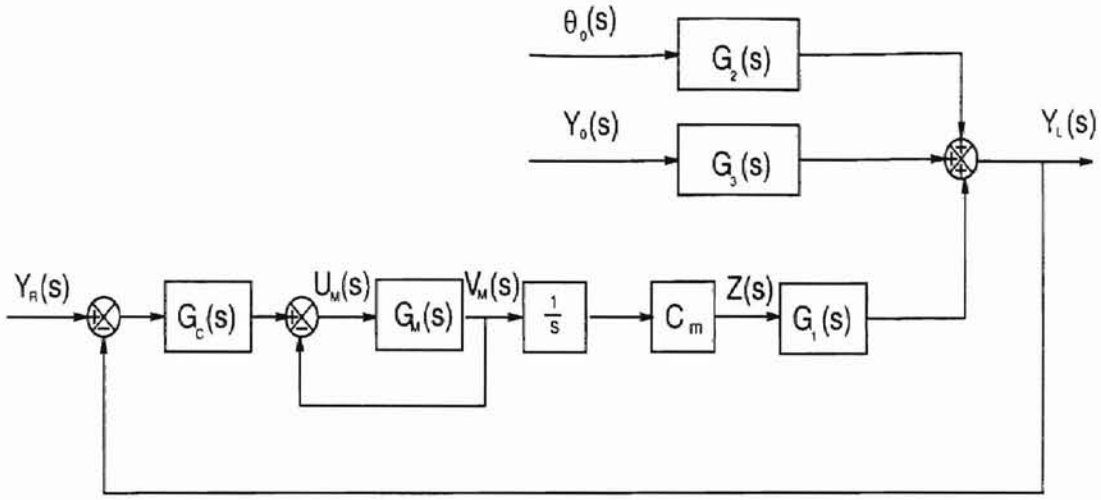

Figure 4.10: Block diagram of lateral control system

disturbances are adopted, which are impulse disturbance, unit step disturbance, and sinusoidal disturbance, respectively. Figures 4.17 through 4.19 compare the response of web system with tachometer and with motor velocity observer, to different kinds of reference input. From the simulation results it can be seen that the performance of the closed-loop system using estimated velocity in the inner-loop is similar to that with tachometer feedback. The simulation results reveal that a motor velocity observer can functionally replace a tachometer.

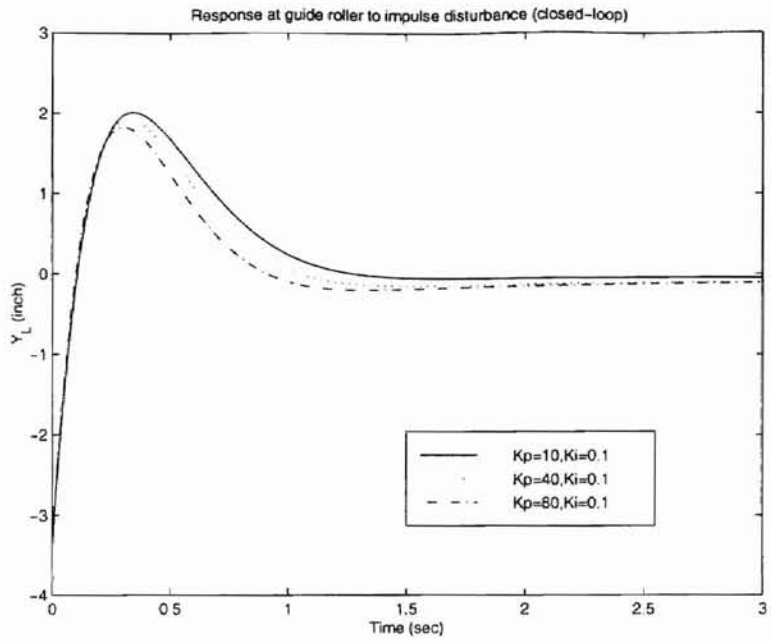

Figure 4.11: Response at Kamberoller guide to an impulse disturbance

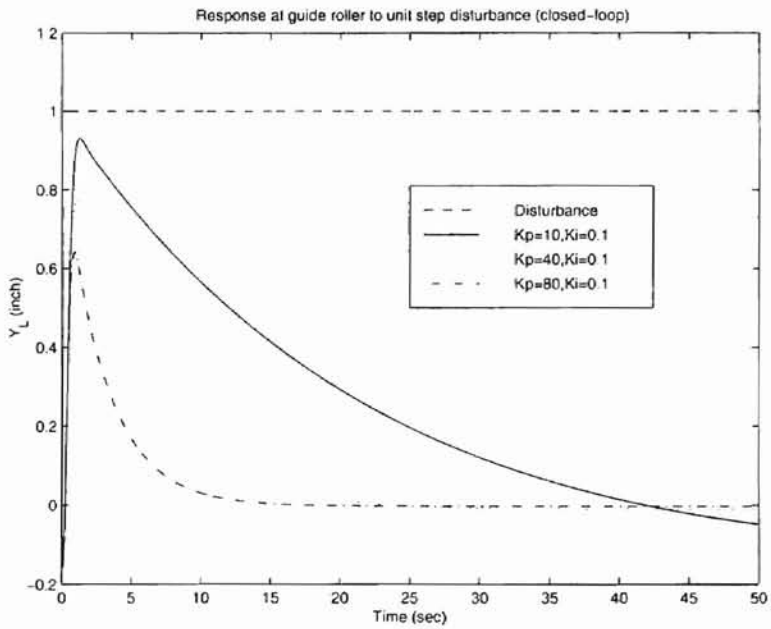

Figure 4.12: Response at Kamberoller guide to a unit step disturbance

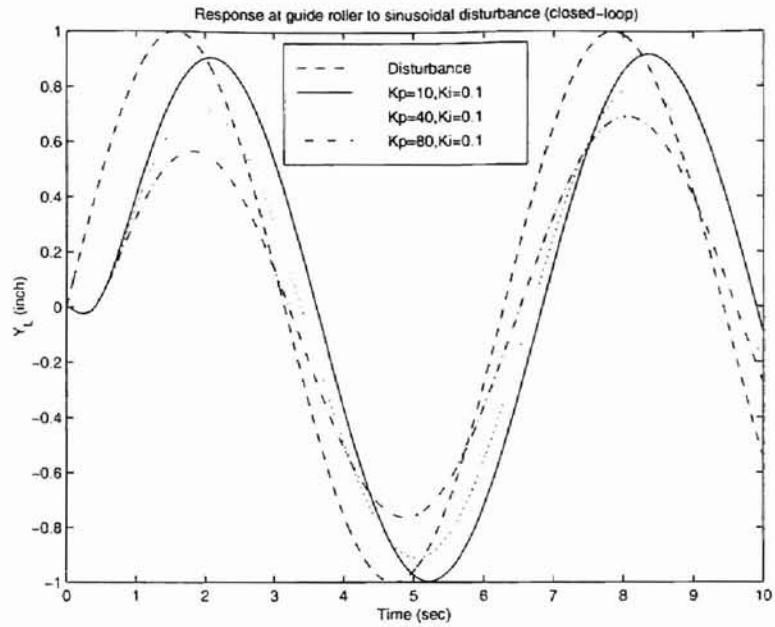

Figure 4.13: Response at Kamberoller guide to a sinusoidal disturbance

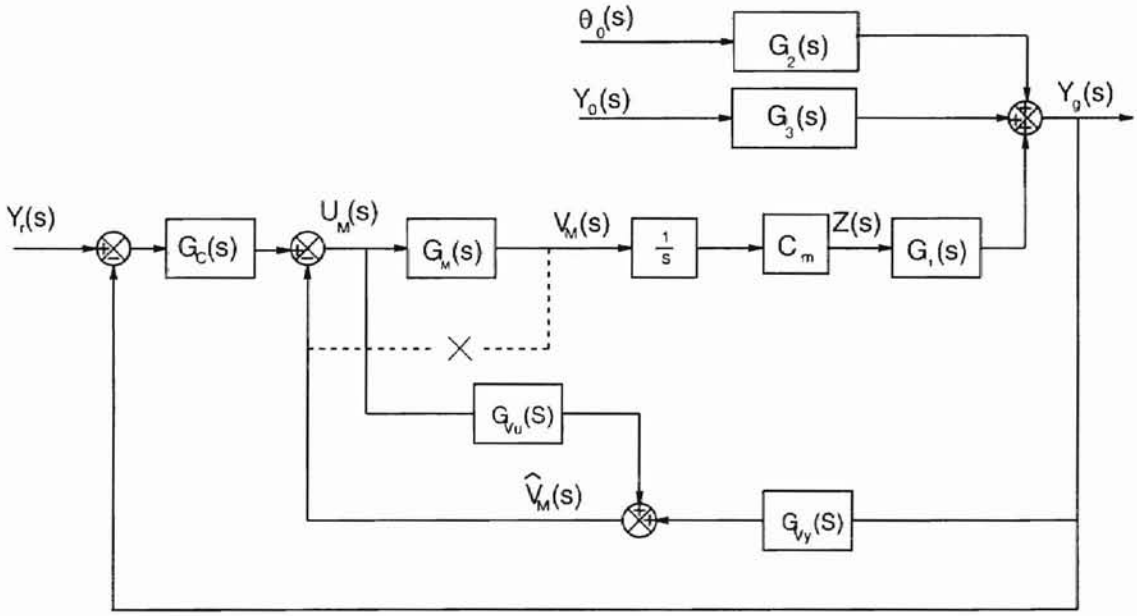

Figure 4.14: Lateral control system with estimated motor velocity feedback

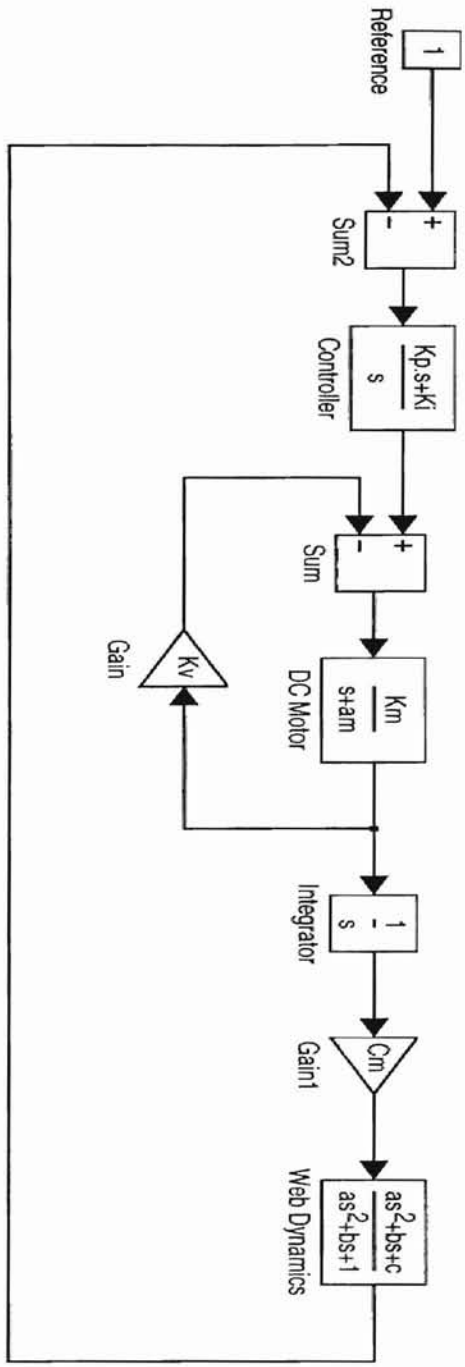

Figure 4.15: Simulink block diagram using tachometer feedback

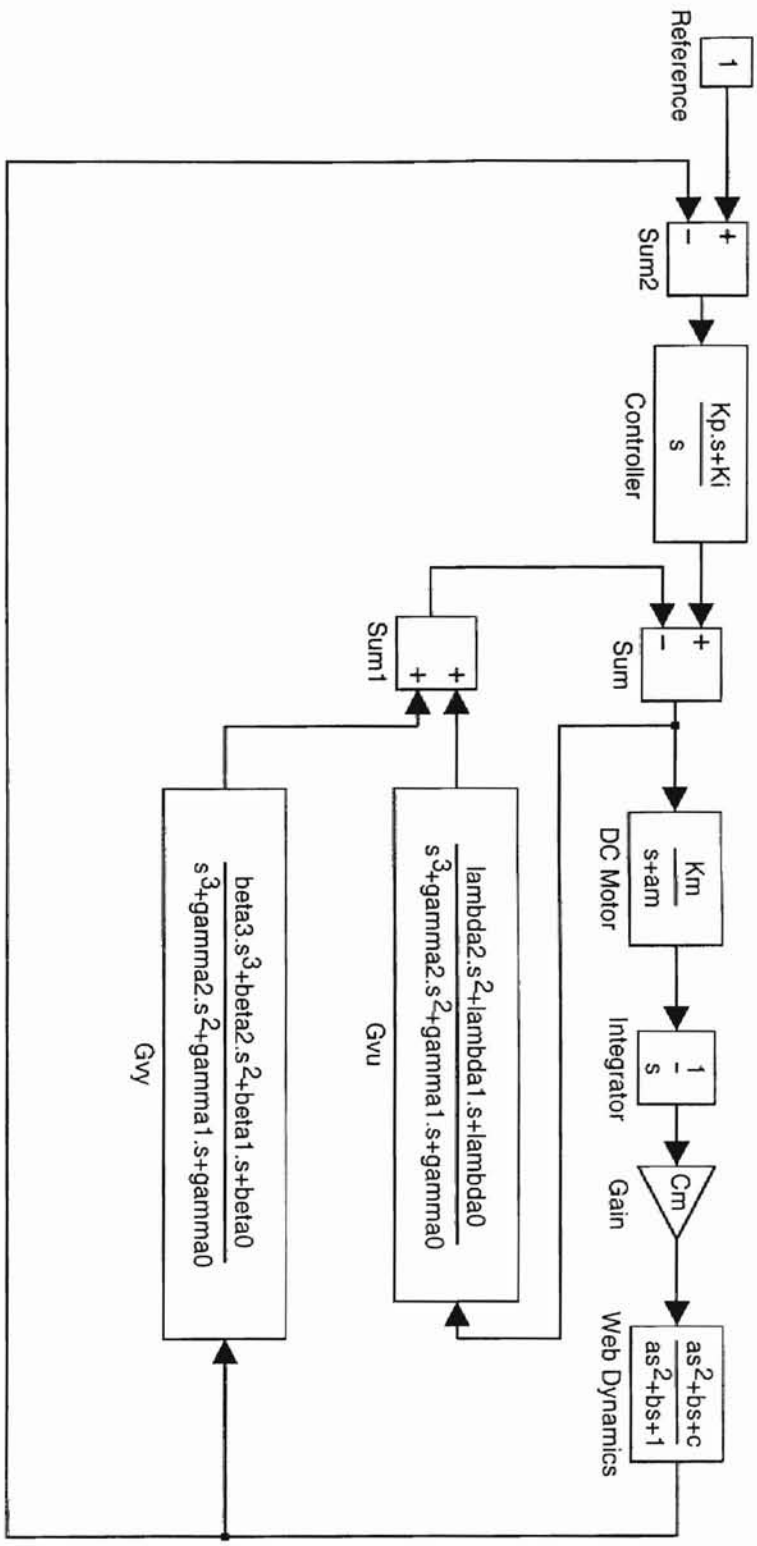

Figure 4.16: Simulink block diagram using estimated motor velocity feedback

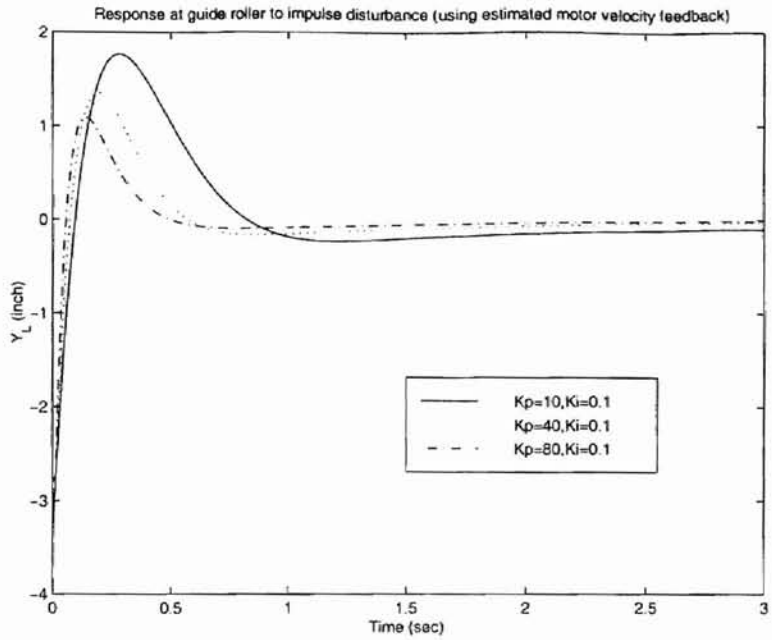

Figure 4.17: Response using estimated motor velocity feedback (impulse disturbance)

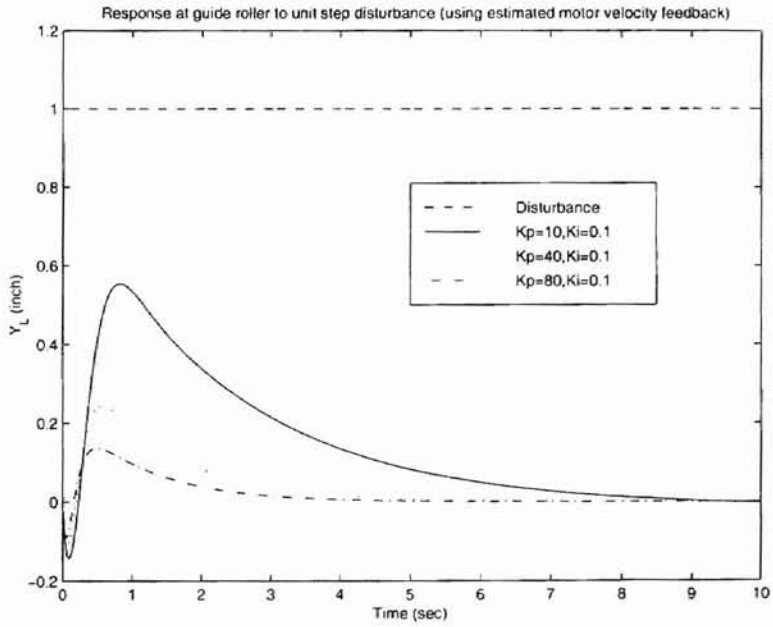

Figure 4.18: Response using estimated motor velocity feedback (unit step disturbance)

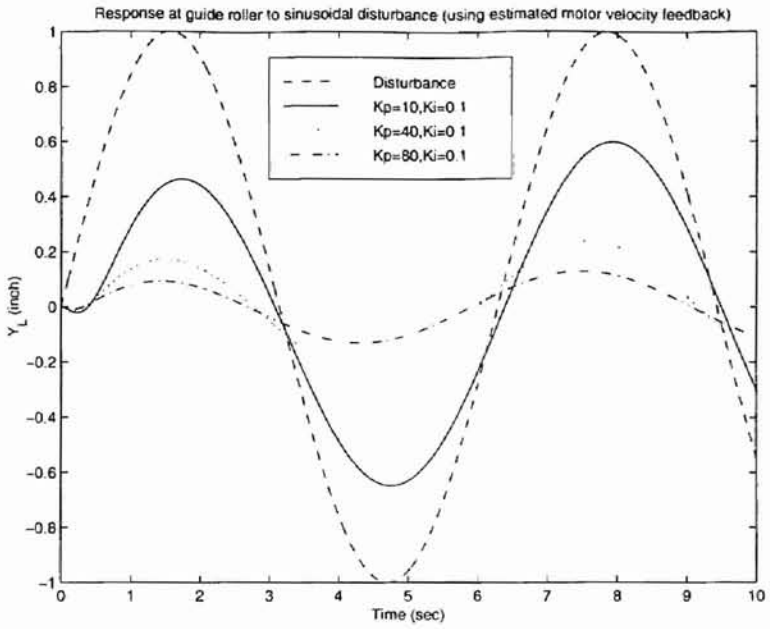

Figure 4.19: Response using estimated motor velocity feedback (sinusoidal disturbance)

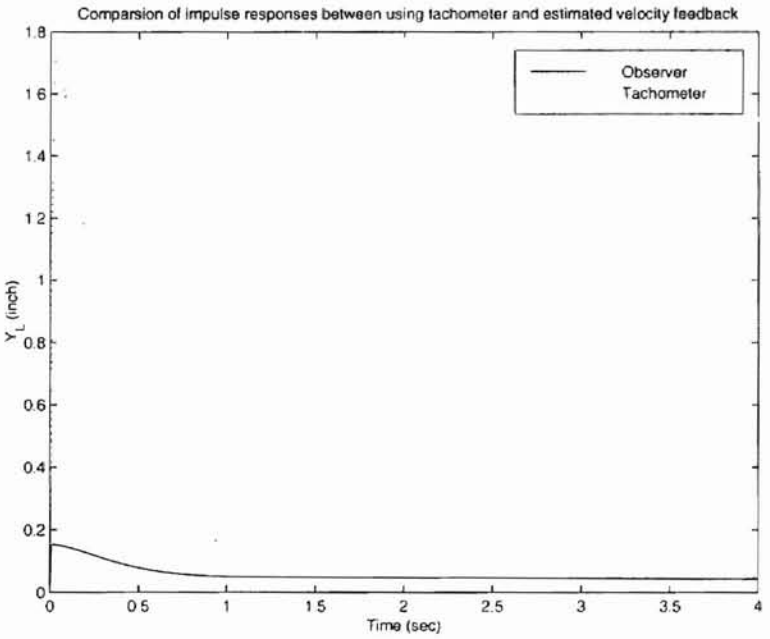

Figure 4.20: Impulse reference response using estimated motor velocity feedback

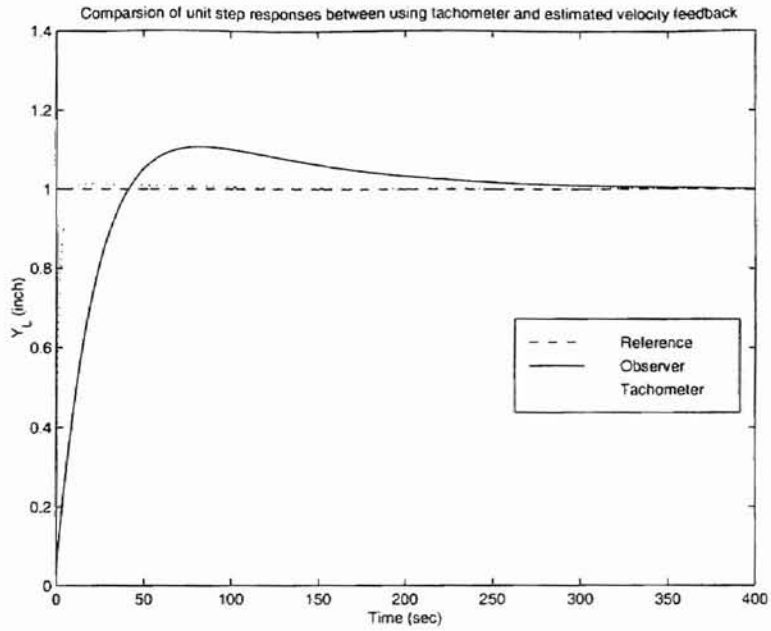

Figure 4.21: Unit step reference response using estimated motor velocity feedback

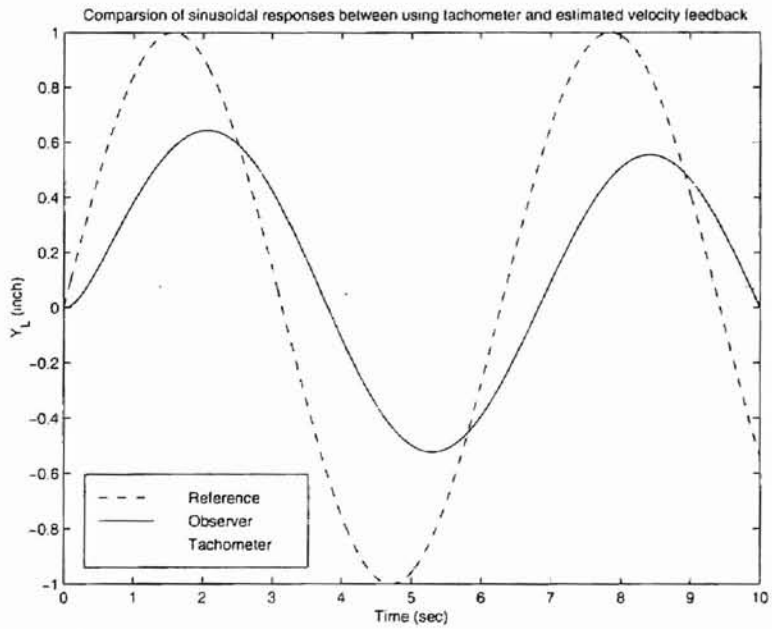

Figure 4.22: Sinusoidal reference response using estimated motor velocity feedback

Chapter 5

Experimental Setup

This chapter describes the open-architecture experimental platform that is developed for conducting lateral control experiments. The platform consists of a closed-loop web line as shown in Fig. 5.1. The term closed-loop web line refers to web line without unwind and rewind rolls. This type of a platform mimics most of the features of a process section of a real processing line.

The experimental platform can be divided into two parts: hardware and software. The hardware part consists of the closed-loop web line, signal processors, drivers for the actuators, and computer for implementing control algorithms in real-time. Software part consists of an open architecture real-time program written in C++ programming language. In the following sections we describe the hardware and software elements of the experimental platform. The machine section consists of a number of rollers, with one large master speed roller which is used to transport the web in the line. The main control elements are a Fife remotely pivoted guide and an active dancer mechanism as shown in Fig. 5.1. A functional sketch of the experimental web platform is shown in Fig. 5.2.

The Fife guide mechanism consists of an actuator and an edge sensor immediately downstream of the guide roller. Lateral control of the web in the line is accomplished

using the Fife guide.

5.1 Hardware

The closed-loop web line shown in Fig. 5.1 consists of 15 rollers. A master speed roller, shown as large diameter roller in Fig. 5.1, is used to transport the web in the web-line. Since each roller width is 8 inches, the maximum web width that can be used in the web line is 6 inches. The diameter of each roller is 5 inches, except for the master speed roller, which has a diameter of 10 inches. A nip roller for the master speed roller is used to reduce slip during start-up. An analog controller for the master speed roller is available to obtain the desired transport velocity of the web in the line. The closed-loop web line, as shown in Fig. 5.1, consists of three main control elements: (i) Lateral control system, (ii) Active dancer mechanism, and (iii) Passive dancer mechanism.

5.1.1 Lateral Control System

Lateral control of the web is accomplished by a remotely pivoted Fife guide as shown in Fig. 5.1. The guide mechanism consists of a guide roller on a base which is actuated by a DC motor. An edge sensor downstream of the guide roller gives the web lateral position. From a control viewpoint, the Fife analog control system is given by the sketch shown in Fig. 5.4. The physical elements of the Fife guide and their interaction is shown in Fig. 5.3. The analog lateral control system includes: (i) Fife analog signal processor (A9), (ii) Sensors (edge sensor, tachometer), (iii) DC motor. The A9 signal processor serves as an amplifier and an on-board analog controller. It implements a velocity inner-loop and a position outer-loop as shown in Fig. 5.4. The velocity inner-loop is formed by feedback of the velocity signal of DC motor from the tachometer, which is used to regulate motor velocity by applying proportional

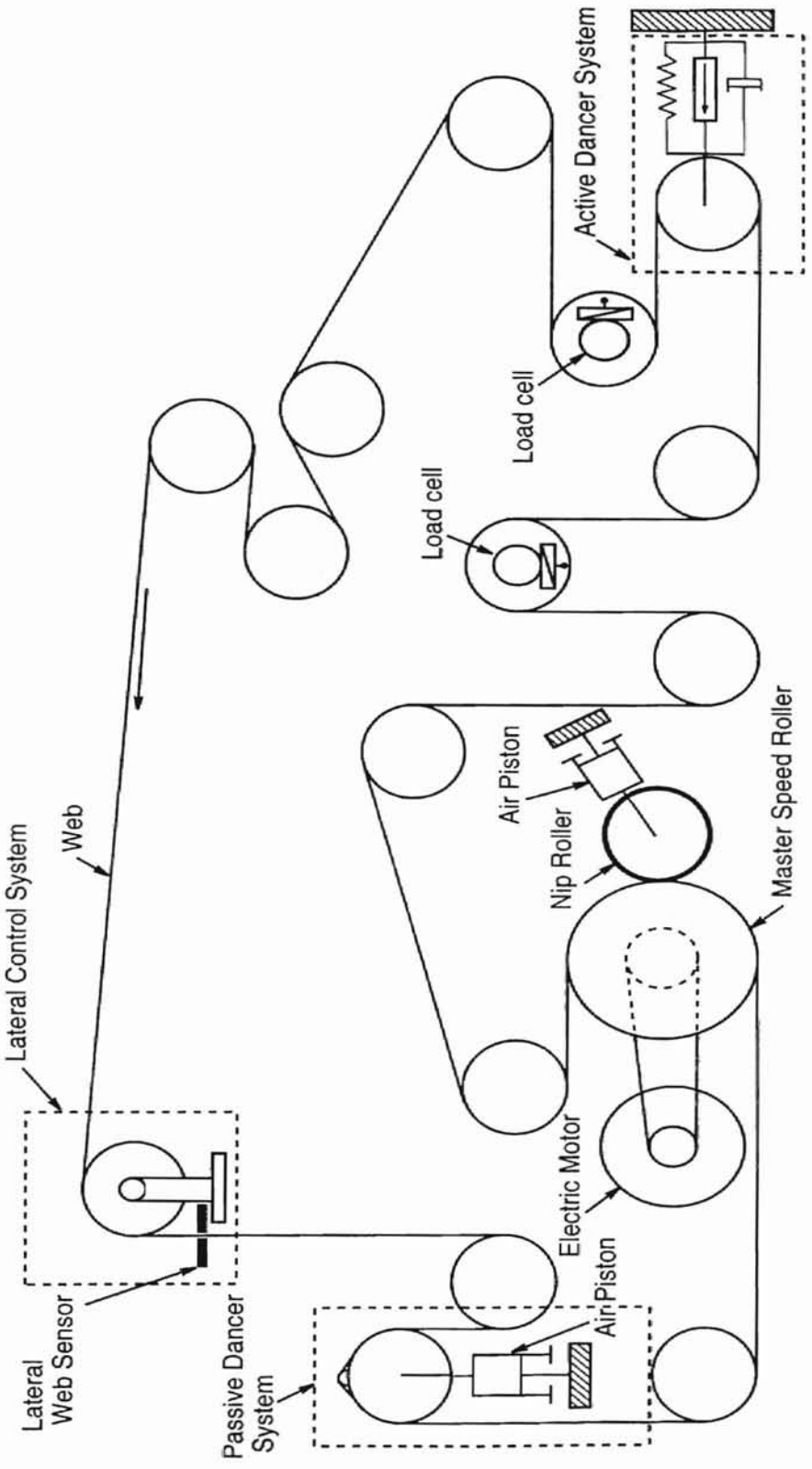

Figure 5.1: Experimental web platform

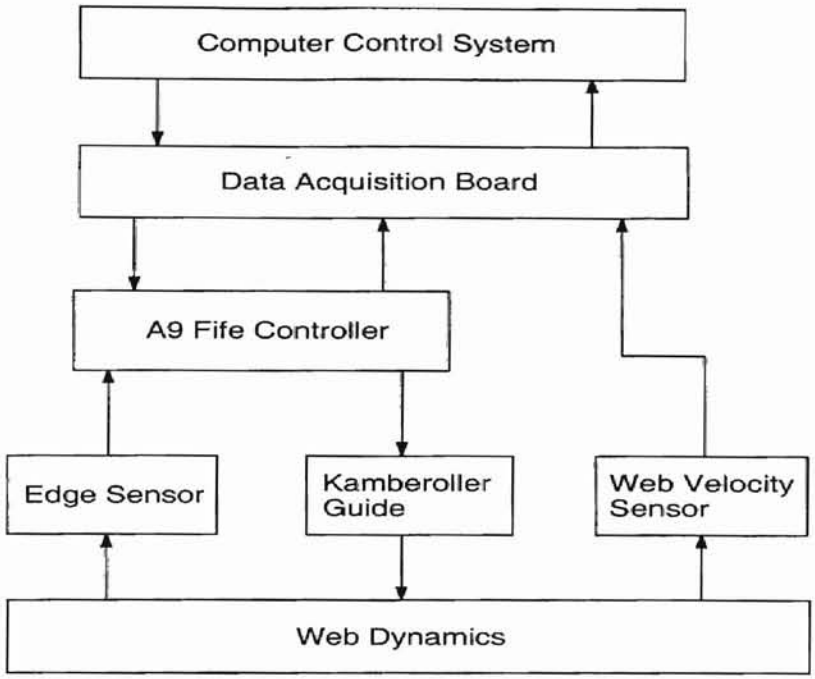

Figure 5.2: Lateral control of the experimental web platform

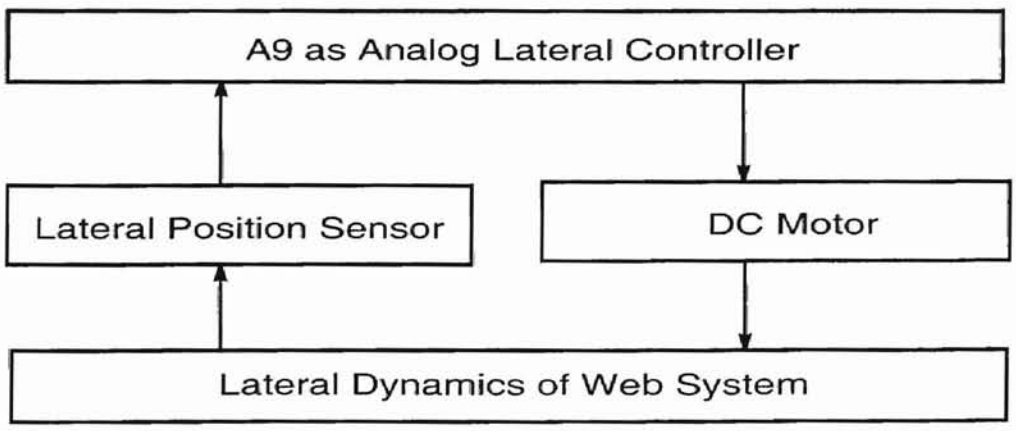

Figure 5.3: Schematic of analog lateral control system

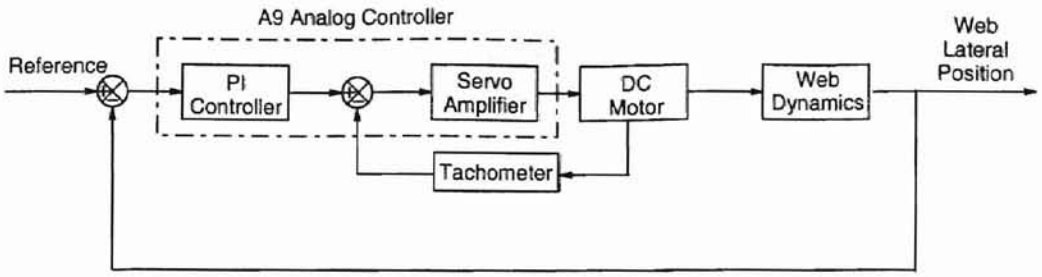

Figure 5.4: Fife analog lateral control system

control. The position outer-loop is formed by feedback of the web lateral position signal from the edge sensor, which regulates the web lateral position by applying proportional and integral control. The edge sensor is a Fife optical position sensor. The DC motor drives the guide roller based on the control signal from A9. To obtain an open-architecture computer control system, we bypass the analog controller used in the A9 processor and instead use the control algorithm generated in the computer. In the computer control system, Fife A9 processor simply serves as an amplifier only. The open-architecture computer control system can be used to implement any desired control algorithm. A schematic of physical elements and their interaction in computer control system is shown in Fig. 5.5. The main component of a Fife guide system is the DC motor. A velocity inner-loop is typically used to stabilize the DC motor. This requires measurement of motor velocity using a tachometer. It is typical that the tachometer may cost up to 25 percent of the cost of the DC motor setup. Considerable reduction in cost can be achieved if other means can be employed for generating a stable inner-loop without using tachometer to measure velocity. To investigate an estimated motor velocity inner-loop, we consider two different conditions for the lateral computer control system. In the first case, shown in Fig. 5.6, a tachometer velocity based inner-loop is used. In the second case, a velocity estimator is designed to estimate the motor velocity based on the input to the motor and the web lateral position, and the estimated velocity is used for

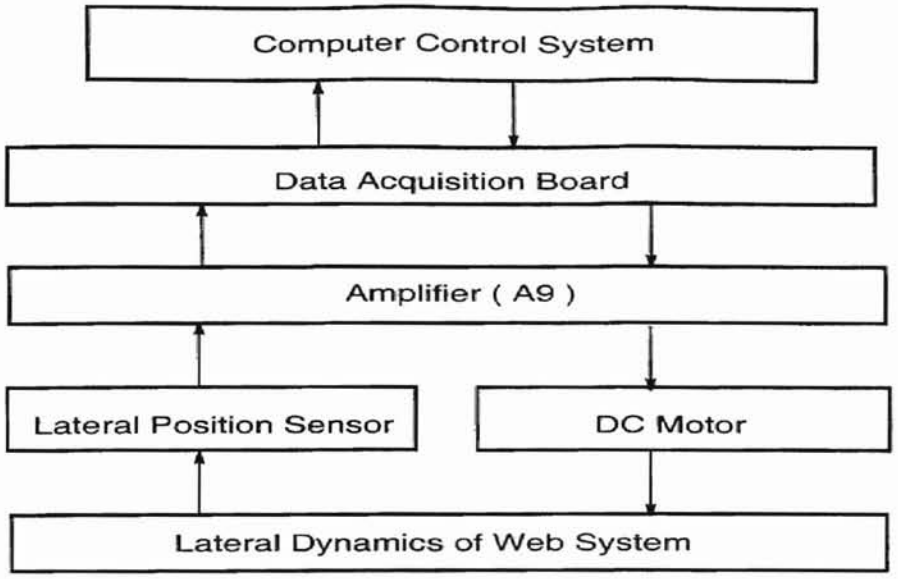

Figure 5.5: Schematic of lateral computer control system with velocity inner-loop

inner-loop as shown in Fig. 5.7.

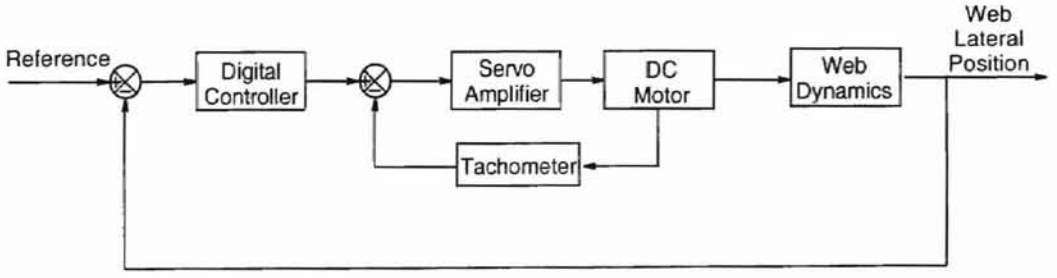

Figure 5.6: Lateral computer control system with tachometer velocity

5.1.2 Computer System

The computer system consists of a 450 MHz Pentium computer with a digital data acquisition board. The data acquisition board is a Keithley DAS 1601, which consists of eight A/D and two D/A channels. The two D/A channels are used to send control input to the amplifiers of the guide actuator and the active dancer motor. The eight A/D channnels are used to acquire the sensor signals. The distribution of the A/D and D/A channels are given in the following.

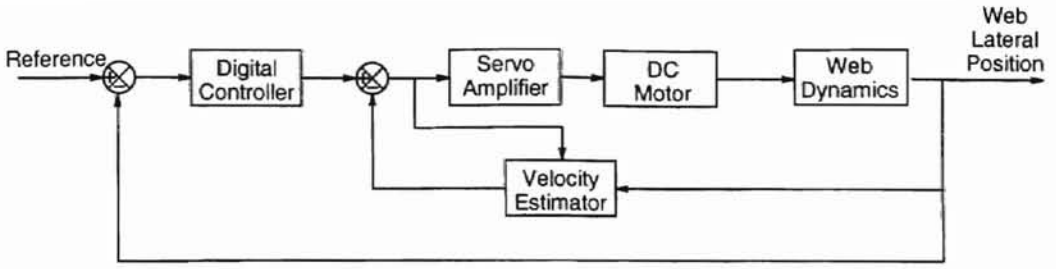

Figure 5.7: Lateral computer control system using velocity estimator

A/D Channel Configuration

- Channel 0 : None
- Channel 1 : Lateral Control Motor Tachometer
- Channel 2 : None
- Channel 3 : Upstream Load-cell
- Channel 4 : Dancer Motor Tachometer
- Channel 5 : Downstream Load-cell (After Amplifier)
- Channel 6 : Upstream Load-cell
- Channel 7 : Edge Sensor

D/A Channel Configuration

- Channel 0 : Dancer Motor
- Channel 1 : Lateral Control Motor

5.2 Software Structure

The software for real-time control and data analysis is written in C++ programming language, and can be divided into off-line software and real-time software as shown

in Fig. 5.8. MATLAB software and C++ programming language are used for data analysis and off-line simulation. The real-time software, which is written in C++ based on Windows platform, implements the following functions in a modular way: data acquisition, data storage, real-time data display and plotting, control algorithm, state observer algorithm, and control signal output.

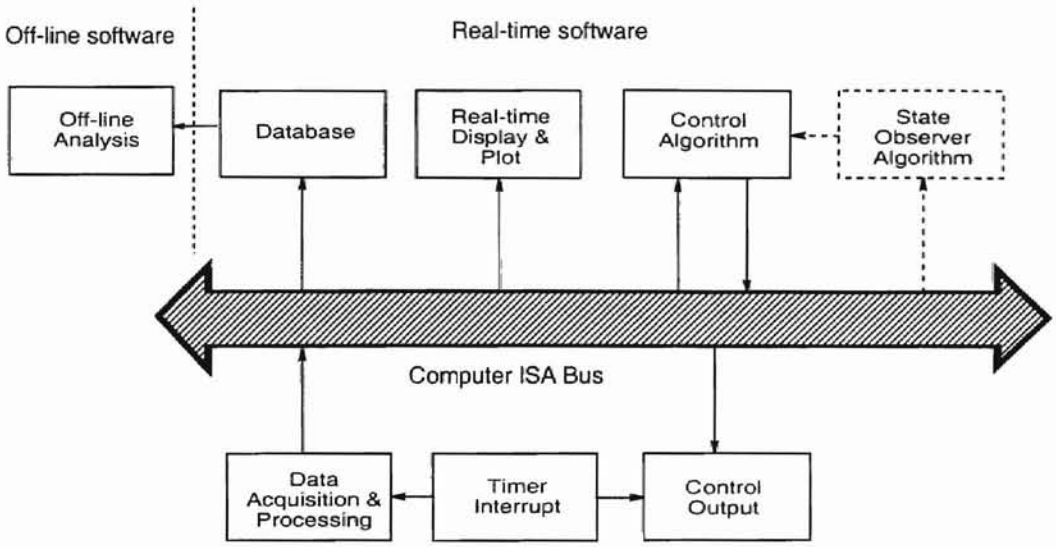

Figure 5.8: Software for web handling system

5.2.1 Real-time Software

The individual blocks of the real-time software shown in Fig. 5.8 are explained in the following.

- **Timer interrupt:** Timer interrupt serves as the "clock" of the real-time control system. As shown in Fig. 5.8, timer interrupt determines both the sampling period and the control period of the computer-control system. For all the control experiments, the sampling period and the control period are the same, and is taken to be 20 milliseconds. It is well known that when a continuous-time system is discretized, if the sampling frequency is not fast enough, then discretized

control system can go unstable. From the well known Shannon sampling condition, we know that the sampling frequency should be at least twice the highest frequency content of the sensed signal. Considering the dynamic characteristics of the web system, the chosen sampling frequency of 50 Hz is fast enough. Moreover, since computer control is used, the sampling period can be set at any value by just a change of the variable in the real-time control program.

- **Data acquisition and processing:** At each sampling time, current information on web lateral position (for lateral control) and web tension (for tension control) is read from A/D channels on the digital data acquisition board. More specifically, the information collected include: the lateral positional signal from edge sensor; the tachometer signal from the DC motor of Kamberoller guide: force information from upstream load-cell and down stream load-cell, tachometer signal from the DC motor of the active dancer mechanism. The supporting software for this function module is DAS-1600/1400 series standard software package, which is shipped with the data acquisition board. This software package includes support functions for Microsoft Windows and function libraries for writing application programs under $Windows^{TM}$ in Borland C++ Builder.

- **Control output:** During each sampling period, after the control algorithm is evaluated, the control signals are output through D/A channels on the digital data acquisition board, and then sent out to DC motors after amplification to drive the active dancer (for tension control) and Kamberoller guide (for lateral control).

- **Real-time display and plot:** Based on the data acquired through data acquisition board, real-time information on web tension and lateral position is plotted, so that the users can have a direct sense on the performance of the

control designs. Other parameters such as controller gains are displayed on computer screen, and can be modified in real time.

- **Database:** Data from the sensor signals acquired from A/D channels is written into a database for later off-line analysis, which is mainly performed using MATLAB software package.

- **Control algorithm:** This block implements the control algorithm via a control function. The function can be suitably modified based on the design of the controller.

- **State Observer Algorithm:** This block contains function for implementation of a minimum-order observer to estimate the motor velocity. The inputs to this function at each sampling period is the web lateral position and the control input to the DC motor. The motor velocity is estimated in real-time via this functional block.

Chapter 6

Experimental Results

The main focus in this set of experiments is to study the analog control system of Fife signal processors and to use computer control to emulate and improve Fife control designs. Further, a motor velocity estimator is designed and is implemented to circumvent the use of tachometer signals for inner-loop feedback. The following experimental conditions are used during lateral control experiments.

- Web velocity: 424 feet/min
- Average web tension: 9.7 lbf
- Computer control sampling period: 20 milli-seconds
- Web material: polyester film

6.1 Emulation of Fife A9 by computer

In this set of experiments the control algorithm used in Fife A9 controller is emulated in the computer, i.e. we by-pass the analog A9 PI controller and implement the PI control algorithm using the computer. Three conditions are considered while emulating Fife A9 controller: no disturbance, pulse disturbance and step disturbance. The step disturbance in our case is actually a long pulse disturbance since appropriate

mechanisms to create an actual step disturbance was unavailable. For the following experiments a long pulse disturbance is considered as a step disturbance. The lateral position signal from edge sensor under the three experimental conditions are shown in Fig. 6.1. Fig. 6.2 shows the motor velocity (tachometer signal) for both computer control and A9 controller implementation. The lateral pulse disturbance in the web is obtained using a small width non-transparent tape on the side of web containing the edge sensor. Since the edge sensor is an optical sensor, the non-transparent tape on the web (polyester film) is perceived as a pulse disturbance. Increasing the width of the non-transparent tape on the web results in a step of finite duration. In Fig. 6.1, the dotted lines indicate the disturbance profile on the web. The disturbance profile is also shown in Fig. 6.2 to indicate the time instance of the disturbance. In all the experiments, the lateral web position shown is in inches and the motor velocity is in volts. The following observations can be made from the experimental results (Figures 6.1 and 6.2):

- By tuning the control gains for computer control, similar performance as that of the Fife A9 controller is obtained. In all three cases, i.e. no disturbance, step disturbance and pulse disturbance, the system shows the same response pattern.

- Due to the connection tape used to form the web in the experimental platform, a periodic small pulse disturbance exists in all three cases in addition to the introduced disturbances.

- Notice that with rising edge of the step disturbance, the edge sensor signal increases, which is immediately pushed back to the reference zero position by the control action of the guide. Also, with the falling edge of the step disturbance, the edge of the web moves to the negative side, and then is pushed back to the

reference position due to control action of the guide.

- Also, when pulse disturbance appears on the web, the control action of the web guide is to push the web to keep the reference position, and when the pulse disturbance disappears, overshoot is observed due to control action and the web returns to the zero reference position.

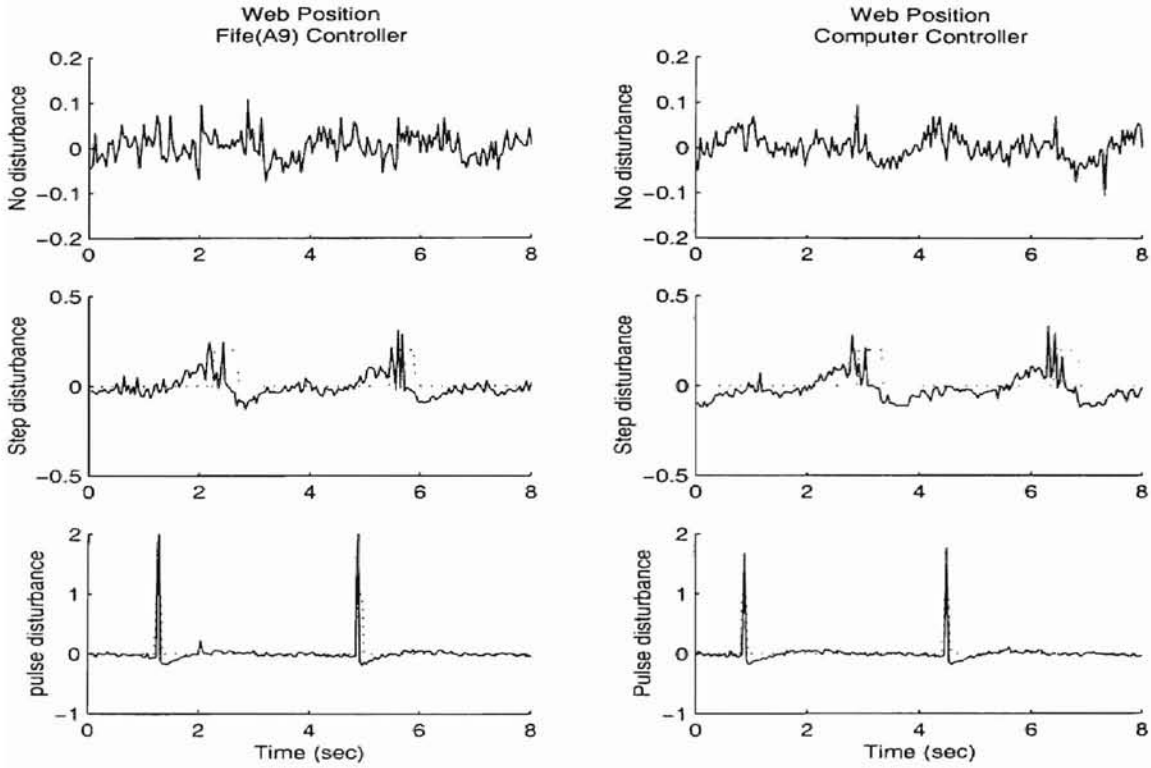

Figure 6.1: Web Position: Fife(A9) controller and computer controller

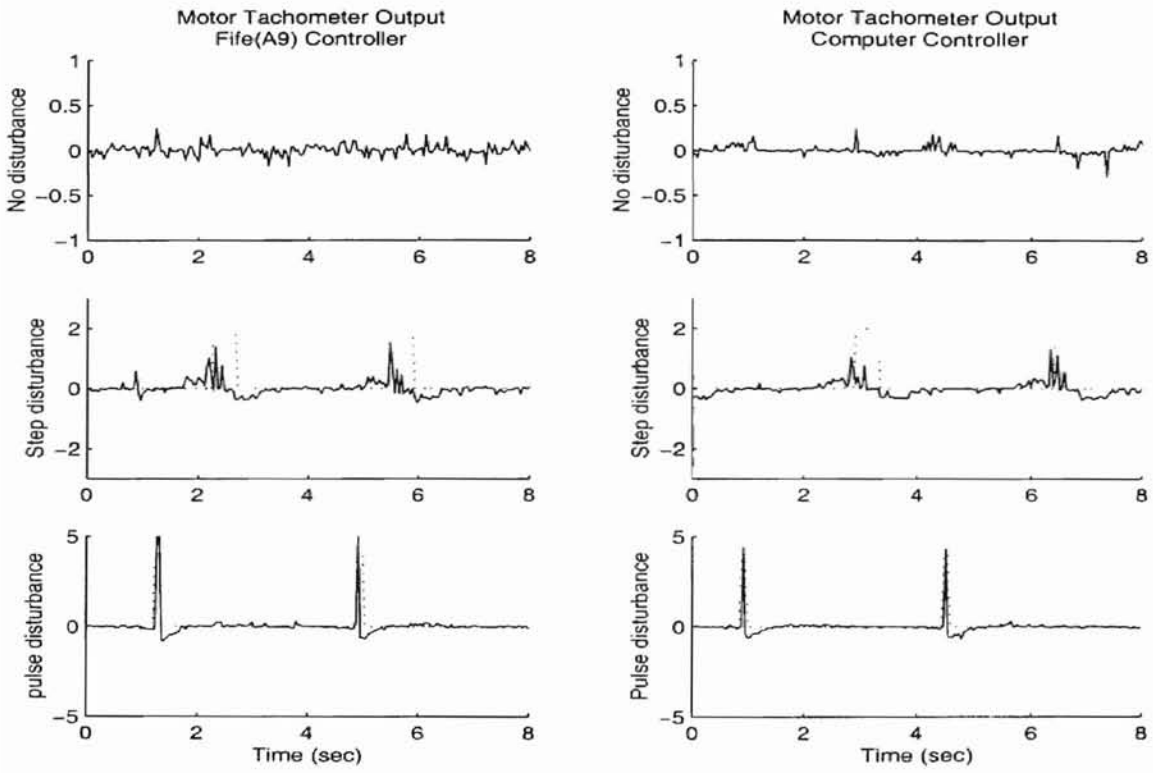

Figure 6.2: Motor Velocity: Fife(A9) controller and computer controller

6.2 Solutions without tachometer

For the purpose of stabilizing the system in the absence of motor tachometer, two approaches are considered. One is using finite difference of edge sensor signal to obtain lateral velocity of the web, which is used as a derivative action in the outer feedback loop. The second solution is to design a minimum-order velocity observer using edge sensor signal and motor control signal to get an estimation of motor velocity. This estimated velocity is used for inner-loop feedback. Figures 6.3 and 6.5 show the experimental results using finite difference approach. The observations from these experimental results are summarized below.

- Compared to the results obtained without inner-loop feedback, which is shown in Fig. 4.2, the edge sensor signals in Fig. 6.3 are smoother and the overshoot due to the disturbance is smaller. The finite difference velocity in feedback acts as a D-action and thus can stabilize the system.

- Although using the finite difference velocity as D-action in the outer-loop feedback has a stabilizing effect, it performs poorly in the presence of disturbances, see second and third row plots in Fig. 6.5. Moreover, the finite difference velocity signal depends on the noise level in the position signal, which makes it unusable in some instances when the lateral position signal noise is high.

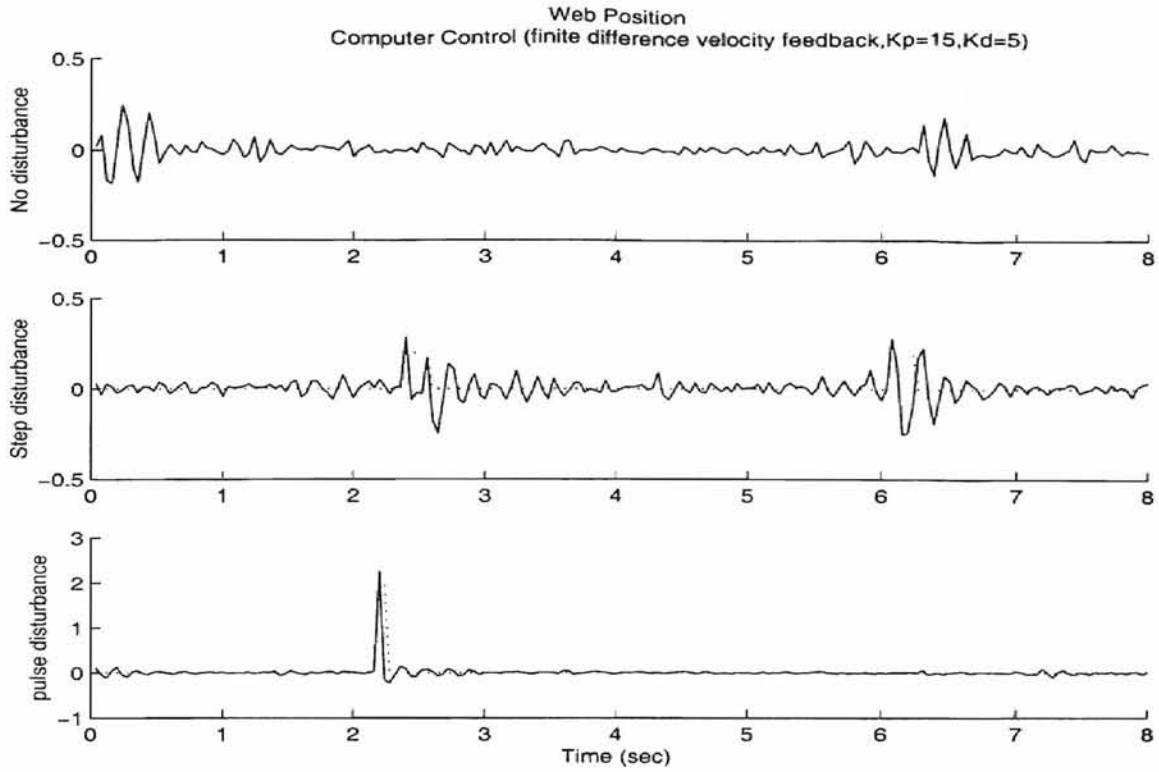

Figure 6.3: Web position: computer control using finite difference velocity feedback

The experimental results using velocity observer are shown in Figures 6.6 and 6.8. The following observations can be made from these results.

- Compared with Fig. 6.3, the edge sensor signals in Fig. 6.6 are more stable. In all the three cases, the oscillations and overshoot due to disturbances are smaller. The use of estimate velocity in controller can significantly improve the performance of the system without a tachometer.

- The velocity observer is capable of effectively picking up the motor velocity changes in presence of step disturbance and large pulse disturbance.

- Estimated velocity feedback in the inner-loop can provide similar closed-loop performance as that of the system with tachometer feedback (compare Figures 6.1 and 6.6).

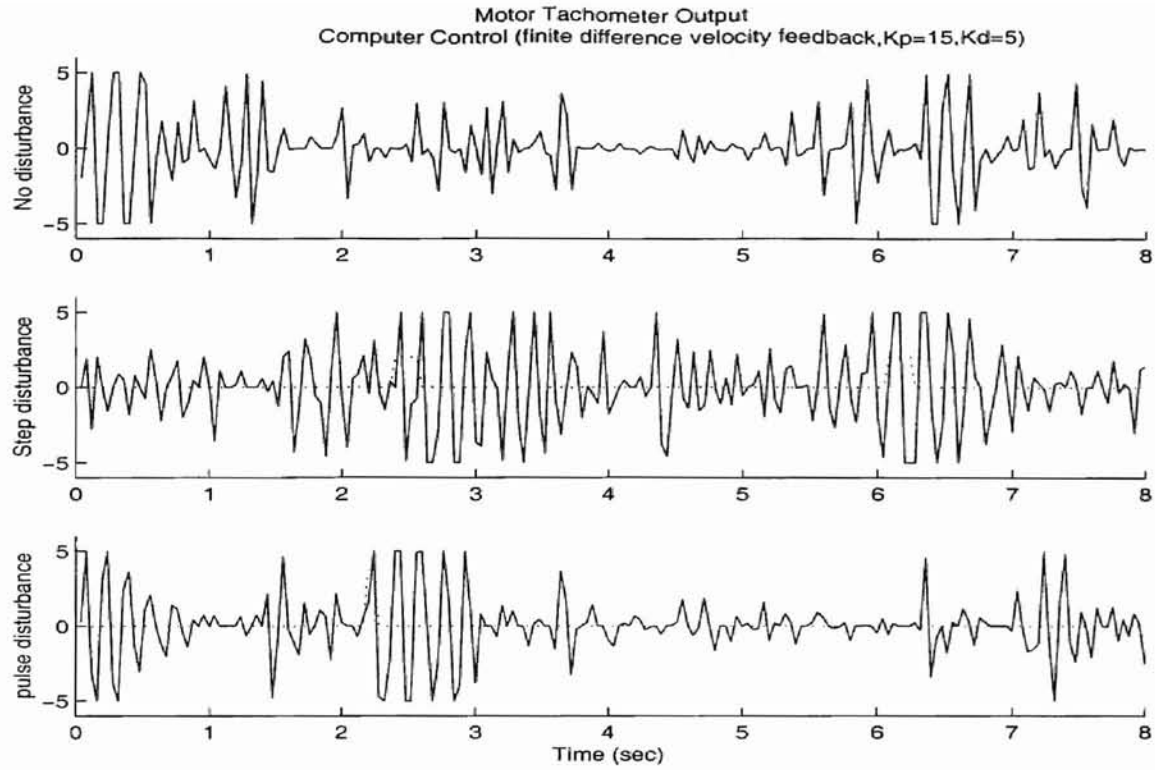

Figure 6.4: Motor velocity: computer control using finite difference velocity feedback

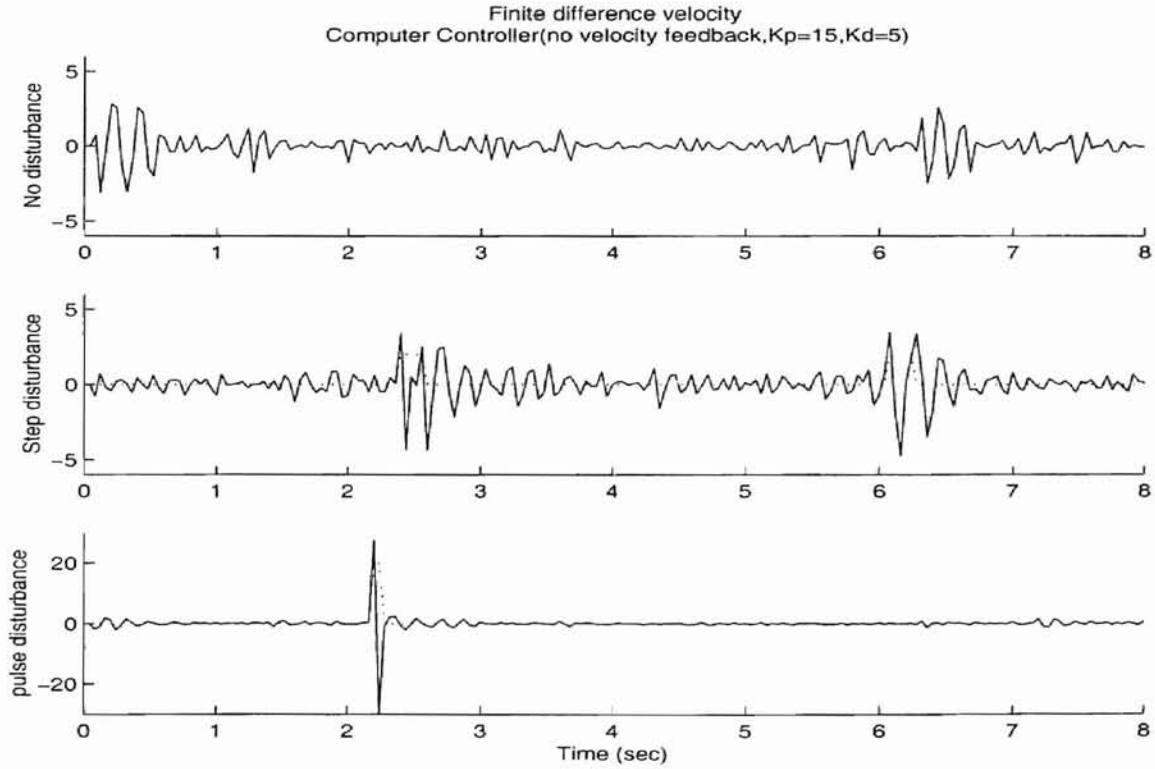

Figure 6.5: Finite difference velocity: computer control using finite difference velocity feedback

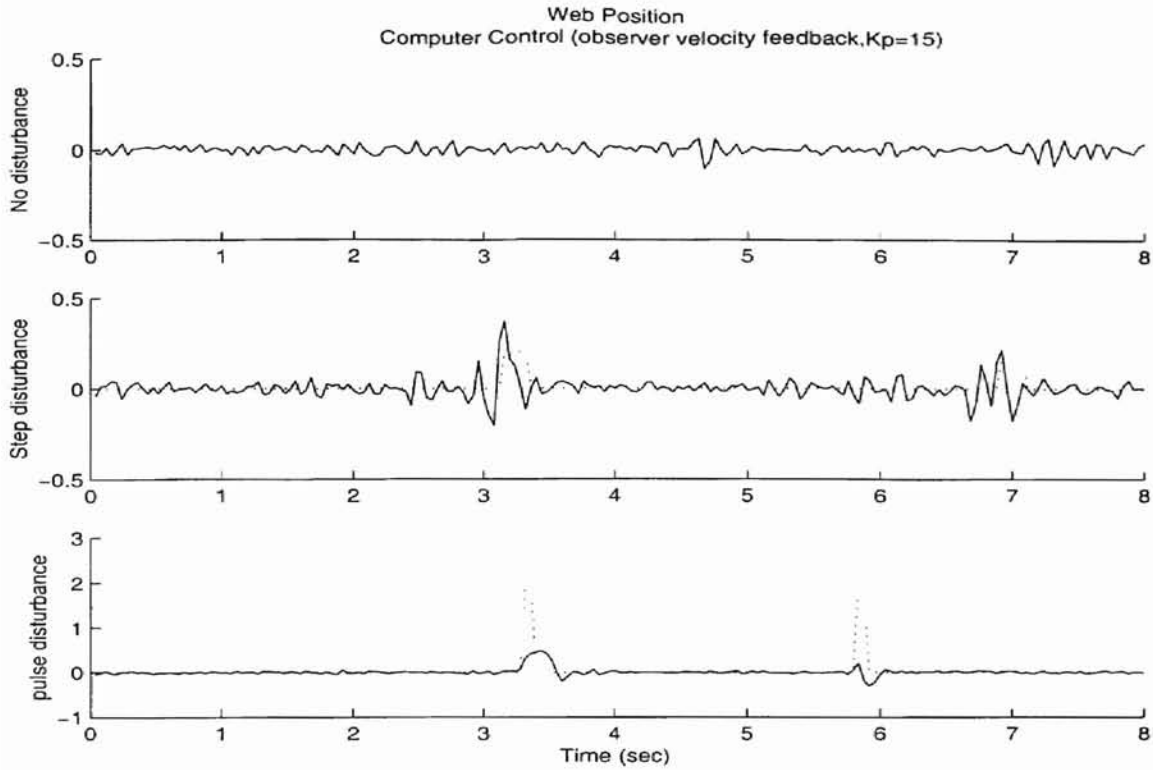

Figure 6.6: Web position: computer controller using velocity observer

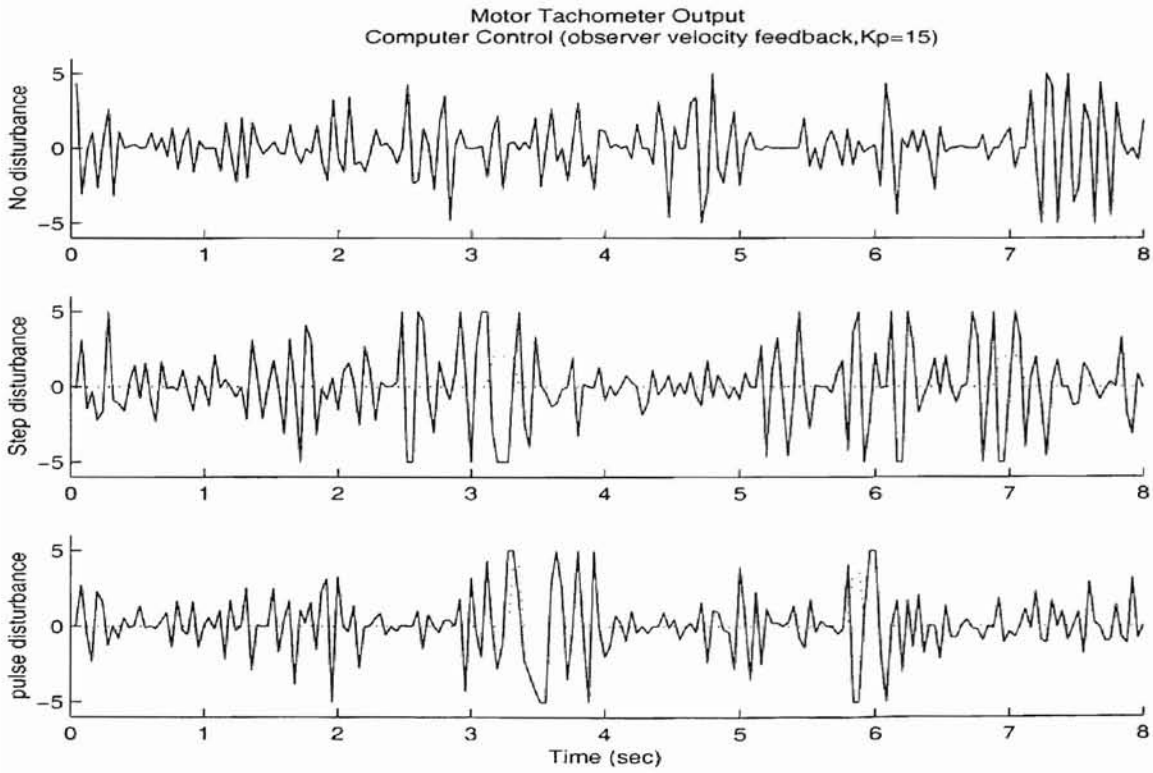

Figure 6.7: Tachometer velocity: computer controller using velocity observer

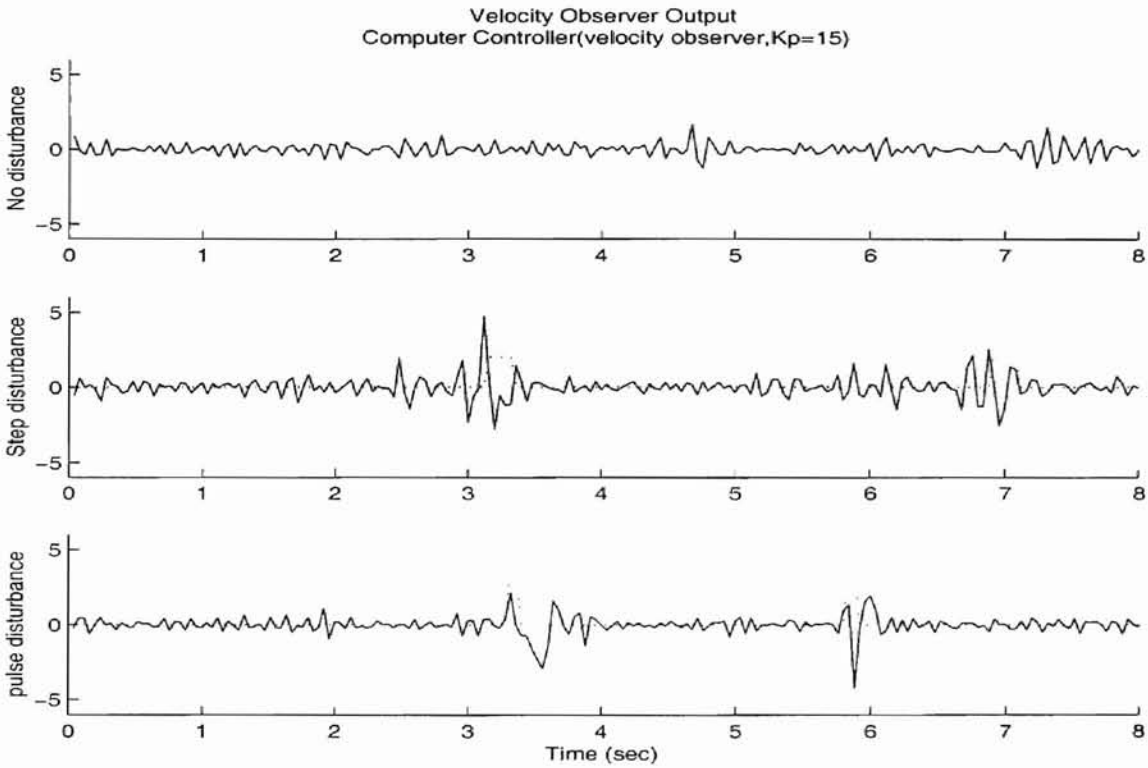

Figure 6.8: Estimated velocity: controller using velocity observer

6.3 Comparison of controllers

To investigate the effects of finite difference velocity and observer estimated velocity on the web system, the transient response of three different controllers are compared: (1) Fife A9 controller with tachometer velocity feedback, (2) computer controller using finite difference velocity and (3) computer controller using observer estimated velocity. Figures 6.9, 6.10 and 6.11 show the velocity from the tachometer, finite difference velocity, and observer estimated velocity, respectively, for the three cases. Figures are enlarged to investigate the time shift.

- Finite difference velocity and velocity observer introduce a time shift. This is expected and is confirmed by the experiment results of all three cases, i.e. Figures 6.9, 6.10 and 6.11.

- It is surprising that the finite difference velocity is time ahead (as opposed to time delay) of tachometer signal. Two possibilities may contribute to this effect:

  - a time delay circuit has been inserted in A9 controller considering the system delay;

  - tachometer dynamics may introduce the time delay;

- When magnitude of disturbance is not large, i.e. for cases of no external disturbance (Fig. 6.9) and step disturbance (Fig. 6.10), both finite difference velocity and observer velocity can provide estimation for motor velocity. However, the velocity observer provides a better velocity estimate.

- When the disturbance is large, consider the case of pulse disturbance (Fig. 6.11), finite difference velocity completely failed to follow the change in motor velocity. Furthermore, the finite difference velocity estimation becomes worse if web position sensor signal is noisy.

- The velocity observer provides a very good estimate of motor velocity. But introduces some time delay when compared with tachometer velocity. This time delay can be reduced by using a higher signal sampling frequency than the control sampling frequency.

- The most attractive feature of the velocity observer is that it can provide a good and relatively smooth motor velocity estimate. Thus, the control gains can be chosen higher to provide faster response.

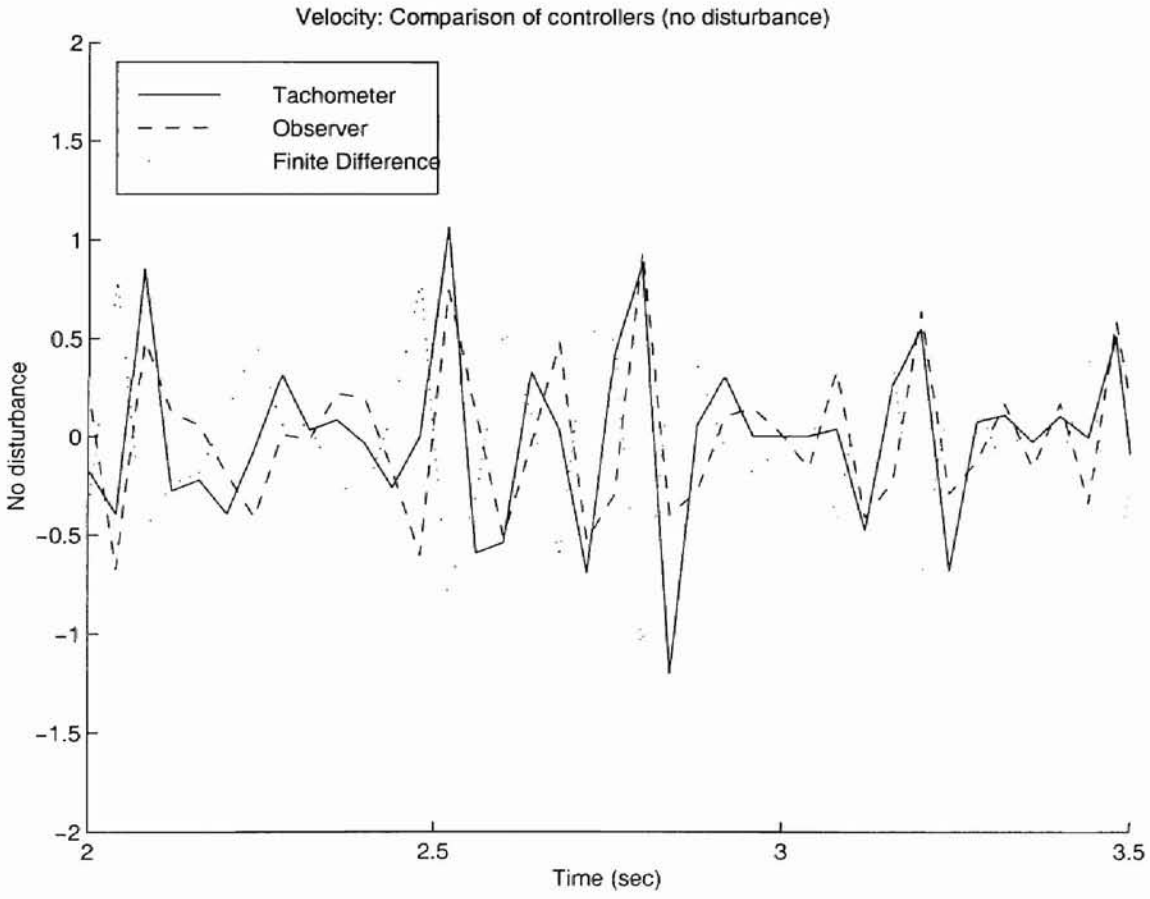

Figure 6.9: Comparison of velocities from three controllers: no disturbance

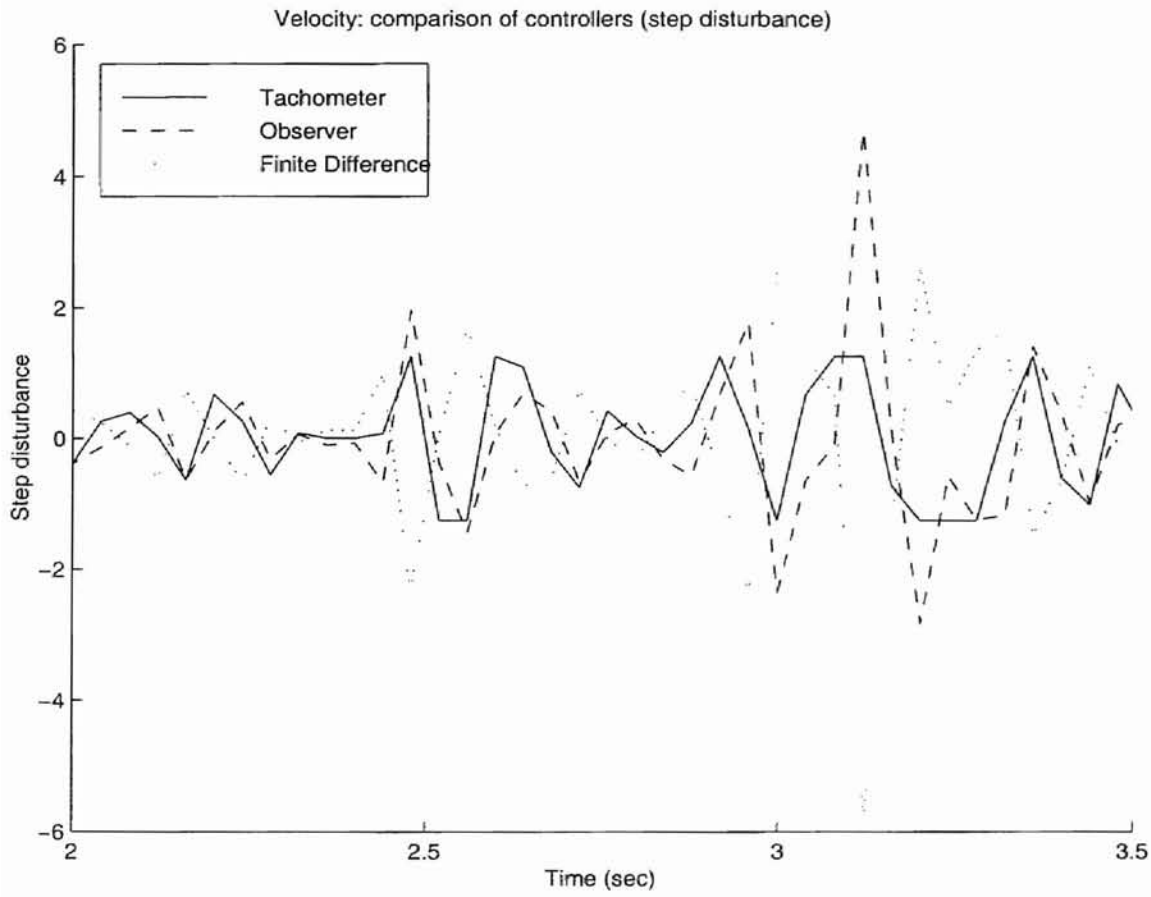

Figure 6.10: Comparison of velocities from three controllers: step disturbance

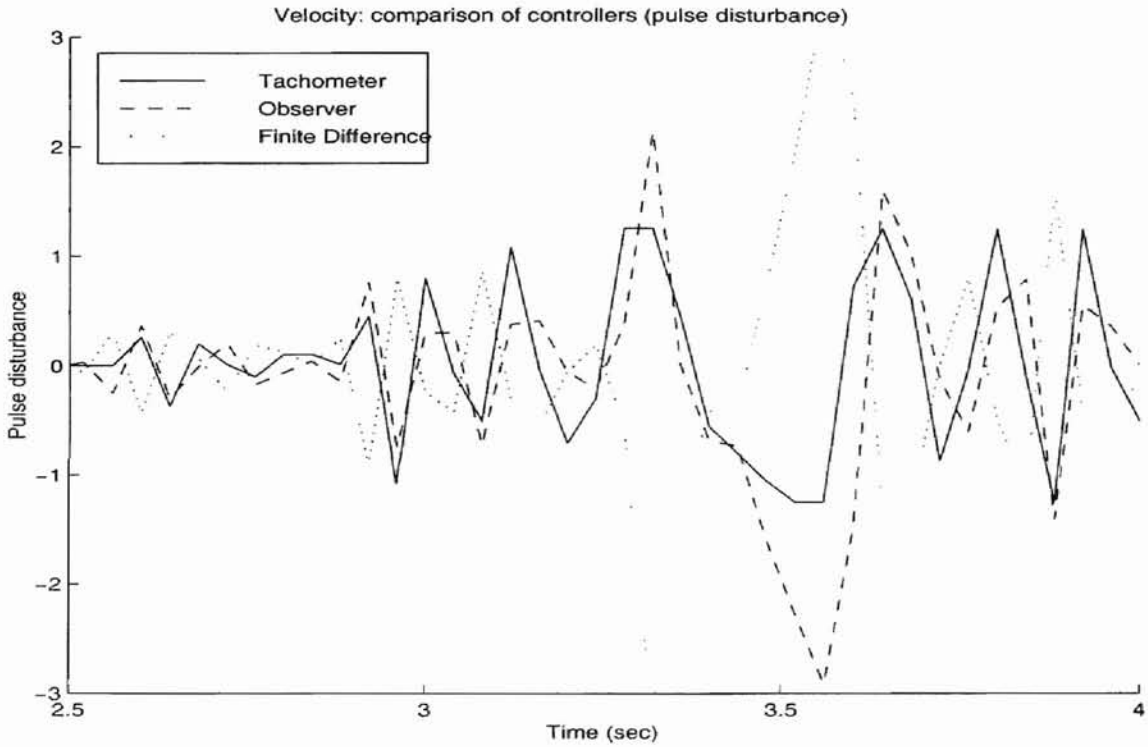

Figure 6.11: Comparison of velocities from three controllers: pulse disturbance

Chapter 7

Conclusion and Future Research

7.1 Conclusion

The objective of this research was to circumvent the use of the tachometer signals for the inner-loop feedback with a motor velocity estimator. Specifically, the equations developed by Shelton for a remotely pivoted steering guide and for lateral deflection of web were to be verified. Once verified these equations could be used for other web line application. Chapter 2 lists the basic types of automatic control systems and guiding mechanisms used in the industry. The control system on the traction machine in OSU is the electromechanical type coupled with the remotely pivoted guide. Shelton's model for the remotely pivoted steering guide is rederived, which forms a basis for all the experiments in this thesis. It has been experimentally verified in Section 4.2 that the velocity inner-loop feedback is very essential for satisfactory lateral control of web. Equation (4.24) is our desired velocity estimator that lateral motion of the web is digitally controlled. Open loop dynamic response of the web for a step, impulse and a sinusoidal disturbance are conducted which show that the web system can follow the disturbance after a short time period as shown in Figures 4.7, 4.8 and 4.9. The open loop dynamics of the system also appears to be characterized by a low pass filter.

Experiments having been conducted using both Fife A9 PI controller and the digital PI controller using the computer. Results show that the computer control is very similar to the Fife A9 analog controller. Two solutions were offered for the purpose of stabilizing the system in the absence of motor tachometer:

- Finite difference of edge sensor signal to obtain the lateral velocity of the web.
- Estimating the velocity of the web using minimum-order observer design.

The results using the finite difference method is found to be unsatisfactory since the finite difference velocity signal depends on the noise level in the position signal, which makes it unusable at some instances when the lateral position signal noise is high. On the other hand, the results using velocity observer are found to be more effective since the estimated velocity feedback in the inner-loop can provide similar closed-loop performance as that of the system with tachometer feedback.

7.2 Future Work

Investigation of the effect of different kinds of controllers (like adaptive control, robust control) on the lateral control of web will be undertaken in the future. The study will involve use of ultrasonic sensors and an offset pivoted guide (displacement guide) will replace the remotely pivoted guide.

Little research has been done for the area of web due to uneven nip loading. However, research has been done for the rubber covered rolls. Foreman assumed that the web achieves the velocity of the rubber rolls in the contact region. The velocity in this region should be greater than the velocity of the covering away from the contact zone. Foreman formulated the following equation for change in velocity per unit

velocity.

$$\frac{\Delta V}{V} = 0.35\frac{R_o^0.5\delta^1.5}{t^2} \tag{7.1}$$

An accurate model and basis for this greater velocity could provide a more accurate strain.

An investigation of modulus could also be useful. Research could also be performed on the small deflection assumption of the rubber covered roll. Being able to determine the point where this assumption does not apply could be useful in predicting the lateral deflection of the web. This could give a more accurate description of lateral web movement. The effect of friction between rollers and the web would also be interesting. Investigation into this area could show a relationship between friction and lateral web movement. Once the equations for lateral deflection and effective nip load have been refined, they could be then used for web guiding. By using an edge sensor and a feedback controller, the nip setup could be used as a web guidance system.

Bibliography

[1] J.J. Shelton, *Lateral Dynamics of a Moving Web*, Ph.D.thesis. Oklahoma State University, 1968.

[2] J.J. Shelton and K.N. Reid, *Lateral Dynamics of a Real Moving Web*, ASME Journal of Dynamic Systems, Measurement, and Control, vol. 93, no. 3, pp. 180-192, 1971.

[3] J.J. Shelton and K.N. Reid, *Lateral Dynamics of an Ideal Moving Web*, ASME Journal of Dynamic Systems, Measurement, and Control, vol. 93, no. 3, pp. 187-186, 1971.

[4] K.I. Hopcus, *Unwind and Rewind Guiding*, Proceedings of the Second International Conference on Web Handling, June 6-9, 1993.

[5] G.E. Young and K.N. Reid, *Lateral and Longitudinal Dynamic Behavior and Control of Moving Webs*, ASME Journal of Dynamic Systems, Measurement, and Control, vol. 115, no. 2B, pp. 309-317, 1993.

[6] G.E. Young, J.J. Shelton and C.E. Kardamilas, *Modeling and Control of Multiple Web Spans Using State Estimation*, ASME Journal of Dynamic Systems, Measurement, and Control, vol. 111, pp. 505-510, 1989.

[7] C.E. Kardamilas and G.E. Young, *Stochastic Modeling of Lateral Web Dynamics*, Proceedings of the American Control Conference, San Diego, CA, May 23-25, 1990.

[8] C.E. Kardamilas, *Stochastic Modeling and Control of Lateral Web Dynamics*, Ph.d.thesis, Oklahoma State University, 1990.

[9] G.E. Young, J.J. Shelton and B. Fang, *Interaction of Web Spans: Part I-Statics*, ASME Journal of Dynamic Systems, Measurement, and Control, vol. 111, pp. 490-496, 1989.

[10] G.E. Young, J.J. Shelton and B. Fang, *Interaction of Web Spans: Part II-Dynamics*, ASME Journal of Dynamic Systems, Measurement, and Control, vol. 111, pp. 497-504, 1989.

[11] P.B. Lindley, *Load-Compression Relationships of Rubber Units*, Journal of Strain Analysis, vol. 1, no. 3, pp. 190-195.

[12] A.R. Foreman, *Application of Rubber Covered Rolls to Pinch Rolls and Bridles*, Iron and Steel Engineer, pp. 111-120, 1964.

[13] J.J. Shelton, Informal notes on web deformation due to nonuniform nip pressure, 1994.

[14] M.N. Ahmad, *Lateral Deflection of a Web due to a Differentially loaded Nip*, Masters Thesis, Oklahoma State University, 1995.

[15] J.J. Shelton, *Effects of Web Camber on Handling*, Proceedings of the Fourth International Conference on Web Handling, June 1-4, 1997.

[16] P.R. Pagilla, K.N. Reid and K. Hopcus, *Modeling and Advanced Control of Web Handling Systems*, Project Number: AR928-021, Contract Number: 5401, January 2000.

[17] K. Ogata, *Discrete-Time Control Systems*, Prentice Hall, Englewoods Cliffs, New Jersey, 1995.

Appendix A

Derivation of Velocity Observer

A typical control system with estimated state feedback is shown in Fig. A.1

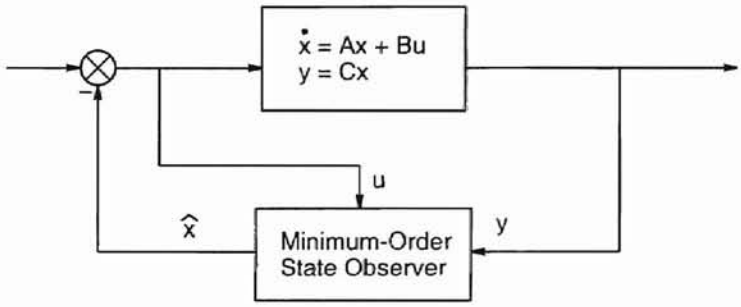

Figure A.1: Typical control system with estimated state feedback

The transfer function of web guiding system, which is a remotely pivoted steering guide is given by the following equation:

$$\frac{Y_L(s)}{Z(s)} = \frac{s^2 + \frac{f_2(KL)}{\tau}s + \frac{f_2(KL)}{\tau^2 x_1}}{s^2 + \frac{f_2(KL)}{\tau}s + \frac{f_2(KL)}{\tau^2}} \tag{A.1}$$

A state space model of the above system is given by:

$$\begin{bmatrix} \dot{x}_1 \\ \dot{x}_2 \\ \dot{x}_3 \\ \dot{x}_4 \end{bmatrix} = \underbrace{\begin{bmatrix} 0 & 1 & 0 & 0 \\ 0 & -a_m & 0 & 0 \\ 0 & 0 & 0 & 1 \\ \beta & 0 & -\alpha_1 & -\alpha_2 \end{bmatrix}}_{A} \begin{bmatrix} x_1 \\ x_2 \\ x_3 \\ x_4 \end{bmatrix} + \underbrace{\begin{bmatrix} 0 \\ k_m \\ 0 \\ 0 \end{bmatrix}}_{B}$$

$$y = \underbrace{\begin{bmatrix} 0 & 0 & 1 & 0 \end{bmatrix}}_{C} \begin{bmatrix} x_1 \\ x_2 \\ x_3 \\ x_4 \end{bmatrix}$$

The state variables x_1, x_2, x_3 and x_4 correspond to motor angle, motor angular velocity, web lateral position, web lateral velocity, respectively. For our web system, the web lateral position x_3, is measured by the optical sensor. Thus, the minimum-order observer is designed to estimate the state variables x_1, x_2 and x_4.

The procedure for deriving the observer is summarized below.

(1) Choose a matrix C_* such that

$$C_* = \begin{bmatrix} 1 & 0 & 0 & 0 \\ 0 & 1 & 0 & 0 \\ 0 & 0 & 0 & 1 \end{bmatrix}$$

Consider the following similarity transformation matrix,

$$T^{-1} = \begin{bmatrix} C_* \\ C \end{bmatrix} = \begin{bmatrix} 1 & 0 & 0 & 0 \\ 0 & 1 & 0 & 0 \\ 0 & 0 & 0 & 1 \\ 0 & 0 & 1 & 0 \end{bmatrix}$$

Therefore,

$$T = \begin{bmatrix} 1 & 0 & 0 & 0 \\ 0 & 1 & 0 & 0 \\ 0 & 0 & 0 & 1 \\ 0 & 0 & 1 & 0 \end{bmatrix}$$

(2) Apply similarity transformation to matrices A, B, and C.

$$\tilde{A} = T^{-1}AT$$

Therfore,

$$\tilde{A} = \begin{bmatrix} 1 & 0 & 0 & 0 \\ 0 & 1 & 0 & 0 \\ 0 & 0 & 0 & 1 \\ 0 & 0 & 1 & 0 \end{bmatrix} \begin{bmatrix} 0 & 1 & 0 & 0 \\ 0 & -a_m & 0 & 0 \\ 0 & 0 & 0 & 1 \\ \beta & 0 & -\alpha_1 & -\alpha_2 \end{bmatrix} \begin{bmatrix} 1 & 0 & 0 & 0 \\ 0 & 1 & 0 & 0 \\ 0 & 0 & 0 & 1 \\ 0 & 0 & 1 & 0 \end{bmatrix}$$

$$\tilde{A} = \begin{bmatrix} 0 & 1 & 0 & 0 \\ 0 & -a_m & 0 & 0 \\ \beta & 0 & -\alpha_2 & -\alpha_1 \\ 0 & 1 & 1 & 0 \end{bmatrix} \equiv \begin{bmatrix} A_{11} & A_{12} \\ A_{21} & A_{22} \end{bmatrix}$$

where

$$A_{11} = \begin{bmatrix} 0 & 1 & 0 \\ 0 & -a_m & 0 \\ \beta & 0 & -\alpha_2 \end{bmatrix}; \quad A_{12} = \begin{bmatrix} 0 \\ 0 \\ -\alpha_1 \end{bmatrix}; \quad A_{21} = \begin{bmatrix} 0 & 0 & 1 \end{bmatrix}; \quad A_{22} = \begin{bmatrix} 0 \end{bmatrix}$$

Also,

$$\tilde{B} = T^{-1}B$$

Therefore,

$$\tilde{B} = \begin{bmatrix} 1 & 0 & 0 & 0 \\ 0 & 1 & 0 & 0 \\ 0 & 0 & 0 & 1 \\ 0 & 0 & 1 & 0 \end{bmatrix} \begin{bmatrix} 0 \\ k_m \\ 0 \\ 0 \end{bmatrix} = \begin{bmatrix} 0 \\ k_m \\ 0 \\ 0 \end{bmatrix} \equiv \begin{bmatrix} B_1 \\ B_2 \end{bmatrix}$$

where

$$B_1 = \begin{bmatrix} 0 \\ k_m \\ 0 \end{bmatrix}; \quad B_2 = \begin{bmatrix} 0 \end{bmatrix}$$

$$\tilde{C} = CT = \begin{bmatrix} 0 & 0 & 1 & 0 \end{bmatrix} \begin{bmatrix} 1 & 0 & 0 & 0 \\ 0 & 1 & 0 & 0 \\ 0 & 0 & 0 & 1 \\ 0 & 0 & 1 & 0 \end{bmatrix}$$

Therefore,

$$\tilde{C} = \begin{bmatrix} 0 & 0 & 0 & 1 \end{bmatrix}$$

(3) Define the following matrix,

$$E = A_{11} - LA_{21}$$

where L is the observer feedback gain matrix which is given by $[l_1 \quad l_2 \quad l_3]^T$. The observer gains, l_1, l_2 and l_3 are obtained by choosing the desired poles of the observer matrix E. The matrix E is

$$\begin{aligned} E &= \begin{bmatrix} 0 & 1 & 0 \\ 0 & -a_m & 0 \\ \beta & 0 & -\alpha_2 \end{bmatrix} - \begin{bmatrix} l_1 \\ l_2 \\ l_3 \end{bmatrix} \begin{bmatrix} 0 & 1 & 1 \end{bmatrix} \\ &= \begin{bmatrix} 0 & 1 & 0 \\ 0 & -a_m & 0 \\ \beta & 0 & -\alpha_2 \end{bmatrix} - \begin{bmatrix} 0 & l_1 & l_1 \\ 0 & l_2 & l_2 \\ 0 & l_3 & l_3 \end{bmatrix} \\ &= \begin{bmatrix} 0 & 1-l_1 & -l_1 \\ 0 & -a_m - l_2 & -l_2 \\ \beta & -l_3 & -\alpha_2 - l_3 \end{bmatrix} \end{aligned}$$

The characteristic polynomial of E is given by

$$det[sI - E] = s^3 + (\alpha_2 + l_3 + a_m)s^2 + (a_m\alpha_2 + a_m l_3 + l_1\beta)s + (l_2\beta + l_1\beta a_m) \tag{A.2}$$

Let μ_1 , μ_2 ,μ_3 be the desired poles of the observer, i.e. of matrix E. Then the following characteristic equation gives the desired observer poles:

$$det[sI - E] = s^3 + (\mu_1 + \mu_2 + \mu_3)s^2 + (\mu_1\mu_2 + \mu_2\mu_3 + \mu_3\mu_1)s + (\mu_1\mu_2\mu_3) = 0 \tag{A.3}$$

Comparing coefficients of (A.2) and (A.3), we obtain

$$a_m + \alpha_2 + l_3 = \mu_1 + \mu_2 + \mu_3$$

$$a_m\alpha_2 + a_m l_3 + \beta l_1 = \mu_1\mu_2 + \mu_2\mu_3 + \mu_3\mu_1$$

$$\beta l_1 a_m + \beta l_2 = \mu_1\mu_2\mu_3$$

Solving the above equations we obtain the observer gain matrix, L.

(4) Now define matrices J, D, R, S such that,

$$J = A_{11}L - LA_{21}L + A_{12} - LA_{22}$$

$$D = B_1 - LB_2$$

$$\begin{bmatrix} R & S \end{bmatrix} = \begin{bmatrix} I_3 & L \\ O & 1 \end{bmatrix}$$

On computation the matrices J, D, R, S are

$$J = \begin{bmatrix} l_2 - l_1 l_3 \\ -a_m l_2 - l_2 l_3 \\ l_1\beta - \alpha_2 l_3 - l_3^2 - \alpha_1 \end{bmatrix} \equiv \begin{bmatrix} J_1 \\ J_2 \\ J_3 \end{bmatrix}$$

$$D = \begin{bmatrix} 0 \\ k_m \\ 0 \end{bmatrix}; \quad R = \begin{bmatrix} 1 & 0 & 0 \\ 0 & 1 & 0 \\ 0 & 0 & 1 \\ 0 & 0 & 0 \end{bmatrix}; \quad S = \begin{bmatrix} l_1 \\ l_2 \\ l_3 \\ 1 \end{bmatrix}$$

$$T\begin{bmatrix} R & S \end{bmatrix} = \begin{bmatrix} 1 & 0 & 0 & 0 \\ 0 & 1 & 0 & 0 \\ 0 & 0 & 0 & 1 \\ 0 & 0 & 1 & 0 \end{bmatrix} \begin{bmatrix} 1 & 0 & 0 & l_1 \\ 0 & 1 & 0 & l_2 \\ 0 & 0 & 1 & l_3 \\ 0 & 0 & 0 & 1 \end{bmatrix} = \begin{bmatrix} 1 & 0 & 0 & l_1 \\ 0 & 1 & 0 & l_2 \\ 0 & 0 & 0 & 1 \\ 0 & 0 & 1 & l_3 \end{bmatrix}$$

The estimated state vector is given by

$$\hat{x}(t) = \begin{bmatrix} 1 & 0 & 0 & l_1 \\ 0 & 1 & 0 & l_2 \\ 0 & 0 & 0 & 1 \\ 0 & 0 & 1 & l_3 \end{bmatrix} \begin{bmatrix} \hat{z}(t) \\ y(t) \end{bmatrix} \tag{A.4}$$

where $\hat{z}$ is given by the observer error dynamics,

$$\dot{\hat{z}}(t) = E\hat{z}(t) + Du(t) + Jy(t) \tag{A.5}$$

Taking Laplace transform of the above equation, we obtain

$$(sI - E)\hat{Z}(s) = DU(s) + JY(s)$$

$$\begin{bmatrix} s & -1 & l_1 \\ 0 & s + a_m & l_2 \\ -\beta & 0 & s + \alpha_2 + l_3 \end{bmatrix} \begin{bmatrix} \hat{Z}_1(s) \\ \hat{Z}_2(s) \\ \hat{Z}_3(s) \end{bmatrix} = \begin{bmatrix} 0 \\ k_m \\ 0 \end{bmatrix} U(s) + \begin{bmatrix} J_1 \\ J_2 \\ J_3 \end{bmatrix} Y(s)$$

The above equation can be divided into three parts:

$$s\hat{Z}_1(s) - \hat{Z}_2(s) + l_1\hat{Z}_3(s) = J_1Y(s) \tag{A.6}$$

$$(s + a_m)\hat{Z}_2(s) + l_2\hat{Z}_3(s) = k_mU(s) + J_2Y(s) \tag{A.7}$$

$$-\beta\hat{Z}_1(s) + (s + \alpha_2 + l_3)\hat{Z}_3(s) = J_3Y(s) \tag{A.8}$$

Solving equations (A.6), (A.7) and (A.8) we get

$$\begin{aligned} \hat{Z}_2(s) \;=\; & \frac{k_ms^2 + (k_m\alpha_2 + k_ml_3)s + l_1k_m\beta}{s^3 + (a_m + \alpha_2 + l_3)s^2 + (\alpha_2a_m + l_3a_m + l_1\beta)s + (l_1a_m\beta + l_2\beta)}U(s) \\ & + \frac{J_2s^2 + (J_2\alpha_2 + J_2l_3 - J_3l_2)s + (l_1J_2\beta - J_1l_2\beta)}{s^3 + (a_m + \alpha_2 + l_3)s^2 + (\alpha_2a_m + l_3a_m + l_1\beta)s + (l_1a_m\beta + l_2\beta)}Y(s) \end{aligned}$$

To obtain the transfer function relating the estimated motor velocity, $\hat{X}_2(s)$ to $U(s)$ and $Y(s)$, we use equation (A.4). From (A.4),

$$\hat{x}_2(t) = \hat{z}_2(t) + l_2y(t)$$

Therefore,

$$\hat{X}_2(s) = \frac{\beta_3s^3 + \beta_2s^2 + \beta_1s + \beta_0}{s^3 + \gamma_2s^2 + \gamma_1s + \gamma_0}Y(s) + \frac{\lambda_2s^2 + \lambda_1s + \lambda_0}{s^3 + \gamma_2s^2 + \gamma_1s + \gamma_0}U(s) \tag{A.9}$$

where

$$
\begin{aligned}
\gamma_2 &= a_m + \alpha_2 + l_3 \\
\gamma_1 &= \alpha_2 a_m + l_3 a_m + l_1 \beta \\
\gamma_0 &= l_1 a_m \beta + l_2 \beta \\
\beta_3 &= l_2 \\
\beta_2 &= l_2 a_m + \alpha_2 l_2 + l_2 l_3 + J_2 \\
\beta_1 &= J_2 \alpha_2 + J_2 l_3 - J_3 l_2 + \alpha_2 a_m l_2 + l_3 a_m l_2 + l_1 l_2 \beta \\
\beta_0 &= l_1 J_2 \beta - J_1 l_2 \beta + l_1 a_m l_2 \beta + \beta {l_2}^2 \\
\lambda_2 &= k_m \\
\lambda_1 &= k_m \alpha_2 + k_m l_3 \\
\lambda_0 &= l_1 k_m \beta
\end{aligned}
$$

Appendix B

Matlab Script File

```
Cm=0.012; am=53; Km=1413*Cm; Km1=1413;
x1=88;                          %instant center (inch)
L=46;           % in
v=400*12/60;    % in/sec
Tension=10;         % lb

T=L/v;
K=sqrt((Tension-v^2*1.7*10^(-8))/(10800*(1+0.008658*Tension)));
KL=K*L;

fff1=KL^2*(cosh(KL)-1)/(KL*sinh(KL)-2*(cosh(KL)-1))
fff2=KL*(KL*cosh(KL)-sinh(KL))/(KL*sinh(KL)-2*(cosh(KL)-1))
fff3=KL*(sinh(KL)-KL)/(KL*sinh(KL)-2*(cosh(KL)-1));

a=T^2/fff1 b=fff2*T/fff1 c=4/3*fff2/fff1

Kp1=10; Kp2=40; Kp3=80; Kp4=4; Kd=0; Ki=0.1; Kv=0.744;
```

```
beta=(c-1)/a; alpha1=b/a; alpha2=1/a;

mu1=50; mu2=50; mu3=50;

M=[0 0 1;beta 0 am;beta*am beta 0]; N=[mu1+mu2+mu3-am-alpha2
   mu1*mu2+mu2*mu3+mu3*mu1-am*alpha2
   mu1*mu2*mu3];

LL=inv(M)*N;

l1=LL(1); l2=LL(2); l3=LL(3);

J1=l2-l1*l3; J2=-am*l2-l2*l3; J3=beta*l1-alpha2*l3-l3*l3-alpha1;

beta3=l2; beta2=l2*(alpha2+l3+am)+J2;
beta1=l2*(am*(alpha2+l3)+beta*l1)+J2*(alpha2+l3)-J3*l2;
beta0=(J2*beta*l1-J1*beta*l2)+l2*(am*beta*l1+l2*beta);

gamma0=am*beta*l1+l2*beta; gamma1=am*(alpha2+l3)+beta*l1;
gamma2=alpha2+l3+am;

lambda0=Km*beta*l1; lambda1=(alpha2+l3)*Km; lambda2=Km;

gvu=tf([lambda2,lambda1,lambda0],[1,gamma2,gamma1,gamma0]);
gvy=tf([beta3,beta2,beta1,beta0],[1,gamma2,gamma1,gamma0]);
```

```
%*********************  Coef2.m*******************

f1=(K^2)*(cosh(KL)-1)/(KL*sinh(KL)-2*(cosh(KL)-1));

f2=K*(KL*cosh(KL)-sinh(KL))/(KL*sinh(KL)-2*(cosh(KL)-1));

f3=K*(sinh(KL)-KL)/(KL*sinh(KL)-2*(cosh(KL)-1));


numz=[1,v*f2,v^2*f2/x1];

denz=[1,v*f2,v^2*f1];

g1=tf(numz,denz);


num3R=[0,-v*f3,v^2*f1];

den3R=[1,v*f2,v^2*f1];

g3=tf(num3R,den3R);


gm=tf([0 0 Km],[1 am+Km 0]);


gc1=tf([Kp1 Ki],[1 0]);

gc2=tf([Kp2 Ki],[1 0]);

gc3=tf([Kp3 Ki],[1

0]);


g_close1=g3/(1+gc1*gm*g1);

g_close2=g3/(1+gc2*gm*g1);

g_close3=g3/(1+gc3*gm*g1);
```

```
g_close_ref=gc1*gm*g1/(1+gc1*gm*g1);


close all;


%open loop response (Impulse)
t=0:0.01:5;
%[y1,t]=impulse(tf([1],[1]),t);
%plot(t,y1,'--');
hold on;
[y2,t]=impulse(g3,t);
plot(t,y2,'-');


title('Response at guide roller to impulse disturbance (open
loop)');
xlabel('Time (Sec.)');
ylabel('Amplitude');
hold off;
zoom on;


%   open loop response (step)
figure(2);
t=0:0.01:5;
y2=ones(size(t));
[y1,t]=step(g3,t);
plot(t,y2,'b--',t,y1,'b-');
legend('Disturbance','Response');
```

```
title('Response at guide roller to unit step disturbance (open
loop)');
xlabel('Time (Sec.)');
ylabel('Amplitude');
zoom on;

%   open loop response (sin)
figure(3);
t=0:0.01:10;%open loop response (Impulse)

y1=sin(t); sin1=sin(t);
[y2,t]=lsim(g3,sin1,t);
plot(t,y1,'b--',t,y2,'b-');
legend('Disturbance','Response');
title('Response at guide roller to sinusoidal disturbance (open
loop)');
xlabel('Time (Sec.)');
ylabel('Amplitude');
zoom on;

%%%%%%%%%%closed-loop response%%%%%%%%%%%%%%

%close loop response (Impulse)
figure(4);
t=0:0.01:3;
%[y1,t]=impulse(tf([1],[1]),t);
```

```
%plot(t,y1,'--');
[y1,t]=impulse(g_close1,t);
[y2,t]=impulse(g_close2,t);
[y3,t]=impulse(g_close3,t);
plot(t,y1,'b-',t,y2,'b:',t,y3,'b-.');
legend('Kp=10,Ki=0.1','Kp=40,Ki=0.1','Kp=80,Ki=0.1');
title('Response at guide roller to impulse disturbance
(closed-loop)');
xlabel('Time (Sec.)');
ylabel('YL  Amplitude');
zoom on;

%close loop response (unit step)
figure(5);
t=0:0.01:10;
y4=ones(size(t));
[y1,t]=step(g_close1,t);
[y2,t]=step(g_close2,t);
[y3,t]=step(g_close3,t);
plot(t,y4,'b--',t,y1,'b-',t,y2,'b:',t,y3,'b-.');
legend('Disturbance','Kp=10,Ki=0.1','Kp=40,Ki=0.1','Kp=80,Ki=0.1');
title('Response at guide roller to unit step disturbance
(closed-loop)');
xlabel('Time (Sec.)');
ylabel('YL  Amplitude');
hold off;
```

```
zoom on;

%close loop response (sin step)
figure(6);
t=0:0.01:10;
y4=sin(t);
[y1,t]=lsim(g_close1,y4,t);
[y2,t]=lsim(g_close2,y4,t);
[y3,t]=lsim(g_close3,y4,t);
plot(t,y4,'b--',t,y1,'b-',t,y2,'b:',t,y3,'b-.');
legend('Disturbance','Kp=10,Ki=0.1','Kp=40,Ki=0.1','Kp=80,Ki=0.1');
title('Response at guide roller to sinusoidal disturbance
(closed-loop)');
xlabel('Time (Sec.)');
ylabel('YL  Amplitude');
zoom on;


%%%%%%%%%%closed-loop response with velocity observer%%%%%%%%%%%%%%%

g_obs1=g3*(1+gvu)/(1+gvu+gm*g1*(gc1+gvy));
g_obs2=g3*(1+gvu)/(1+gvu+gm*g1*(gc2+gvy));
g_obs3=g3*(1+gvu)/(1+gvu+gm*g1*(gc3+gvy));
g_obs_ref=gm*gc1*g1/(1+gvu+gm*g1*(gc1+gvy));

%closed-loop response with velocity observer (Impulse)
```

```
figure(7);
t=0:0.01:3;
%[y1,t]=impulse(tf([1],[1]),t);
%plot(t,y1,'--');
[y1,t]=impulse(g_obs1,t);
[y2,t]=impulse(g_obs2,t);
[y3,t]=impulse(g_obs3,t);
plot(t,y1,'b-',t,y2,'b:',t,y3,'b-.');
legend('Kp=10,Ki=0.1','Kp=40,Ki=0.1','Kp=80,Ki=0.1');
title('Response at guide roller to impulse disturbance (using
estimated motor velocity feedback)');
xlabel('Time (Sec.)');
ylabel('YL  Amplitude');
hold off;
zoom on;

%closed-loop response with velocity observer (unit step)
figure(8); t=0:0.01:10;
y4=ones(size(t));
[y1,t]=step(g_obs1,t);
[y2,t]=step(g_obs2,t);
[y3,t]=step(g_obs3,t);
plot(t,y4,'b--',t,y1,'b-',t,y2,'b:',t,y3,'b-.');
legend('Disturbance','Kp=10,Ki=0.1','Kp=40,Ki=0.1','Kp=80,Ki=0.1');
title('Response at guide roller to unit step disturbance (using
estimated motor velocity feedback)');
```

```
xlabel('Time (Sec.)');
ylabel('YL  Amplitude');
zoom on;

%closed-loop response with velocity observer (sin)
figure(9);
t=0:0.01:10;
y4=sin(t);
[y1,t]=lsim(g_obs1,y4,t);
[y2,t]=lsim(g_obs2,y4,t);
[y3,t]=lsim(g_obs3,y4,t);
plot(t,y4,'b--',t,y1,'b-',t,y2,'b:',t,y3,'b-.');
legend('Disturbance','Kp=10,Ki=0.1','Kp=40,Ki=0.1','Kp=80,Ki=0.1');
title('Response at guide roller to sinusoidal disturbance (using
estimated motor velocity feedback)');
xlabel('Time (Sec.)');
ylabel('YL  Amplitude');
zoom on;


%responses to impulse disturbance using tachometer and estimated velocity feedba
%%%% impulse response
figure(10); t=0:0.01:3;
%[y1,t]=impulse(tf([1],[1]),t);
%plot(t,y1,'--');
[y1,t]=impulse(g_close_ref,t);    %with tach
```

```
[y2,t]=impulse(g_obs_ref,t);      %with estimated
plot(t,y1,'b-',t,y2,'b:'); legend('Observor','Tachometer');
title('Comparsion of impulse responses between using tachometer
and estimated velocity feedback');
xlabel('Time (Sec.)');
ylabel('YL  Amplitude');
hold off;
zoom on;

%%%% unit step response
figure(11);
t=0:0.01:10;
y4=ones(size(t));
[y1,t]=step(g_close_ref,t);    %with tach
[y2,t]=step(g_obs_ref,t);      %with estimated
plot(t,y4,'b--',t,y1,'b-',t,y2,'b:');
legend('Reference','Observor','Tachometer');

title('Comparsion of unit step responses between using tachometer
and estimated velocity feedback');
xlabel('Time (Sec.)');
ylabel('YL Amplitude');
zoom on;

%sin response
figure(12);
```

```
t=0:0.01:10;
y4=sin(t);
[y1,t]=lsim(g_obs_ref,y4,t);
[y2,t]=lsim(g_close_ref,y4,t);
plot(t,y4,'b--',t,y1,'b-',t,y2,'b:');
legend('Reference','Observor','Tachometer');

title('Comparsion of sinusoidal responses between using tachometer
and estimated velocity feedback');
xlabel('Time (Sec.)');
ylabel('YL Amplitude');
zoom on;
```

VITA

Shaibal Sailaza Mandal

Candidate for the Degree of

Master of Science

Thesis: LATERAL CONTROL OF A WEB USING ESTIMTED VELOCITY FEEDBACK

Major Field: Mechanical Engineering

Biographical:

Education: Received Bachelor of Engineering degree in Mechanical Engineering from University of Mumbai, Maharashtra, India in May 1998. Completed requirements for the Master of Science degree at Oklahoma State University in July, 2000.

Professional Experience: Graduate Research Assistant, Web Handling Research Center, School of Mechanical and Aerospace Engineering, Oklahoma State University, March 1999 to July 2000. Trainee Engineer in Bhabha Atomic Research Center, Trombay, India, August 1997 to April 1998.